A Study of the Forming Limits of Cold and Hot Forming of Aluminium Alloy Sheets with Multi-point Tooling

Song Yang

The University of Strathclyde

A thesis submitted to the Department of Design, Manufacturing and Engineering Management for the degree of Doctor of Philosophy

Copyright Statement

The copyright of this thesis belongs to the author under the terms of the United Kingdom Copyright Acts as qualified by the University of Strathclyde Regulation 3.50. Due acknowledgement must always be made of the use of any material contained in, or derived from, this thesis.

Author's Declaration

This thesis is the result of the author's original research. It has been composed by the author and has not been previously submitted for examination which has led to the award of a degree.

Signed:

Date: 19/08/2020

Dedicated to

my father and mother

my wife, Lina Hou

whose love, sacrifice and encouragement have
helped me tremendously

Acknowledgements

In the first place, I would like to express great thanks to my supervisor, Professor Yi Qin, for his professional guidance and support to my research. Since I graduated from a different undergraduate course background, Professor Qin has spared no effort to help me in developing an understanding of mechanical engineering knowledge and making a connection with my previous knowledgebase. Professor Qin also provided me with many opportunities for engagement with research projects and conferences, which has broadened my horizon and vision. He shared his knowledge of research and generous attitude to life during my research period, which has helped to develop me with a stronger heart when dealing with academic difficulties and those encountered in life.

I also would like to thank Dr Erkan Oterkus, from the Department of Naval Architecture, Ocean and Marine Engineering. He gave me an impressive education and support when I was an undergraduate student and provided me with the chance to study for my PhD in the Department of Design, Manufacturing and Engineering Management. He gave me tremendous advice during my PhD study.

Special thanks also to Taufik Bin Mohamed Supri and Michael McPhillimy for their efforts in multi-point tool design and Daniel Melville for his efforts in contact-cooling tool design. Thanks also to the friends and colleagues in the Department of Design, Manufacturing and Engineering Management, especially Quanren Zeng, Wenlong Chang, Jie Zhao, Andreas Remier, Yihui Zhao, Xinyu Yang, Yankang Tian, Hao Wu, Senyong Chen, Hongying Jiang, Mutian Li, Cong Niu, etc, for sharing all their experience and giving constructive advice.

Last but not least, without reservation my grateful thanks to all the people I have met in the past years in Glasgow and Harbin, for all their support during these unforgettable days.

Publications

1. Hijji, Hasan, Yi Qin, Kunlan Huang, M. Bin Zulkipli, Song Yang, and Jie Zhao. "Forming alumina (Al2O3) by micro-FAST." In *Proc. of the 14th Int. Conf. on Manufacturing Research, Loughborough*, pp. 61-66. 2016.

2. Hijji, Hasan, Yi Qin, Kunlan Huang, Song Yang, Muhammad Bin Zulkipli, and Jie Zhao. "Fabrication of micro components with MSZ material using electrical-field activated powder sintering technology." In *Advances in Manufacturing Technology XXX: Proceedings of the 14th International Conference on Manufacturing Research, Incorporating the 31st National Conference on Manufacturing Research, September 6–8, 2016, Loughborough University, UK*, vol. 3, p. 55. IOS Press, 2016.

3. Yang, Song, Michael McPhillimy, Taufik Bin Mohamed Supri, and Yi Qin. "Influences of process and material parameters on quality of small-sized thin sheet-metal parts drawn with multipoint tooling." *Procedia Manufacturing* 15 (2018): 992-999.

4. Zhao, Yihui, Taufik Bin Mohamed Supri, Song Yang, and Yi Qin. "A new static method of calibration for low-cost laser triangulation systems." *Measurement* 156 (2020): 107613.

5. Yang, Song, Jie Zhao, Yankang Tian, and Yi Qin. "Pilot prototype production line for the hot-forming of aluminium alloy sheets with fast contact-cooling and multi-point tooling. " 10th EASN Conference on Innovation in Aviation & Space to the Satisfaction of the European Citizens (2020). Conference presentation, Sept. 2020

Abstract

Multi-point forming (MPF) is a special category of sheet metal forming techniques with good operational flexibilities due to using two sets of adjustable pins along the machine ram direction. These pins represent the acting points of the desired forming-tool surface contours. Although this technology has already been widely used for the shaping of panel components, it has been little tested for the forming of lightweight metal sheets with high strength.

Forming of lightweight metallic materials, such as aluminium alloys, has been widely deployed in the Aerospace and Automotive industry. Nevertheless, some challenges still exist when the forming takes place under different process and machine-set conditions, especially materials such as high strength aluminium alloy sheets.

Hot stamping technology is capable of improving the material properties and forming limits while reducing the forming-force requirement and springback. This could be enhanced particularly by integrating an intermediate fast cooling process into the process chain of the forming of aluminium alloys. However the spray cooling that is currently popular in industry cannot achieve the required high cooling rates, while introduction of an intermediate fast cooling process into an industry process is hampered by lack of the industrially viable tooling.

To address the issues mentioned above, this PhD research studies the feasibility of combining multi-point forming and hot-forming to shape the high-strength Aluminium alloy sheets. This is done with a view to improving the manufacturing flexibility while the capability of forming high-strength sheet-metals is maintained. This new capability was further enhanced by developing a fast contact-cooling facility and integrating it

into a pilot prototype production line. The fundamental and process studies combined with the two test cases, deep drawing and stretch forming with multi-point tooling, suggest a feasible alternative route for the forming of lightweight high-strength sheet-metals. The pilot line established shows that the fast contact-cooling technology is effective for application in an industrial metal forming process.

With this pilot line, the aluminium sheets heated up by the electrical furnace were subjected to the intermediate cooling prior to the loading into the multi-point tooling for forming. Different cooling rates, such as 50 °C/s and 100 °C/s, have been tested, and their effects on the forming limits for different component-forms investigated. AA6082 sheet blanks were used as the raw material; several square cups with different depths were formed; and the temperatures of the sheet blanks were monitored during the tests through a built-in monitoring system.

The tests conducted demonstrated that the integration of fast contact-cooling into a production process is feasible and its associated cost could be relatively low. It also demonstrated that introducing a high-temperature forming configuration into a multi-point tooling forming process is feasible, which extends the existing process capabilities. The test results showed that proper cooling rates, which are achievable easily with the facility developed, could improve forming limits of the high strength aluminium alloys greatly, although, in general, the higher the cooling rate, the better results are obtained. At the same time, the fast-cooling configuration design could, potentially, lead to significant process-time saving, due to the extremely short cooling time involved.

Contents

List of Figures

xiii

List of Tables

Nomenclature

AEM – Applied Element Method

ALE – Arbitrary Lagrangian Eulerian adaptive mesh

CAD – Computer-Aided Design

CAE – Computer-Aided Engineering

CAM – Computer-Aided Manufacturing

CCM – Classical Continuum Mechanics

CFD – Computational Fluid Dynamics

CMM – Coordinate Measuring Machine

CNC – Computer Numerical Control

CZE – Cohesive Zone Element

DFC – Ductile Fracture Criteria

EMF – Electromagnetic Forming Method

EPFM – Elastic Plastic Fracture Mechanics

FDM – Finite Difference Method

FE – Finite Element

FEA – Finite Element Analysis

FEM – Finite Element Method

FLC – Forming Limit Curve

FLCN – Forming Limit Curve at Necking

FLCF – Forming Limit Curve at Fracture

FLD -Forming Limit Diagram

FLDCRT – Maximum value of FLD damage initiation criterion

FLSD – Forming Limit Stress Diagram

GTN model – Gurson, Tvergaad and Needleman's damage model

HFQ - solution Heat treatment, cold-die Forming and Quenching

LEFM – Linear Elastic Fracture Mechanics

MK model – Marciniak and Kuczynski model

MP – Map Solution

MPF – Multi-Point Forming

PLC effect – Portevin-LeChatelier effect

RT – Room Temperature

SBFEM – Scaled Boundary Finite Element Method

SEF – Strain Energy Function

SHT – Solution Heat Treatment

SHT+NC – Solution Heat Treatment with Natural Cooling

SHT+FC – Solution Heat Treatment with Fast Cooling

SHT+EFC – Solution Heat Treatment with Extra Fast Cooling

SMPF – Sectional Multi-Point Forming

SPIF – Single Point Incremental Forming

SSSS – Supersaturated Solid Solution

TRL – Technical Readiness Level

UTS – Ultimate Tensile Strength

VBF – Variable Binder Force

XFEM – Extended Finite Element Method

Chapter 1 Introduction

1.1 Background

Sheet metal forming plays an important role in various fields of applications, e.g., producing complex three-dimensional shape parts, providing a good surface finish, enabling lightweight structures, etc. Nevertheless, for some processes where the shaped die-surfaces will have to be provided, these forming dies are often fixed to specific shapes, and lack flexibility for re-use and re-configurations. Multi-point forming (MPF) is regarded as a flexible-tooling technology for sheet forming with high flexibility through adjustment of its two sets of movable pins (upper and lower set in vertical direction usually) to desired heights, forming a continuous three-dimensional tooling contour. The idea of configurable dies was first presented in 1969 by Nakajima [1], but it was not until 1992 the concept of 'multi-point forming' was first defined. Usually each set of pins consist of matrices of dome-like punches which must be packed as tightly as possible, only with very little clearance. The pin size should be selected carefully as it has been proven that the occurrence of defects has a negative relationship with the surface area of contact spots [2]. Indentations can be reduced by use of cushions and wrinkles can be suppressed to some extent by applying blank holders since an in-plane bias can be produced by binding the material at the edges [3]. However, overload fracture should be carefully avoided during the process. In overload fracture the applied stress between the die and the workpiece is higher than the ultimate strength of the die material which can cause a serious safety hazard when releasing a large amount of energy. Plastic deformation results from irreversible deformation due to the stress in a local point or a widespread area exceeding the yield strength of the material.

1

At present aluminium and its alloy are popular for metal sheets, since lightweight technology is developing fast around the world to reduce weight and improve fuel consumption, especially in Aerospace and Automotive industry [4]. Aluminium is one of the most cost-effective lightweight materials, due to its excellent mechanical properties such as high strength to weight ratio, good plasticity, good corrosion resistance, etc. Based on aluminium alloy designations, some alloy materials have good formability at room temperature, which is suitable for cold forming, but there are still significant challenges when forming high/ultra-high strength alloys due to restricted formability and large springback [5]. To overcome these difficulties and meet production demands, hot forming technology is useful for such materials having low ductility with large, complex geometries while maintaining a low cost. The formability and material flow condition can be improved at elevated temperature, thus the force required for deformation can be greatly reduced. In a hot sheet metal forming process, the aluminium alloy sheets are heated to the solution heat treatment (SHT) temperature and held for a while to achieve uniform temperature distribution and desired micro-structure. Then the sheets are transferred to the cold die for forming, followed with the in-die quenching [6]. In this study, a contact fast cooling step is introduced between the solution heat treatment (SHT) and the forming step for the preservation of the obtained micro-structure. The cooling step is fast and controllable, for example, to decrease the temperature of the sheets from approximately 480 °C to 350 °C with various cooling rates for high strength aluminium alloys. The Centre for Precision Manufacturing (CPM) in Design, Manufacturing and Engineering Management has been working on this hot forming technology for several years, but little work has been done on testing the integration of fast cooling into an industrially viable industrial forming process chain. At the same time, multi-point tooling offers opportunities for flexible forming, and for testing different forming configurations when solid dies are not appropriate. Also hot forming of metallic sheets with a multi-point forming tool has not been tested yet. The Finite Element Method (FEM) is a robust analysis tool for investigating

2

the formability, stress and strain distributions during sheet metal forming. The associated input parameters at elevated temperatures, however, need to be determined by experiment, due to the lack of sufficient material property data for the heated metallic sheets subjected to fast cooling.

1.2 Research aims and objectives

1.2.1 Aims

The reported research deals with the study of multi-point tooling sheet metal stamping at elevated temperatures. The aim was to develop a hot multi-point tooling stamping process chain for the forming of high-strength aluminium alloys which integrates heating, intermediate fast-cooling, forming and aging in a complete production line. It was expected to deliver a high-efficient and cost-effective sheet-metal forming technology with improved process capability and flexibility for the forming of high-strength sheet metal parts.

1.2.2 Objectives

In order to reach the aim proposed, the following objectives were planned:

1. To develop a new understanding of the factors that influence the forming limits in multi-point tooling sheet-metal forming both experimentally and numerically.

2. To identify knowledge gaps in hot forming with multi-point tooling and to develop methods and technological measures to fill the gaps identified.

3. To investigate the roles of intermediate fast-cooling in sheet metal hot forming and to develop technology and tools for implementing the intermediate fast-cooling in hot-stamping of sheet metals.

4. To integrate the heating, multi-point tooling, intermediate fast-cooling and hot forming into a complete process chain and to demonstrate it through setting up a pilot production line.

Overall, the proposed work is a pioneering work combining a multi-point forming tool with hot stamping and fast cooling for practical applications. Successful outcomes of the research should significantly enhance the manufacturing capability and efficiency of the forming of sheet metal parts with high/ultra-high strength materials.

1.3 Research methodology

To achieve the aim and objectives, the following methodologies were employed:

- Conducting a comprehensive literature review on the sheet forming of aluminium alloys especially the multi-point forming, including the material property characterisation, tool configurations, tool applications, common tool failures and numerical methods for analysing forming performance.

- Conducting tensile tests on selected working materials and characterising their properties which would generate sufficient data for general analysis as well as provide input to the FE simulations of the forming processes.

- Conducting FE simulations of cold deep drawing with multi-point tooling to study the effects of materials and process parameters such as forming geometry, type of the working material, blank holding force, interface lubrication and use of a rubber cushion, etc.

- Carrying out experimental investigations into cold deep drawing with multi-point tooling under different conditions and conditioning the FE model based on the comparison of the measured data and the results predicted by the simulations.

- Conducting FE simulations of deep drawing of the heat-treated and fast cooled high-strength aluminium alloy sheet materials to study the differences between the cold and hot forming configurations when the multi-point tooling is used, including the improvement on the formability.

- Developing a hot stamping process chain by integrating the blank heating, multi-point tooling, intermediate fast-cooling and hot forming, and investigating into the effect of the intermediate fast-cooling and cooling-rates on the formability enhancement.

- Conducting experiments and simulations of hot stretch forming with multi-point tooling to study the springback occurring due to the hot-forming, and considering particularly the hot sheet-forming with the intermediate fast cooling introduced.

- Drawing conclusions from the research on the forming process, the process chain, integrated forming facility and forming limits, with particular reference to the introduction of a hot-forming configuration into the multi-point forming, and the fast, intermediate contact cooling

of aluminium alloys sheet metals. These are followed by developing several recommendations for the future work.

The relationship among these research methodologies was illustrated in a block diagram shown in Figure 1-1.
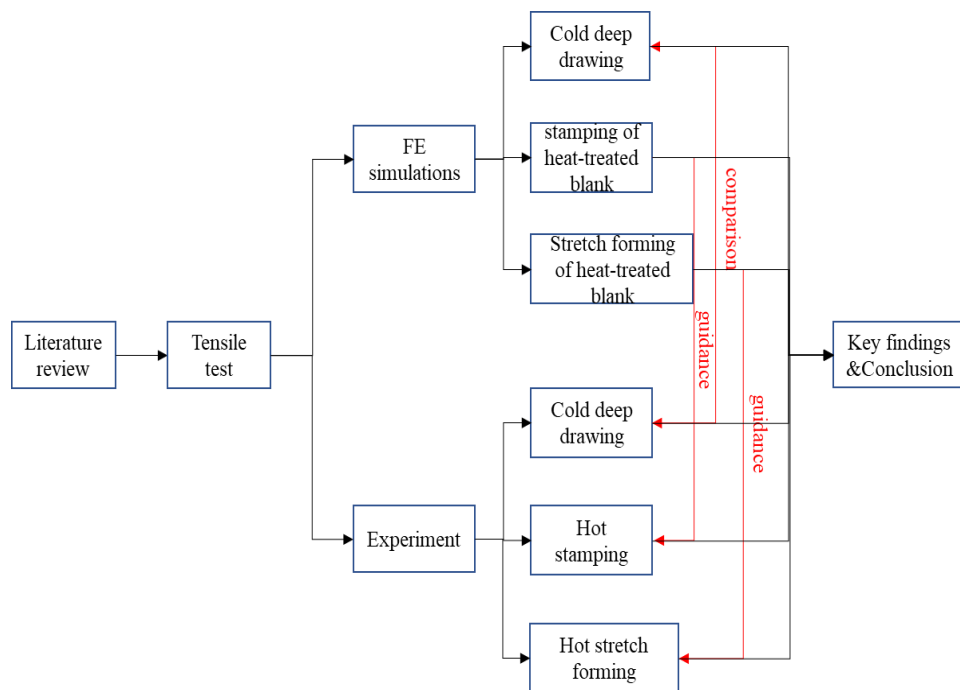
Figure 1-1 Block diagram of research methodology

1.4 Thesis structure

This thesis presents a high-efficient and cost-effective hot multi-point forming technology with an intermediate cooling system to hasten industrial applications. The structure of the thesis is:

Chapter 2 reviews existing literature on the development of widely used sheet metal forming processes and the advantages of the multi-point forming process. In addition, this chapter contains a comprehensive review

of hot stamping in the fields of process setup and equipment, including heating, forming and quenching. The investigations of material characteristics of aluminium alloys are described. Implementation of finite element simulation into such engineering problems is discussed. The knowledge gap is discussed to guide the following research.

In Chapter 3, the selected material characteristics from tensile tests are discussed. Test sample dimensions and test setup are introduced. A schematic illustration of the proposed fast cooling procedure for high strength aluminium alloy is illustrated. Stress-strain relation is given in a plotted curve with relative property parameters.

In Chapter 4 finite element (FE) simulation of the proposed multi-point forming process is described through the commercial software Abaqus. A material model is defined based on the results from tensile tests. Simulation procedures, including model geometrical setup, elements, meshing and boundary conditions are discussed. Central profile of the formed parts, pressure and equivalent strain distribution for cold multi-point forming are discussed to study the effect of influencing factors on shape performance. A feasibility study of formability improvements on the heat treated high-strength aluminium alloy is described. Analysis of the simulated formed parts provides a guide for the experimental setup.

In Chapter 5, the experimental setup for cold multi-point forming is discussed. Several metal sheets formed under different factors are measured, including sheet material properties, dimensions of curvatures to be formed, holding force, lubrication condition, and use of rubber as cushions. Results are analysed based on the measurement of the surface finish under different conditions.

Chapter 6 discusses the innovative idea and design of the intermediate cooling system. The assembly and setup of the whole hot multi-point sheet

7

forming production line with the intermediate cooling system is discussed. The improvements of production line design on process control, reliability and system robustness are discussed. A series of test and validation trials are conducted to determine the forming limit and surface finish of hot stamping demonstrators using the manufacturing production line.

Chapter 7 studies the effects of cooling rate on springback at elevated temperature in stretch forming using the proposed prototype production line. Numerical and experimental results are discussed to investigate the improvements from the fast cooling procedure.

Based on the research work done above, achievements, contributions to knowledge and the future work are summarised in the last chapter.

Chapter 2 Literature Review

2.1 Introduction

The trend in flexible sheet metal forming technology has developed quickly in recent years in line with other innovations within the forming industries. Meanwhile, demands for aluminium alloys are increasing to replace steel especially in automotive and aerospace industries. But since the thickness of metal sheets are always small compared with dimensions in other directions and ductility of some materials are poor at room temperature, fatigue cracks often occur and develop if concentrated cyclic stresses are too high. The production of high strength parts with desired shapes requires advanced knowledge and experience of the process procedures. In this chapter, a detailed review of sheet forming techniques with multi-point tools is given along with research on the hot forming techniques for aluminium alloy components. Lastly the identification of classical finite element modelling for determining forming performance is well reviewed.

2.2 Sheet forming of aluminium alloys

Metal forming is an engineering process of fashioning metal parts through mechanical deformation without any mass change. In the last few decades, metal forming approaches have experienced significant developments due to improved methodologies. Bulk metal forming and sheet metal forming are two typical groups of forming processes based on different metal shapes as indicated in Table 2-1. Bulk metal forming is characterized by substantial changes of cross sections, wall thickness or height under pressure or temperature changes during deformation. While in sheet metal forming the metal with a high surface area to volume ratio is modified in geometry with almost uniform wall thickness. In most circumstances the

wall thickness is not changed significantly, otherwise, in some cases extreme thinning may cause a process ductile failure named localized neck generating stress concentration [7]. In general, the permissible range of forming deformation depends to a large extent on the metallurgical and mechanical properties of the materials, especially the stress-strain elastic-plastic relationship.

Table 2-1 Differences between bulk and sheet metal forming [8]

Category	Characteristics	Examples
Bulk Metal Forming	Small surface-to-volume ratio Large amount deformation	Forging, extrusion, rolling
Sheet Metal Forming	Large surface-to-volume ratio of the initial workpiece Small change in the thickness	Deep drawing, bending, multi-point forming

2.2.1 Sheet metal forming and applications

Traditional sheet metal forming has experienced tremendous development beginning in the last third of the 19th century along with the prosperity of automobile industry as well as aircraft industry [9]. Products of automobile bodies, airplane wings, sinks and cooking pots are all from different types of sheet forming, showing great strength-to-weight ratio with high elastic modulus and high yield strength [10]. Low-carbon steel, aluminium or titanium are common sheet materials and these sheet plates need to be cut first before forming to different shapes. In general sheet metal forming includes bending, rolling forming, spinning, stretch forming and deep drawing, etc [9].

Bending

Bending is most widely applied in sheet metal forming in which a piece of sheet metal is to be bent at an angle to form the desired shape within a prescribed force. It was first investigated by Ludwik with assumptions to regulate the process involving relationship between width and thickness and material properties [10] [11], and a bend could be characterized by several parameters, such as bend line, bend axis, bend angle and outside mould line, etc. Mostly a simple bending operation only deforms along one axis, but a multitude of operations can be performed to create complex parts.

Both tension and compression exist in a bending operation where the outside part of the sheet undergoes tension by increasing the length, while the shortening of the inner length results compression [12]. But the length of neutral axis remains almost unchanged because it is the boundary line in the middle of thickness without any tension or compression. For a pure elastic bending the sheet will return to the original shape when releasing the bending movement. But for an elastic-plastic material, permanent deformation results and residual stresses in the material will generate slight springback after unloading. Most times over-bending is necessary for this elastic recovery compensation to achieve the desired shape to a precise amount, resulting in a greater bending radius and smaller bending angle than initially formed [13] [14].

Today numerical control bending is widely used and produces products from mass produced small workpieces, such as brackets, to the fabrication of up to 6 metres in length products such as a chassis [15] [16]. With the help of other forming processes, some complex parts such as pipes and wires can be produced with high volume using different materials.

11

Roll forming

Roll forming is defined as progressive forming of sheet metal through a series of bending operations along the roll forming line under contoured rolls on both sides of the sheet while maintaining the same material thickness at room temperature [17]. Desired surfaces can be achieved through plastic deformation forced by rollers. The roll forming line is also referred as the mill, which connects the tooling system to the blank. In general, cantilevered mill, duplex mill, through-shaft duplex mill, standard mill and rafted mill are most common mill types in industry according to the positions and arrangements of the roll stations [9]. With the help of the finite element method, the strain distributions of a sheet with a variety of cross section profiles can be obtained, where the profiles can be either open or closed tube-like shapes [18] [19] [20].

Roll forming has developed significantly during the past 50 years, with literature showing that it accounted for around 30 percent of flat steel products from North American steel mills [21]. Long continuous body structure parts with constant cross section in the automotive industry are produced using roll forming providing low cost and high volume, examples are bumpers, frame rails and roof bows [22].

Spinning

During a spinning process, cylindrical and other products are formed from a piece of sheet metal by applying force on one side. Traditional spinning can be regarded as a tension – compression forming processes because in the deformation zone both tangential compressive and radial tensile stresses exist. A general spinning system consists of spindle, mandrel, clamp, head and tail stock and roller tool, located on a manual or CNC lathe. During spinning the mandrel and the blank are securely clamped between the head and tail stock for high speed rotation, then a force can be

applied by the roller to make the blank bend [23] [24]. Here the mandrel has the solid form of the internal shape of the part to be pressed, but for some complex shapes a multi-piece mandrel may be used, which is similar to the deep drawing process. Conventional spinning and shear spinning are two distinct spinning methods, depending the action of the roller to the blank together with the mandrel [25]. The spun part can achieve a smaller diameter of the blank and constant thickness under conventional spinning, while shear spinning is able to obtain an equal outer diameter but reduced thickness.

Shape parts of almost any shapes with rotational symmetry can be produced through spinning process, and for special requirements, elliptical components and bulges are possible as well [26]. In industry hollow shape parts like cylinder, cone and hemisphere are common, which include cookware, musical instruments, aircraft nose cones, etc [27].

Stretch forming

Stretch forming is a tensile metal forming process in which a piece of sheet metal is stretched and bent simultaneously over the tool in order to form large contour parts under the applied tensile force in the direction of the workpiece axis. The piece of sheet is securely gripped along its edges and pulled towards the form die by pneumatic or hydraulic forces, usually in vertical direction [28]. Stretch forming process can be divided into simple stretch forming and tangential stretch forming, depending on the relative position between the sheet blank and the desired contour punch [10]. In simple stretch forming the sheet blank is gripped by rotatable grippers and deformed directly by moving the desired contoured punch. This always makes the sheet metal deform first from the position around which contacts the top of the punch, as the punch moves continuously, the sheet blank can reach the final desired shape of the punch [9] [29]. While in tangential stretch forming it is separated to two distinct stages. At first the sheet blank

13

is stretched up to the yield point to obtain uniform strains, but for the sheets without uniform properties, strains of some parts may exceed the yield strain of the material, normally 2-4% [9] [30]. Then the stretched blank contacts tangentially to the contour of the former without any relative motion during the whole process.

Stretch forming products are always large and vary from a simple curved surface to complex non-uniform cross section areas and always possess large radius bend over the entire extent of the parts. High accuracy and smooth surface finish are typical advantages, especially for ductile materials, which show crucial potential in aircraft and automobile industries [31]. Panel parts such as doors, roofs, vehicle body panels and wing panels are most popular stretch formed parts.

Deep drawing

Deep drawing is a metal forming process in which sheet metal is stretched into the desired hollow part shape of a die cavity under the push force of the punch, maintaining almost the same thickness of the original material sheet. Usually a deep drawing system consists of a blank, blank holder, punch and die. During the process, the blank is clamped by the blank holder over the die and forced down by the hydraulically powered punch [32] [33]. Lubrication can be used to reduce wear between the punch and the blank by improving the material flow. It should be noticed that since the mean normal stress during deep drawing is tensile, the maximum possible strains allowed in a single draw may be limited by the material formability [9] [34] [35]. So many successive draws can be carried out to reach the desired shape within the formability limit.

Most deep drawn parts have a depth more than half of the diameter of the part with a variety of cross sections. Shape and dimensional errors, defects in the workpiece or in the surface, unsatisfactory material properties are

three main aspects of failure modes, which should be carefully avoided [9] [36]. With the help of numerical methods, especially finite element simulation, defects and stress distribution can be improved at the initial design stage, leading to significant economic and technical gains [37]. Ductile metals perform most effectively in the deep drawing process and typical products include automotive bodies, fuel tanks, kitchen sinks, cans and pots, etc [38].

Other sheet forming processes

Other sheet metal forming processes include single-point incremental forming, hydroforming, magnetic-pulse forming, multi-point forming, etc. The review on some of those processes is presented in Section 2.2.3 where the processes for the forming of panel components are particularly reviewed. Laser forming is another category of the forming techniques which now becomes more important for improving process capability and extending forming limits in sheet metal forming. Also most of the above named processes can incorporate laser-beam heating as an assisting means for sheet metal forming [39] [40] [41].

2.2.2 Material and property characterisation

2.2.2.1 Material property characterisation

A comprehensive understanding of sheet material behaviour is important to ensure a satisfactory industrial production flow. Depending on different forming operations, material properties required the special design test procedures will vary according to formability as well as suitability. For commonly used steel and nonferrous metals such as aluminium, magnesium, titanium and their alloys, etc, most material properties can be obtained from tensile tests so that unsuitable materials can be sorted out

under different sheet forming processes as mentioned above. The characteristics for sheet metals to be known in advance are generally yield strength, elongation, strain-hardening exponent and anisotropy, etc, the details of which are given in Table 2-2.

Table 2-2 Sheet metal characteristics

Characteriatic	Importance
Yield strength	Determines the stress that a material can withstand without any permanent deformation, i.e. plastic deformation (normally takes the value of 0.2% permanent deformation of the original dimension)
Elongation	Describes the capability of the sheet metal to stretch without failure, can be a reference of material deformation shape
Strain-Hardening Exponent	Measures the achievable maximum formability for different materials under the same restraints, normally a harder metal may have a higher resistance to plastic deformation
Anisotropy (planar)	Exhibits different behaviour with relative planar directions during plastic deformation, especially for rolled sheets
Anisotropy (normal)	Referred to as the ratio between width-strain and thickness-strain. Determines the thinning behaviour of sheet metals, important in deep drawing and stretch forming process

The above basic parameters measure the formability of sheet metals to undergo the desired shape change without any failure. In order to show the levels of formability, the forming limit diagram/curve (FLD/FLC) is introduced. Sheet metal is marked with small circles, and stretched over a punch and deformation is observed in failure areas [42] [43]. FLD/FLC shows the boundary between safe and failure zones through a plotted curve of major strain along with minor strain at the critical necked or fractured position of the sheet metal. In order to construct the diagram, it is reported in literature that experiments were conducted by using a hemispherical punch and rectangular or circular blanks [38] [44] [45]. Originally the FLD/FLC curve was only valid for determination of forming limits under proportional loading with some specific speeds, later research focused on different loading paths, and higher speeds and strain paths were investigated and details will be proposed in Section 2.3.3.1 [46] [47] [48].

Residual stresses, springback and wrinkling are all characteristics to measure the limit of forming range. For the deep drawing process, the drawing ratio measures the drawing boundary by determining the ratio of the maximum possible blank dimension to the dimension of the drawn part. Springback is a measurement of the elastic recovery of the sheet metal after unloading. For the determination of a more complete assessment, some direct methods, such as the folding test for bending, Ericksen test, hydraulic bulge test and Swift cup test for a stretch forming process, Sachs wedge test and Fukui conical cup test for a deep drawing process have been used [38] [49] [50] [51] [52]. Many testing methods have been proposed to predict the parameters of a material sheet for different processes, but it should be noticed that the results are not all completely accurate if one simple test method is used. So usually the formability performance should be predicted and tested using different forming tests [9]. After evaluating the formability parameters, design of the final shape is also an important consideration, since in some circumstances the material formability may not be capable of obtaining the desired formed shape.

2.2.2.2 Aluminium alloys

Aluminium and its alloys are widely used in fields of automotive, aerospace, transportation, petrochemical engineering and many other industries, due to the advantages of excellent physical and mechanical properties such as low density, good corrosion resistance and high strength to weight ratio [6] [53]. Compared with cast alloys, wrought alloys are good for press working and it is identified with a four digit number based on different alloying elements. According to the alloy phase equilibrium diagram and heat treatment characteristics, aluminium alloys can be classified as heat treatable alloys (2XXX, 6XXX, 7XXX) and non-heat treatable alloys (1XXX, 3XXX, 4XXX, 5XXX) [54]. Typically the heat treatable alloys are high strength which are widely used in automotive, naval architecture and aerospace applications [53] [55] [56]. For non-heat treatable alloys, they often exhibit low to medium strength with good corrosion resistance and are often used as welding parts due to good weldability [57] [58].

Although an enhanced formability of high strength aluminium alloys can be achieved at an elevated temperature (usually above 300°C), the desirable micro-structures are destroyed and softening occurs. Heat treatment is important to restore these micro-structures and improve their mechanical properties while maintaining the same shape and size [59]. It is basically a heating-heat preservation-cooling process where material phase transition occurs. Annealing, solution heat treatment and aging are commonly used heat treatment methods in industry for heat treatable alloys. After annealing the heterogeneity of chemical composition is removed so that the plasticity is enhanced. Solution heat treatment can contribute to an unstable supersaturated solid solution (SSSS) which can cause thermal distortion and it therefore must come with a rapid quenching to obtain the optimal mechanical properties by freezing the supersaturated solid solution (SSSS) [60]. Then the alloys can be significantly strengthened and

18

hardened. Aging is a heat treatment method where the supersaturated solid solution (SSSS) is kept from being decomposed at a certain temperature for a certain time. Natural aging occurs at room temperature while a faster artificial aging is conducted above room temperature. 2XXX, 6XXX and 7XXX aluminium alloys are often in a heat treated (T) condition, such as T4 and T6 [61] [62]. Non-heat treated aluminium alloys are normally cold formed in annealed (O), as fabricated (F) or strain hardened (H) condition [54]. In this thesis the formability of AA6082-T6 is studied.

2.2.3 Forming of aluminium alloy panel components

To meet the industrial requirements of forming panel components with complex shapes, various forming techniques have been proposed and tested. Extensive research has been conducted on improving the formability and surface finish of high strength materials, including well developed techniques and state of the art testing methods. In this section groups of forming techniques for aluminium alloys are reviewed.

Hydroforming

Sheet hydroforming is originally based on a patent granted in 1955 and now it is a preferred method that uses pressurized hydraulic fluid to provide the shaping force to improve the material flow and formability of aluminium alloy sheets [63] [64]. Significant advantages of this process are friction reduction at the flange due to the fluid lubricant and surface defects reduction due to the liquid pressure medium [6] [65] [66]. Additionally, a reduction of the tooling cost can be achieved by requiring only one punch [67]. However, the cycle time for manufacturing automotive components is slow and sometimes the press cannot provide sufficient forming loads, leading to a high manufacturing cost [67] [68].

At room temperature hydrodynamic deep drawing is a typical hydroforming process where oil or another liquid pressure medium is used to improve the drawing ratio by pressing the material onto the punch for complex and large components [69] [70]. The Amino process is another form of hydroforming which includes a punch, a water chamber and a process control system, where water-based fluid is employed for deeper draws by delaying failure [67]. Since high strength aluminium alloys exhibit poor formability at room temperature but increased ductility at an elevated temperature, elevated hydroforming techniques on complex shapes have become popular [71]. To overcome the die-set limitation that the sheet cannot be heated separately and transferred to the die, researchers heated the sheet and the die at the same time using an external furnace or heating bands [6] [72] [73]. Oil and gas are popular pressurising mediums whose working temperature ranges determine the required pressure of the forming process [74]. Blank holder and liquid pressure should be carefully considered and designed to avoid flange wrinkling and tearing, especially for high strength aluminium alloys [75].

Incremental forming

For small batch sizes or prototype sheet metal part production, the high cost and lead times issue in conventional sheet forming processes can be eliminated or reduced by using incremental sheet metal forming. This is classified as either a die-less process (SPIF, single point incremental forming) or with a back support die [76]. The process is generally comprised of tool path generation using CAD geometry, generation of CNC code and then using a CNC milling machine to form 3D components [77]. During this process a conventional CNC machine is used instead of a hydraulic press and design of the tool path change is easy through the CNC programming without any dies. Another merit can be the small forming load. Research has shown that optimisation of process parameters, such as tool shape, tool size and feed rate, is very critical in forming an

accurate shape [78] [79]. However poor production efficiency, thinning of the formed sheets and geometry springback limit the process development and need to be improved [6] [80].

A straight groove test is efficient for assessing the formability in the incremental forming [81]. Fratini et.al. studied the formability of materials with different mechanical properties in 2004 [82]. Several researchers have conducted experiments to characterise the formability of AA1050-O [83] [84]. For high strength alloys, a hot incremental forming works well for improving the formability by using a heating device such as hot air blowers, laser-based heating, electrically-assisted heating, and conduction heaters [6] [85] [86] [87] [88].

Stamping

Stamping is a commonly used forming technique using rigid dies to manufacture sheet parts with net shapes. Cold stamping and hot stamping are two main approaches depending on the temperature applied to the materials to be formed. Cold stamping is a good option for annealed components with comparatively high formability through intense pressure below the materials' recrystallization temperature. After cold stamping the material strength can be heightened by solution heat treatment, low temperature storage, cold sizing and aging [89]. Artificial aging can help to correct the springback and distortion caused by the above heat treatments. Cryogenic treatment can be employed to reduce the residual stress and discontinuous deformation at cryogenic temperatures (usually below -196°C), when the strength and ductility of aluminium alloys will be increased [90]. Research has shown that for AA5XXX the Portevin-LeChatelier (PLC) effect, which is a thermal-strain rate dependent phenomenon, can be minimized and for AA6XXX the yield stress and ultimate tensile stress can be greatly increased [91] [92]. In general, cold stamping is faster and cheaper than hot stamping. But for high strength

aluminium alloys with very poor ductility and formability at room temperature, hot stamping is a useful technology because the reduced flow resistance increases the formability and the high tensile strength resistance reduces springback especially for parts with complex shapes [93].

Hot stamping is normally a heating-forming-quenching process to increase the material tensile strength and it is classified as a direct or indirect method depending on when the forming stage happens. The schematic illustration is shown in Figure 2-1. In the direct hot stamping process the flat sheet is heated and preserved in the furnace for a while before transfer to the forming and quenching tool. However, in the indirect hot stamping process the part is pre-formed to the nearly complete shape before being heated, so only quenching and calibration operation are necessary in the press after austenitisation [94] [95]. Heating the sheets to the solution heat treatment temperature of the aluminium alloys is important for the process accuracy and cost efficiency of hot stamping. To fulfil the requirements of a short heating time and homogeneous blank temperature, induction heating and conduction heating are commonly used in industry with good energy efficiency [96] [89] [97]. The transfer between heating and forming stages must be as quick as possible to avoid cooling of the sheets. The temperature range for effective forming should be tested and studied. After forming the formed parts are normally quenched between the cold dies to a lower temperature. A subsequent aging procedure maybe required for a higher strength. The cooling of the dies should be carefully considered [98].
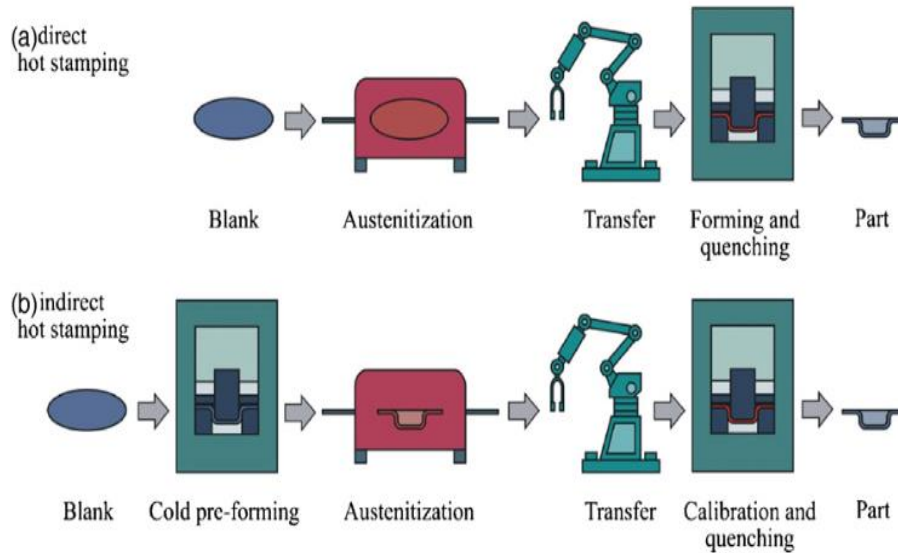
Figure 2-1 Schematic illustration of hot stamping: (a) direct and (b) indirect [94]

In a traditional hot stamping process multi-steps are employed because heat treatment is usually carried out separately after hot stamping to form shell parts, therefore the blank must be heated many times due to the fast heat loss and temperature drop in each stage [60] [93]. Thus, Lin et. al. first proposed an integrated hot stamping-quenching process of high strength aluminium alloys which is called solution Heat treatment, cold-die Forming and Quenching (HFQ) [99]. In HFQ the heat treatment is replaced with die quenching, therefore forming and quenching are combined together in one operation with the cold dies remaining closed, this can guarantee shape accuracy and improve productivity [100]. During the process the blank sheet is initially heated to the solution heat treatment (SHT) temperature and kept for a period to enable the precipitates to be dissolved within the primary α-Al matrix. After this the heated sheet with reduced yield stress is quickly transferred to the cold die to be stamped and further quenched in the closed die to almost room temperature to eliminate springback, with a subsequent artificial aging process followed for heat treatable aluminium alloys to achieve higher strength [101] [6]. A schematic temperature profile diagram is shown in Figure 2-2. By

23

employing different process parameters and strengthening mechanisms, mass production of complex shaped parts of high strength in automotive and aerospace fields can be realized at a low cost. Recently, formability investigations of HFQ process have been conducted on non-heat treatable aluminium alloy 5754 [102], heat treatable aluminium alloy 2024 [103], 6082 [104] [105] and 7075 [100], all show good formability and shape accuracy for complex components.
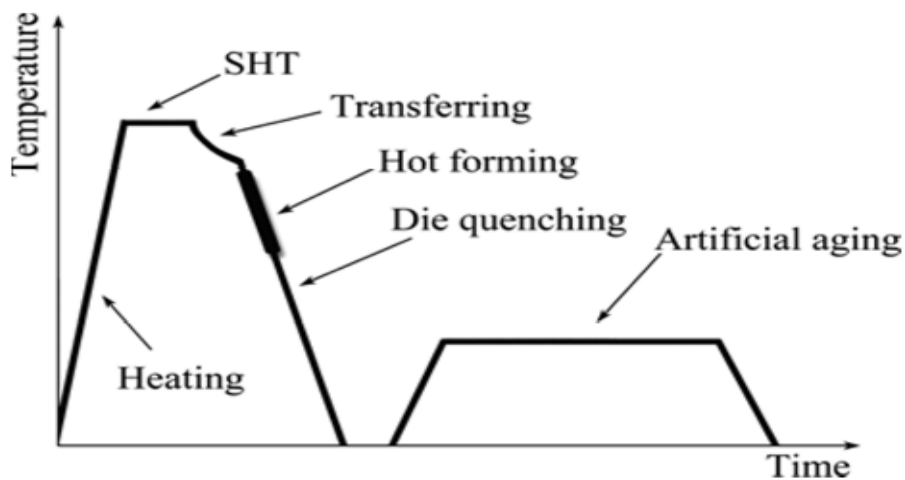
Figure 2-2 Schematic temperature profile of HFQ [106]

Based on the HFQ process, further research has been conducted to address critical issues. Fan et al. proposed a hot forming-quenching integrated process by using warm dies instead of cold dies to reduce the heat loss during the period of transferring and locating the sheet from the furnace to the forming-dies and studied the effects of different die temperatures on the 6A02 aluminium alloy blank strengthening behaviour [60]. In this study the temperature of the forming-dies can be controlled and, after forming, the blank was air cooled to room temperature. Later Yuan and Fan et al. changed previous warm dies to cold-hot dies so that both the heat loss can be improved and quenching process can be employed [107]. In this research the strengthening behaviour and mechanism of 2A12

aluminium alloy were studied by heating the lower die via resistance heating and cooling the upper die by flowing water at 10 °C. Another novel hot stamping process to form high strength aluminium alloy components was proposed by Maeno et al., where quick heating was employed before forming to enable the removal of the solution treatment found in HFQ only for T4 aluminium alloys [89]. In this process solution heat treatment (SHT) temperature (475-520°C) can be applied especially for 2XXX aluminium alloys, while fracture may occur above 450 °C in HFQ. Successful production of high strength aluminium alloy aircraft parts with good dimensional accuracy was achieved.

2.3 Multi-point forming (MPF)

2.3.1 Basic process and tool configurations

Multi-point forming (MPF) is an advanced manufacturing technique for three-dimensional curved surface sheet parts forming without any solid die, featuring short production preparation periods, low manufacturing costs, good panel quality, flexible blank size, sustainable material recycling and good working conditions [3]. The main idea of MPF is using pairs of matrices of elements as flexible dies instead of pre-shaped solid dies used in conventional sheet forming processes. Each of the matrices is movable independently along the ram direction to produce target shapes according to CAD on CNC machine, as shown in Figure 2-3 [108]. By using MPF development time and manufacturing costs of solid dies can be reduced, which is very effective for single or small batch production. Each failed individual pin can be changed separately without changing the whole die. There is a point surface contact between the pins and the formed blank, thus the shape of the pin heads should be carefully considered for surface smoothness. In literature the packed pin heads can be various shapes such as square, hexagonal, triangular or octagonal and square, and the longitudinal movement of each pin is controlled by servo motors, which,

25

however, makes the shape profile not smooth [109] [110] [111]. At present the matrices elements always have dome-like shape heads with hexagonal cross-section shoulders so that the pins can be packed as tightly as possible, only with very little clearance, to avoid straight lines, angles and further defects, as shown in Figure 2-4. The spherical-tipped heads allow tangential contacts with the formed blanks to avoid piercing by sharp edges [110].
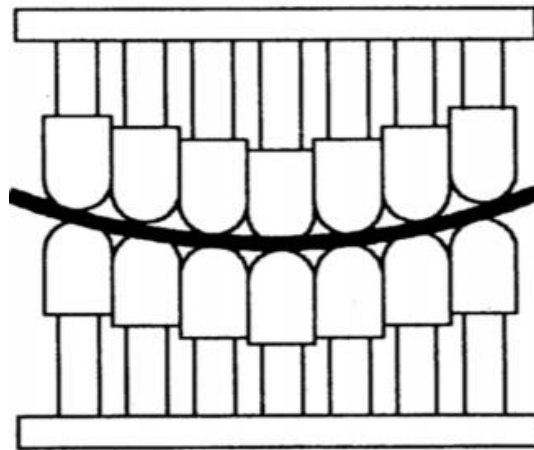
Figure 2-3 Schematic illustration of multi-point forming [2]
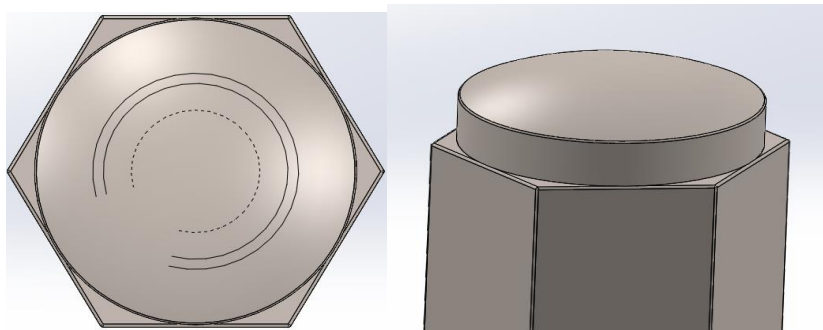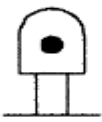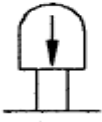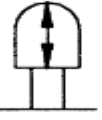
Figure 2-4 Top and side view of a pin with dome-like head and hexagonal shoulder

Two sets of pins can be adjusted through lead screws or hydraulic pressure, manually or automatically [112] [113]. From literature, three ways of adjustment of pins can be conducted depending on the punch positions during the forming [2]. The first is relative fixation where the pins are all moved to the pre-set heights in advance and maintain the same position all the time. In the second way only the upper site pins are controlled and moved to the desired position before forming, while the opposed pins can be moved freely and pressed passively until the final shape is formed. For the last way, all the pins can be adjusted freely during the whole process to the proper shape since the pins are not pre-set and relative movement among pins can be observed. An illustration of these three types of punches was given by Li et. al. in Table 2-3. Four types of MPF are given based on above punches: multi-point die forming, multi-point half die forming, multi-point press forming and multi-point half press forming [2]. Li et.al. proposed a series of equations to calculate the position in height direction (usually z value) of the hemispheric end centre for each pin based on the desired shape, through the definition of two isometric surfaces [114]. The sketch is shown in Figure 2-5, from which S(u,v) represents the target surface of the final shape and r_p is the radius of the spherical surface.

Table 2-3 Adjustment types of pins [2]

Type	Mark	Adjusting method	Controlling force
Fixed		Before forming	Small
Passive		Be made to move in process	None
Active		Freely controlled in process	Large
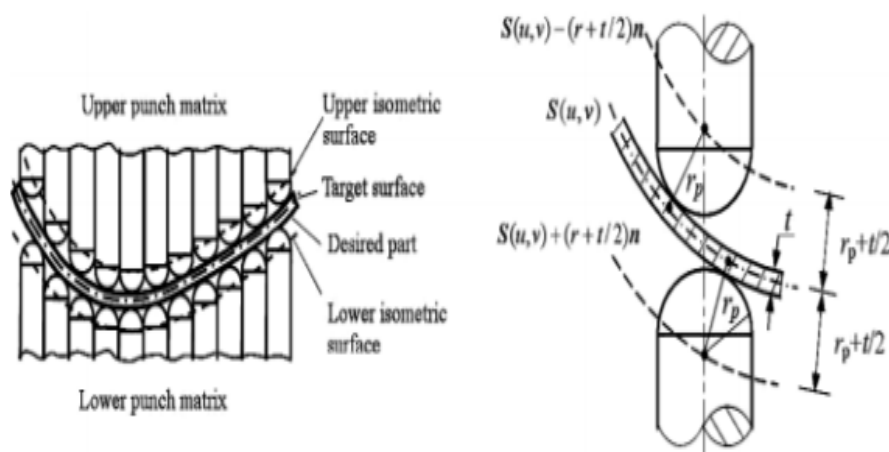
Figure 2-5 Sketch of target surface and isometric surface [114]

High strength steel is a commonly used material for pins, but some new ideas were proposed recently. Zhang et. al. and Elghawail et. al. used polyurethane rubber upper punch instead of the original metal pins to achieve high forming flexibility in which a decrease of wrinkling and springback was proved [115] [116]. Besides the pin shapes, pin size is another important factor. Wang et. al. studied the influence of pin size on surface finish numerically and found that dimples can be reduced with smaller pins [117]. However, the balance between pin size and pin density should be carefully considered due to cost control and pin strength.

2.3.2 Development history and applications

The idea of reconfigurable dies was first presented by Nakajima [1] in 1969, using a die with height adjustable wires on a numerical control milling machine. Following this concept, Nishioka improved this by introducing a universal press with two sets of multiple piston heads in the vertical upper and lower direction, giving a discussion on the surface quality of large sheets of metal, based on local heating methods [118]. Since 1990, reconfigurable discrete dies for sheet metal forming were developed by

28

Hardt and co-workers, where these dies were configured to desired forming surfaces under the control of a numerical machine [119] [120]. At the same time, the concept of 'multi-point forming' was first presented in 1992, and the first automated system using MPF based on repeated forming principles was proposed in 1999 [121] [122]. Together with the rapid development of software simulation, the finite element method was widely used in analysing the stress and strain change during the forming period to improve friction conditions and forming path [123] [124]. The influences of material property, blank thickness, cushion hardness and anisotropy to springback in MPF have been widely investigated and relationships have been given [125] [126] [127].

Later research focused on specific forming process has been investigated with rather good accuracy, such as multi-point sandwich forming, multi-point deep drawing forming, multi-point stretch forming, multi-point forming for rotary surfaces, cyclic multi-point incremental forming and even micro multi-point sheet forming, etc, to extend the range of applications [115] [128] [129] [130] [131] [132]. Le Li and co-workers studied the multi-step multi-point forming technology and found that springback can be reduced if a small deformation was applied at each step for the same final surface [133]. For large size parts, sectional multi-point forming (SMPF) is introduced, with a transitional region defined between the deformed region and undeformed region as shown in Figure 2-6 [3] [134]. This technique makes a small press possible for forming large parts and it is realized by three methods: overlap region method, assortative region method and multi-pass forming method [134] [135].

Nowadays sheet products with small or large areas from MPF are widely used in a number of commercial fields, especially for body panels of automobiles, high speed trains and aircraft. What's more, some crankle-shaped parts in architecture, skull implants in medical engineering and

29

sculpture shells in art all proved the superiority of multi-point forming technology, examples are shown in Figure 2-7 [114].
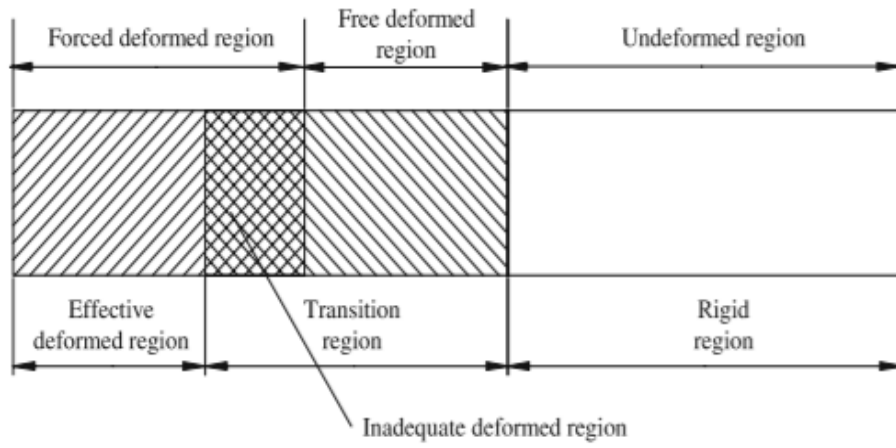
Figure 2-6 Illustration of regions in SMPF [134]
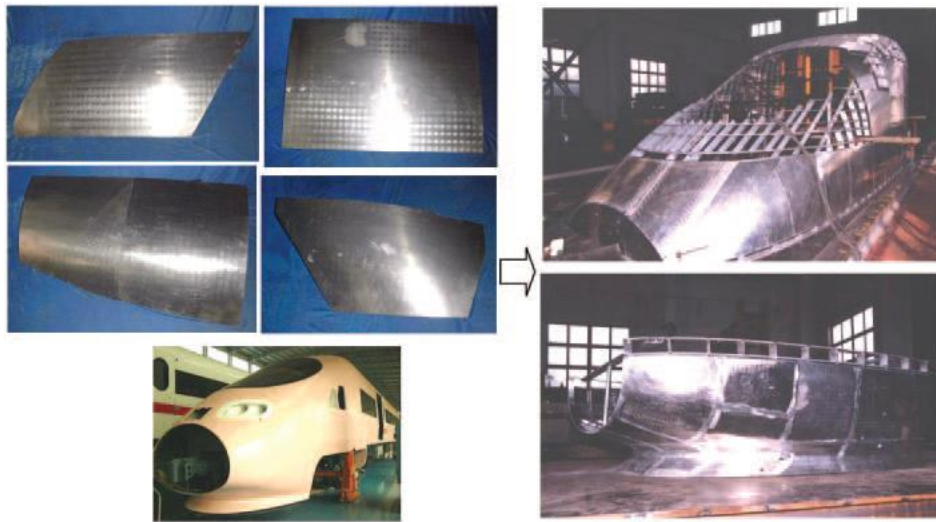
(a)
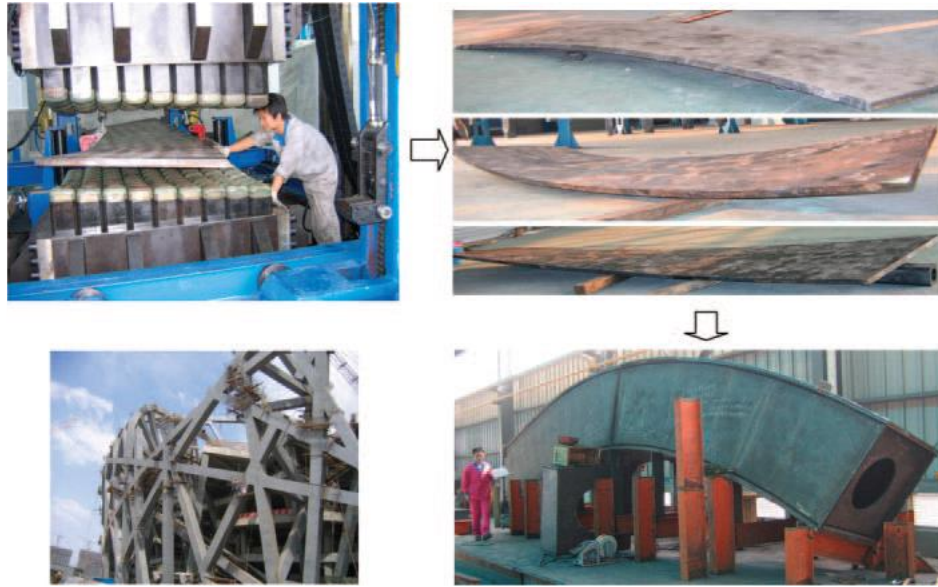
(b)

Figure 2-7 Practical sheet products using MPF method: (a) train body and (b) crankle-shaped parts [114]

2.3.3 Common defects in MPF

In the sheet metal industry, more and more products bear increasing pressure during the process due to special shape requirements or material properties, so how to avoid part defects becomes a major issue. Apart from the defects associated with traditional sheet metal forming processes such as cracking, necking and thinning, additionally surface dimples, wrinkles and unloading springback are the main issues affecting the quality of the metal sheets in multi-point forming due to the discrete dies [136] [137] [138].

2.3.3.1 Cracking, necking and thinning

Localized necking normally results from too much stretching while wrinkling is always from compressive stresses. In general, localized

31

necking can be found by comparing the principle in-plane strain components with a forming limit diagram/curve (FLD/FLC) as introduced by Keeler and Goodwin for linear strain-based paths. However sometimes excessive thinning of the sheet can happen even though the strain is in the safe region, especially in equi-biaxial stretching [42] [43]. Since there is not enough accuracy when complex non-linear strain path changes or non-proportional loading are implemented, the Marciniak and Kuczynski (MK) model was proposed to help make the measurement of the strain forming limit diagram easier, by assuming that the sheet metal has a region of local imperfection where heterogenous plastic flow can develop and localize [139]. Following the development of this concept, a comprehensive failure analysis in a biaxial sheet tension test was introduced and this model was extended to predict not only the major and minor strains, but also the stress limit directly [140]. After several experiments studying the influences of the non-linear strain path under the frame of MK model, Hill described the theory in 1979 for two stage deformation paths [141].

For trial and error investigations, many numerical simulations have been studied to predict FLD/FLSD to investigate the formability of sheet metal parts [142] [143] [144]. The concept of FLD can be classified as forming limit curve at necking (FLCN) and forming limit curve at fracture (FLCF), depending on focus on the onset of necking or fracture [145]. During this period besides FLD/FLSD, other methods were tried to describe the stress state during necking as well, such as the Bridgeman model by Yang and the Variable Binder Force (VBF) trajectory introduced by Cao and Boyce [146] [147].

2.3.3.2 Dimpling

In multi-point forming, dimples occur from stress concentration due to the local discontinuous contacts between the adjustable pins and the formed blanks. Liu et. al. introduced two common forms of dimples, which are

surface dimples and enveloping dimples as shown in Figure 2-8 [148]. Surface dimples are the result of localized plastic deformation in the contact area with large thickness variations, in this condition the upper and lower pins are pressing each other. While enveloping dimple is more like local drawing and the local shape of the blank surface is similar to that of the pin head. The local state of dimples from experiments is given in Figure 2-9. Since the excessive forming force is the main issue contributing to severe dimples, it is necessary to distribute these localized loads [138]. Use of solid elastic cushions in MPF was proved to be effective in reducing dimples through experimental research as well as numerical optimisation [149] [108]. The elastic interpolating layers are placed between formed sheets and dies. A polyurethane pad is a popular option as it exhibits good oil attack resistance as well as wear resistance considering the thickness and the compressive modulus [150]. In addition, the local stress can be reduced by using pins with larger size, but the size may be restricted by the target shape of formed blank. Another alternative method is to design the multi-point deformation path with several intermediate stages until the final shape so that the curves can increase gradually [3] [123].

(a)   (b)
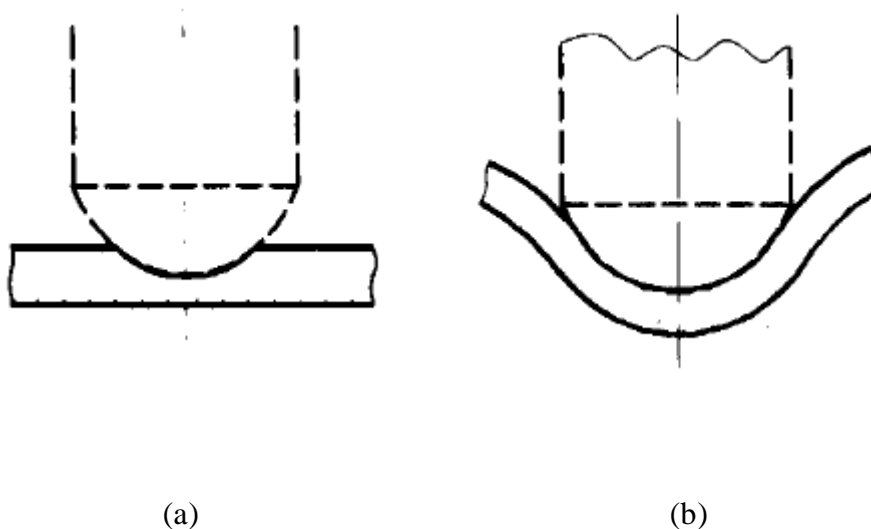
Figure 2-8 Two forms of dimple in MPF: (a) surface dimple and (b) envelope dimple [148]

33
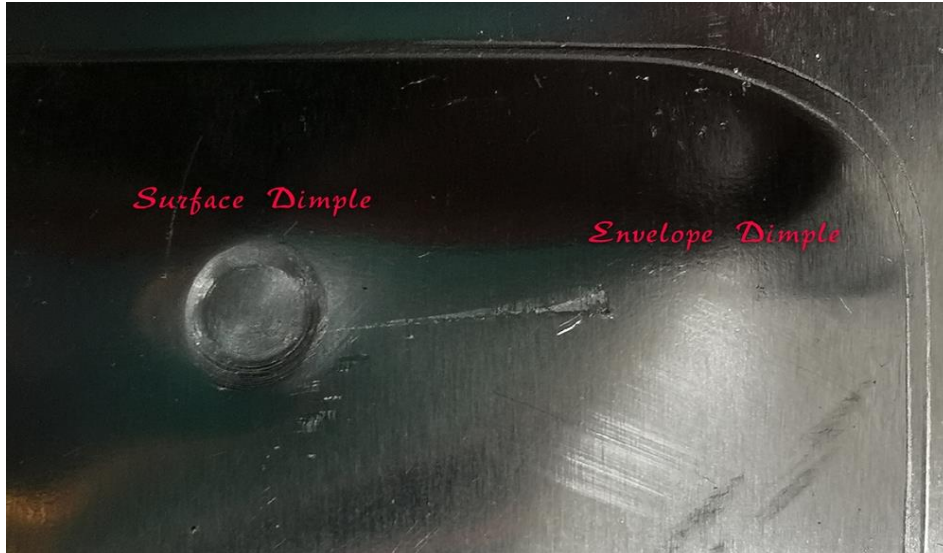
Figure 2-9 Dimples in MPF experiment

2.3.3.3 Wrinkling

Wrinkling is one important failure mode in sheet metal forming due to excessively local compressive stresses that limit the assembly and function of sheet metal components, and this is particularly unacceptable when the surface flatness is crucial. For multi-point forming, wrinkles show new features due to different contact conditions and it is necessary to control the restraining force generated by blank holders and draw-beads. The prediction and prevention methods of wrinkling are generally divided into an analytical approach and FEM numerical simulation. In the past analytical work provided a view to examine the general tendency and the effect of individual parameters on the wrinkles, but mostly it is only limited to simple loading processes such as a column under the axial loading, circular ring under inward tension, annular plate under bending with a conical punch at the centre, etc [151]. Later numerical simulation using the finite element method (FEM) became a prime tool due to its reliability and accuracy without any costly trials, although some results of the FEM code simulation are quite sensitive to details of analysis as well as simplifications of loading conditions.

Wrinkles during multi-point forming can be improved or eliminated by employing a blank holder with lubricant to bind the blank with an in-plane tensile stress especially for complex shapes such as automotive panels [3]. As a smooth and continuous transition surface of the formed sheet between the workpiece and the blank holder is important for wrinkle elimination, Peng et. al. presented two surface design methods, i.e. flexible surface extension and bridge surface extension, to design a high quality blending surface [152]. On the basis of 'ideal forming' introduced by Richmond and co-workers, an optimal forming path technique is proposed by Cai and Li based on minimum plastic work paths [153] [154]. In their work they gave interpolating formulations for an 18 degrees of freedom triangular element for generating a specific forming surface and utilize a real-time control system to avoid wrinkling [154]. Further they proposed a positive definite function and solved the variation problems using FEM to describe the forming path, whose applicability was proved by typical examples [123].

2.3.3.4 Springback

Unloading springback occurs with the removal of the forming force in MPF due to the uneven deformation over thickness and it affects the final shape accuracy significantly [2]. Springback is a phenomenon of elastic recovery and investigations on the influencing factors and elimination methods become necessary. In MPF tiny adjustments of the movable pins can help reduce or eliminate the springback [133]. Alternatively, over-forming can be employed by adding the springback to the desired shape together with repeat forming until the final shape is obtained [155].

Li et. al. first numerically studied the effects of influencing factors (thickness, deformation amount and material properties) on the springback tendency, and then employed multi-step multi-point forming to reduce the springback economically and conveniently [133]. Later the assessed influencing factors of springback in multi-point processes were further

extended to process parameters such as elastic layer thickness, elastic layer hardness and number of punch elements and both experimental tests and numerical simulation were conducted [126]. Zhang et. al. proposed a springback compensation algorithm for doubly curved plate in MPF, using an elastic-perfectly plastic biaxial model to calculate the springback amount in advance and the effectiveness was validated by experiments and simulation [156].

2.4   Sheet metal forming limits and finite element analysis (FEA)

2.4.1 The finite element method

2.4.1.1 Introduction

As the need for MPF has increased in industry, many simulations of the process have been proposed to study the forming capability and defects with the help of the finite element method to provide acceptable die shape design of smooth surfaces [114] [157]. The use of computer-aided engineering (CAE), design (CAD) and manufacturing (CAM) facilitated significant developments in the metal forming industry in the last decades. These computer-aided technologies make it easy to study the requirements for design, control and deformation mechanics of the parameters mentioned above in an economic and accurate way. Among them, simulation of process modelling gives a comprehensive understanding of strain and stress distributions to improve the die performance, and the finite element method (FEM) became popular.

Beside FEM, from the mid of 20th century many mechanical analysis methods were used to study the process parameters with or without computer-aided technology. The slab method [158] [159], the slip-line field method [160], the visio-plasticity method [161], upper-bound

techniques [162], Hill's general method [163] and finite difference method (FDM) [164] are some popular examples. The development of these methods made great contributions to the analysis of forming loads, part geometry changes and metal flow quality during the processes [38]. But for further improvements, they all have had limitations for accurately determining detailed stress, strain, velocity fields and other parameters until the wide use of the finite element method (FEM).

The birth of FEM can be traced back to the 1940s when Courant obtained approximated solutions to the St. Venant torsion problem through a number of triangular elements [165]. After finite elements were first introduced to study the plane elasticity problems by Clough, numerous studies and applications using simulation codes have been made to a broad spectrum of problems including stretch forming, deep drawing, sheet metal stamping, etc, and it soon occupied an important position due to the continuing development of computer technology [166] [167] [168] [169]. This helped people to predict the performance of manufacturing tools with higher accuracy. Later rapid development of FEM was made when it was successfully extended to 3D simulations with elastoplastic properties [170].

2.4.1.2 Methods of analysis

In general engineering problems there are some basic unknowns or field variables which are the key factors for the entire structure prediction. These unknowns are infinite in a continuum. However, the FEM is applied to reduce these unknowns to a finite number by dividing the solution region into small parts and by expressing the unknowns in terms of assumed approximating functions within each part [171]. The basic concept of FEM is discretization and discrete representation of related velocity fields, where the domain of the formed part is discretized into a finite number of subdomains, called finite elements, each with a node inside with assigned values and related derivatives to a specific function.

With the help of the shape function in the global connected elements under boundary conditions, the function can be approximated locally within each element in terms of the initial assigned node values. Element selection is an important factor affecting the results of the formulations, where shell and continuum (solid) elements are normally used depending on different processes. Shell elements are a good choice for the deep drawing process since the bending radius is much larger than the sheet thickness, however, continuum elements perform better in thickness sensitive conditions such as blanking due to its capability of through thickness deformation simulation [172] [173]. Usually four approaches are used to construct the formation of the element equations, these are direct approach, the variational method, the method of weighted residuals and the energy balance approach. The types of basic formulation in FEM can be divided into dynamic explicit, static explicit and static implicit equations. For determination of accurate solutions, five methods were introduced based on different mathematical algorithms and relative movement speed, these are static explicit method, dynamic explicit method, static implicit incremental method, static implicit large step method and static implicit one-step method [174] [175]. The finite element method shows superiority in metal forming projects due to the flexible capability of obtaining a variety of accurate solutions, as well as simplified modifications to different loading conditions.

In recent years many divisions of FEM were made dealing with specific aspects, such as the Applied Element Method (AEM), Generalized finite element method, Mixed finite element method, Scaled boundary finite element method (SBFEM), Extended finite element method (XFEM) and meshfree methods, etc [176] [177]. These special packages greatly enhance the reliability and accuracy of problem analysis under complex conditions, such as fractures, thermal effects, micro-scales, etc [178] [179]. The industrial requirement of sheet metal forming was widely studied to enhance the analysis ability of industrial examples [180] [181]. These provide an important contribution at the initial design stage of a process to

confirm whether the design is acceptable or not. If not, stress concentration points can be checked to optimize the die geometry with improved working performance. At the moment, FEM is used as the analysis fundamental in almost every mechanical engineering discipline, especially in aeronautical, biomechanical, automotive and other structural industries [182] [183] [184].

2.4.1.3 Finite element analysis with Abaqus

Based on fundamental formulations many commercial software packages embedded with FEM were exploited for both academic and industrial use. ABAQUS, DEFORM, LS-DYNA are some typical general use FEM software with good analysis ability for sheet metal forming simulation, while PAMSTAMP, MTLFORM are some famous examples featuring sheet metal deformation simulation specifically. Among them ABAQUS shows a strong efficiency for solving a wide range of linear and non-linear processes under static, dynamic, thermal related and more conditions based on three sub-modules: ABAQUS/Standard, ABAQUS/Explicit and ABAQUS/CFD (computational fluid dynamics). ABAQUS/STANDARD is based on the traditional implicit integration scheme to analyse static problems and some quasi-static problems in an accurate and stable manner. However, for severe deformation with a large number of elements involved, the convergence of the solution is difficult to achieve due to the mesh distortion [185]. In these conditions ABAQUS/Explicit is a better choice since it requires less memory and computation time, especially for problems with many complex contacts and transient loads, but a stability check should be carefully made under general conditions [186] [187]. ABAQUS/CFD can provide advanced computational fluid dynamics capabilities, such as laminar and turbulent flows, natural convection, fluid and solid heat transfer problems. For most solid sheet metal forming processes, ABAQUS/Standard and ABAQUS/Explicit are the two main modules involved [188].

In ABAQUS, besides the processing of the finite element methods, pre-processing and post-processing are two other important stages to input to the product design and visualisation of the results. When using ABAQUS, some issues require attention. During the pre-processing stage, simplification of the model design is an important issue since it is based on a large number of elements. From the literature there are some problems where parameters in the normal direction do not play an important role, using a 2D model instead of a 3D model can save a lot of time and computation space with the same level of accuracy [189] [190]. In addition, when the model is large but the critical area is small, it is better to use different meshing schemes, with extensive elements in the critical part, to balance between efficiency and accuracy. Sometimes small and unconsidered features can be removed during the simulation or replaced by connection elements, such as beam elements or spring elements [191] [192]. Another issue is meshing schemes during the processing stage which dominates the accuracy and convergence of the results. The number of elements should be carefully considered according to the forming condition since a coarse mesh can result in a distorted prediction, while the computational cost is huge if an excessive fine mesh is applied. When referred to severe deformation, ABAQUS provides two remeshing criterion, which are Map-Solution (MP) and Arbitrary Lagrangian Eulerian adaptive mesh (ALE) respectively. ALE is more popular as it is partially automatic combining the features of the Lagrangian method as well as Eulerian methods [186]. But it has some limitations when dealing with large deformation problems.

2.4.2 FE-based damage criteria in sheet metal forming

For sheet metals, their responses to plastic deformation depend on many conditions, such as hardening, anisotropy and yield criteria. The forming limit diagram evaluates the sheet metal formability limits in terms of the minor and major strains as explained in Section 2.3.3.1. FLD are mostly

obtained through experiments in the past, leading to time and cost issues especially at elevated temperatures[193]. Following the development of modelling techniques, many theoretical and numerical models are implemented in the finite element commercial codes for the forming limit prediction. R. Zhang and co works reviewed numerous modelling techniques and indicated that most of them are developed based on bifurcation theory, geometrical imperfection theory and continuum damage mechanics [194]. An illustration of popular developed models in each category is shown in Figure 2-10.

Hill's and Swift's models are classic models following bifurcation theory to predict localized and diffused necking by assuming necking occurs when loading reaches the maximum value [195] [196]. Marciniak and Kuczynski (M-K) model is popular for FLD prediction based on geometrical imperfection theory by introducing a geometrical imperfection on the metal sheets before deformation [139]. When talking about continuum damage mechanics in sheet metal forming, ductile fracture criteria (DFC) can be employed as a supplement of FLD under non-linear plastic loading history to study when and where damage initiates and propagates. Coupled ductile fracture criteria incorporate incremental damage parameter into a relative basic constitutive equation, such as the GTN model and Johnson-Cook, but there are difficulties in embedding with FEM codes [197]. In uncoupled ductile fracture criteria where a damage parameter is proposed in an empirical way, close results have been made for some specific linear and non-linear materials [198] [199]. However, for other materials the lack of reliability and applicability limits DFC development in industry.

Beside the forming limit diagram, there are other damage criteria that can be used in modelling as a supplementary of FEM functions to predict the damage of sheet metal blanks. Since traditional FEM relies on the computational points of classical continuum mechanics (CCM), the spatial

41

derivatives can be undefined when the displacements are discontinuous. In order to avoid the asymptotical infinity of stresses, the traditional approach to predict fracture is linear elastic fracture mechanics (LEFM), using a stress intensity factor to provide external failure criteria through a function of stress and crack size [200]. Elastic Plastic Fracture Mechanics (EPFM) is an alternative method when dealing with elastic-plastic deformation in large regions. Based on the assumption of isotropic and elastic-plastic materials, the strain energy fields or opening displacement near the crack tips can be calculated. To make fracture analysis more generalized, cohesive zone elements (CZE) are introduced into the finite element method [201]. The behaviour of CZE is based on the cohesive law, which is based on a consideration of the cohesive tractions between the adjacent virtual crack surfaces. In 1999 the extended finite element method (XFEM) was introduced to study the crack path in the displacement field without considering the crack location [202]. One of the key features of XFEM is to model fracture and cracks without mesh refinement and crack path tracking. In this condition much research has been conducted to study arbitrary cracks based on XFEM [203] [204].
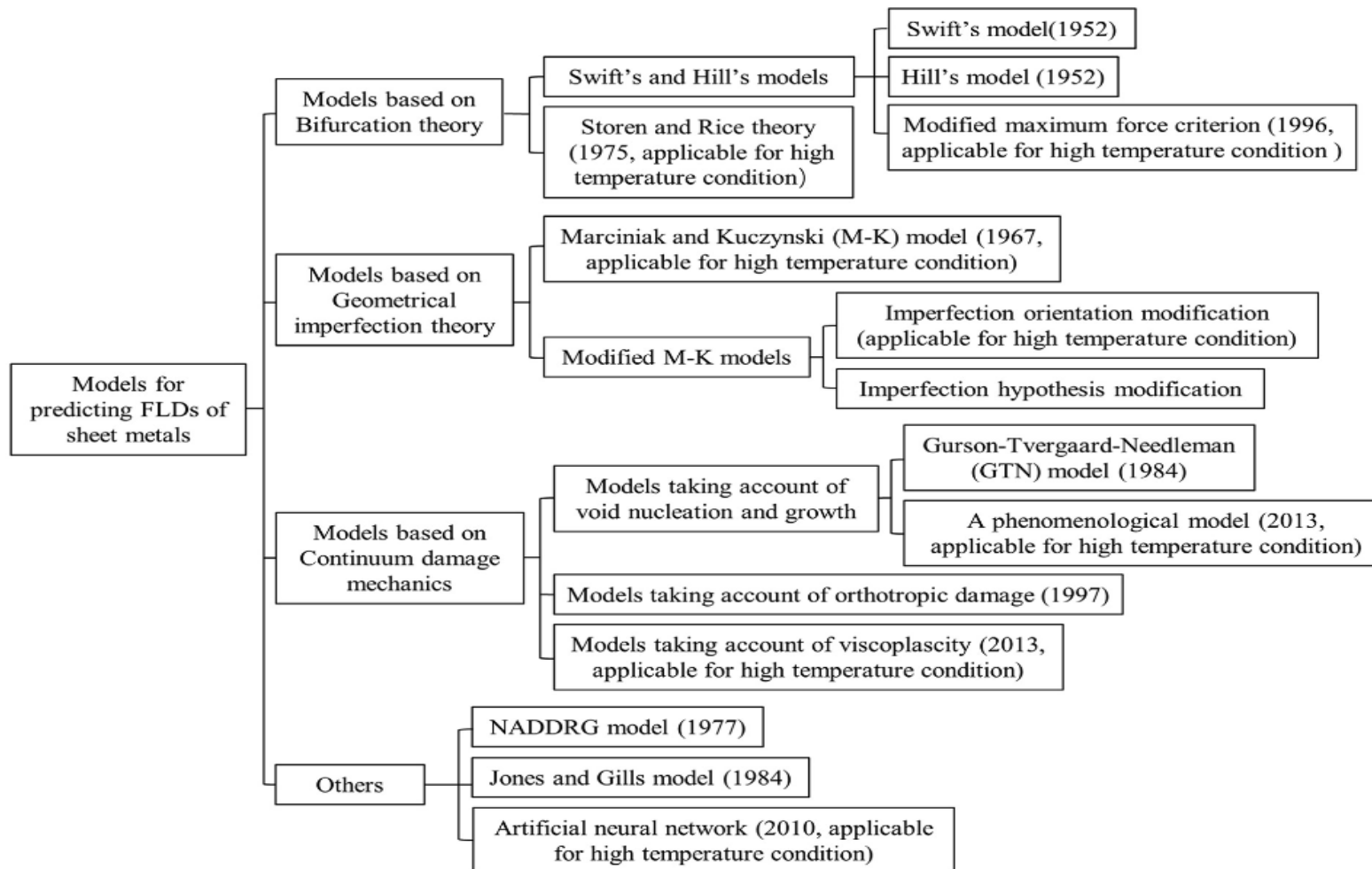
Figure 2-10 Illustration of developed modelling techniques for formability prediction [194]

2.5 Summary of findings and knowledge gaps

Sheet metal forming is one of the most important forming techniques in various fields of applications such as automotive and aerospace industries. High efficiency and accuracy can be achieved in the mass production of high strength-to-weight ratio components. Multi-point forming (MPF) as a special category of sheet metal forming techniques is being used in many industrial sectors, adding flexibility to different shapes/features without need to make different sets of solid dies. As a lightweight material, aluminium alloys are popularly used due to their excellent properties, including low density, good corrosion resistance, high strength-to-weight ratio, etc. Despite many studies having been conducted in multi-point forming (MPF) to improve surface dimpling, wrinkling, formed geometry, etc, there is still much work to do for the forming of lightweight metal sheets with high strength under different machine-set conditions.

Hot stamping technology has been used intensively for the forming of engineering components from aluminium sheets to reduce springback and the forming force required, while the structural integrity and impact safety are maintained. However, hot stamping of high strength aluminium alloys still encounters some problems that are associated largely with the forming of complex shapes and forming die conditions. There is also difficulty in achieving high production rates and a restriction to relatively low forming-limits and hence, to the achievable component-forms. At the same time, air/spray cooling rates are still too low. Therefore, more efforts should be made on integrating hot stamping with multi-point tooling and increasing the cooling rates for production environment applications.

To guide the design and set-up of a prototype pilot production line, finite element analysis can be employed to study the forming performance and formability. Practical models can be built based on material mechanical tests and data from the literature. The simulated results can compare with

44

experimental outcomes to investigate the effects of process parameters and formability improvements.

Chapter 3 Material Testing and Property Characterisation

3.1 Introduction

In this chapter the tensile tests are described to determine the mechanical properties of materials used for the cold and hot multi-point tooling deep drawing trials. Aluminium alloy 1050-H14 and mild steel DC01 were used for cold multi-point tooling deep drawing at room temperature. High-strength aluminium alloy AA6082-T6 was employed to study the influences of cooling rate on mechanical properties in a heat treatment and cooling process, before sending to the multi-point tooling.

Section 3.2 introduces the materials for testing with a detailed test plan. The test procedures are illustrated in section 3.3, including the test sample dimensions and test equipment. Based on the obtained data, the stress-strain curves for the materials are plotted in section 3.4.

3.2 Materials

3.2.1 AA1050-H14 and mild steel

Aluminium alloy 1050-H14 is considered commercially pure with good ductility, reflective finish as well as corrosion resistance. Mild steel DC01 is a good machinable low-carbon material especially in deep-drawing processes. In this tensile test the thickness for both material samples are 1mm and the test plan is shown in Table 3-1.

Table 3-1 Tensile test plan for AA1050 and mild steel

Test No	Blank Material	Rolling Direction
1-3	AA1050-H14	0°
4-6	AA1050-H14	45°
7-9	AA1050-H14	90°
10-12	Mild Steel DC01	0°
13-15	Mild Steel DC01	45°
16-18	Mild Steel DC01	90°

3.2.2 AA6082-T6

The material is commercialised AA6082-T6 with 1.5mm thickness. Uniaxial tensile tests were conducted to identify the mechanical property differences of this high strength aluminium alloy in a heat treatment and cooling process with various cooling rates. The samples were in four groups based on the heating and cooling procedures, which were room temperature (RT), solution heat treatment with natural cooling in the air (SHT+NC), solution heat treatment with fast cooling (SHT+FC) and solution heat treatment with extra fast cooling (SHT+EFC). RT means that the samples were tested directly from T6 condition without any further treatment. In other groups, the test samples were first heated to 480°C for 10 minutes, after which the samples were taken out and cooled either in the air or using our fast cooling system. The cooling rate is variable, which can be 5°C/s, 50°C/s and 100°C/s when performing natural cooling, fast cooling and extra fast cooling. Their relative temperature profiles without forming procedure are given in Figure 3-1, Figure 3-2 and Figure 3-3. The differences of cooling rates for fast cooling and extra fast cooling are realised by the initial temperature of the copper contact plates of the fast cooling station. Temperature of all samples were planned to drop to around 350°C before being formed, so the cooling time may vary within various cooling rates.
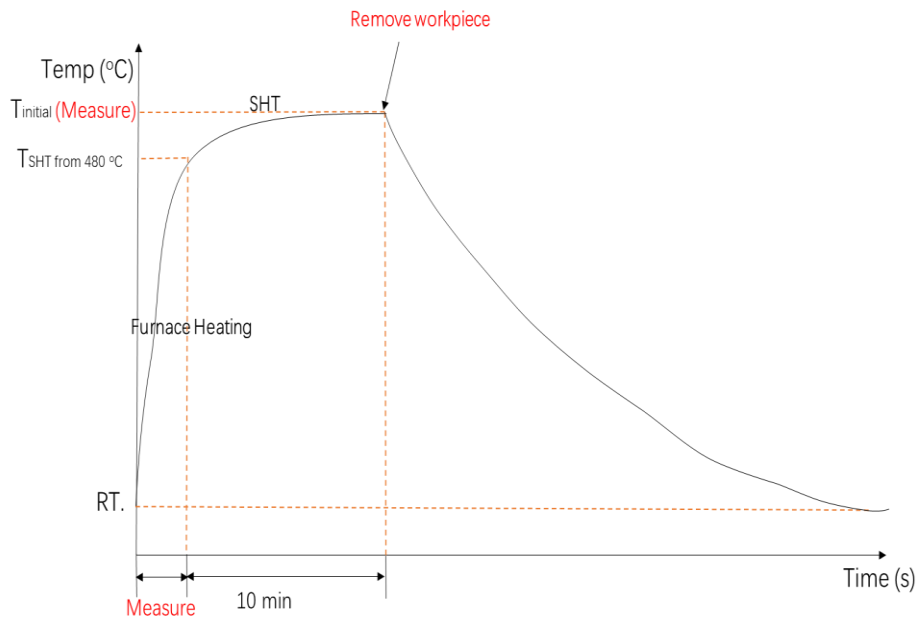
Figure 3-1 Temperature profile of SHT+NC without forming procedure
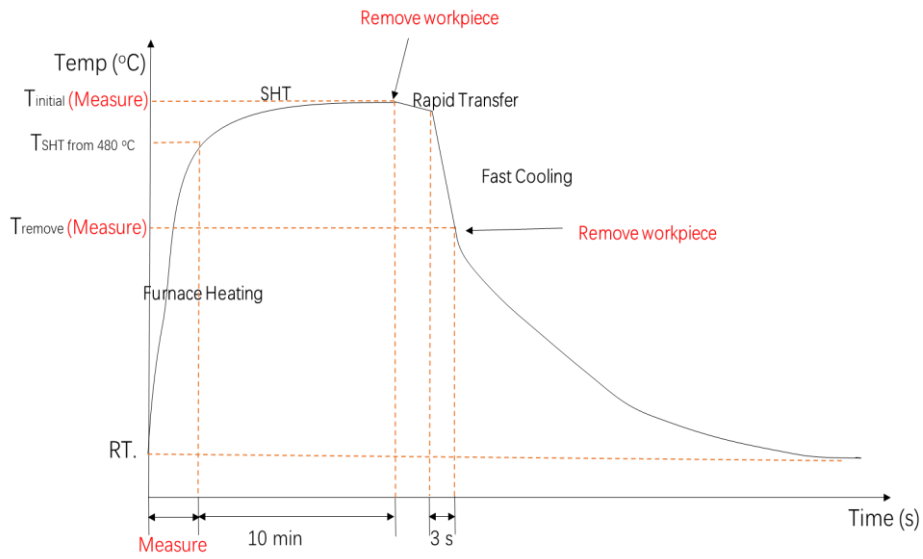
Figure 3-2 Temperature profile of SHT+FC without forming procedure

48
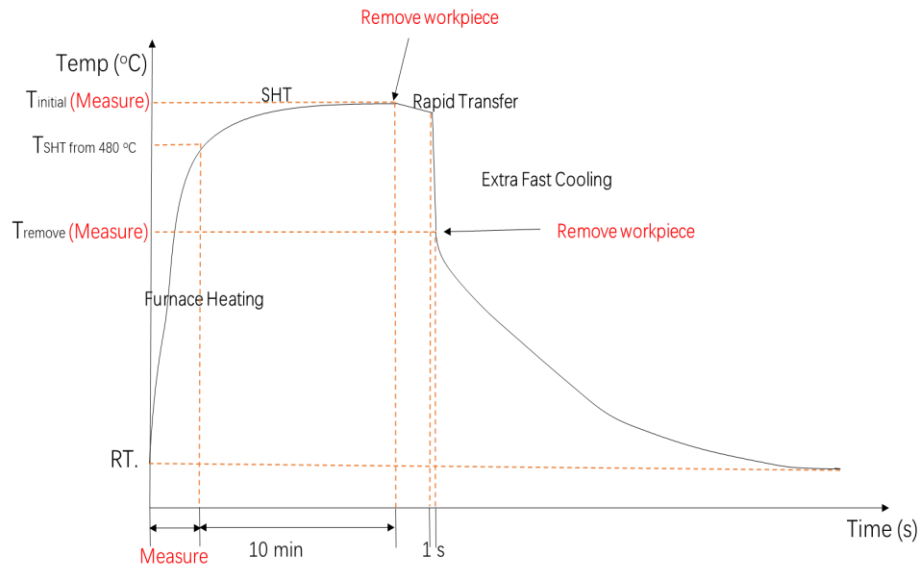
Figure 3-3 Temperature profile of SHT+EFC without forming procedure

The test plan is shown in Table 3-2.

Table 3-2 Tensile test plan for AA6082

Test No	Blank Material	Rolling Direction	Treatment before tensile test
1-3	AA6082	0°	RT
4-6	AA6082	0°	SHT+NC
7-9	AA6082	0°	SHT+FC
10-12	AA6082	0°	SHT+EFC
13-15	AA6082	45°	RT
16-18	AA6082	45°	SHT+NC
19-21	AA6082	45°	SHT+FC
22-24	AA6082	45°	SHT+EFC
25-27	AA6082	90°	RT
28-30	AA6082	90°	SHT+NC
31-33	AA6082	90°	SHT+FC
34-36	AA6082	90°	SHT+EFC

To monitor the temperature change during the heating and cooling period, thermocouples were mounted on the corner of each tensile sample as shown in Figure 3-4. Temperature can be read and saved directly from a laptop through the Omega input data acquisition module. For natural cooling, the samples were placed on the thermal insulation sheet whose thermal conductivity is 0.07W/m.K. at 400℃ instead of ground to avoid inaccurate heat loss.
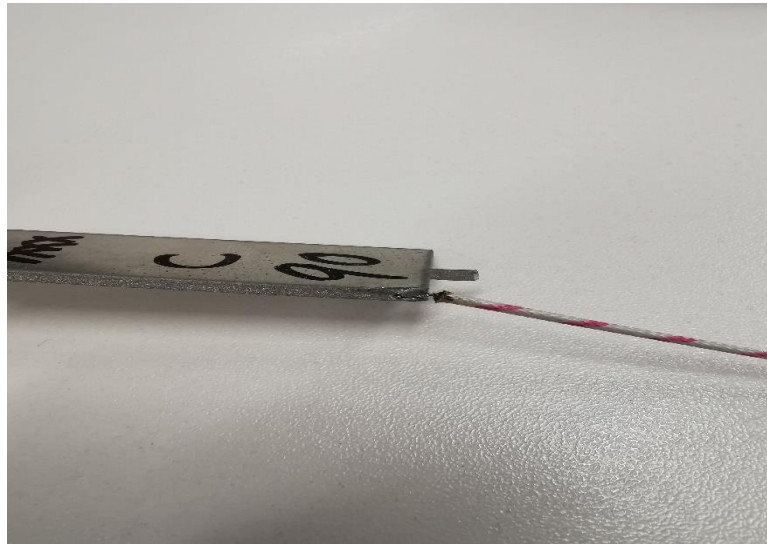
Figure 3-4 Tensile sample mounted with thermocouple

3.3 Procedures

The test machine was an Instron 5969 electromechanical system with an extensometer in the University of Strathclyde as shown in Figure 3-5. Water jet cutter was used to cut the large blank sheets to small samples, whose shape and dimensions is shown in Figure 3-6, following the ASTM E8 Standard. Considering the rolling direction of the large material sheets, the mechanical properties were obtained in three different angles to the

rolling path, which were 0°, 45° and 90°. For each test category three samples were tested. Each side of the test piece was gripped by the holder and when stretching a loading rate of 0.9 mm/min was set until fracture. An extensometer gave the initial length of the test area and monitored the strain increments. After getting the displacement and force values from the software generated file, all the engineering and true stress and strain values can be calculated to get the stress-strain curves.
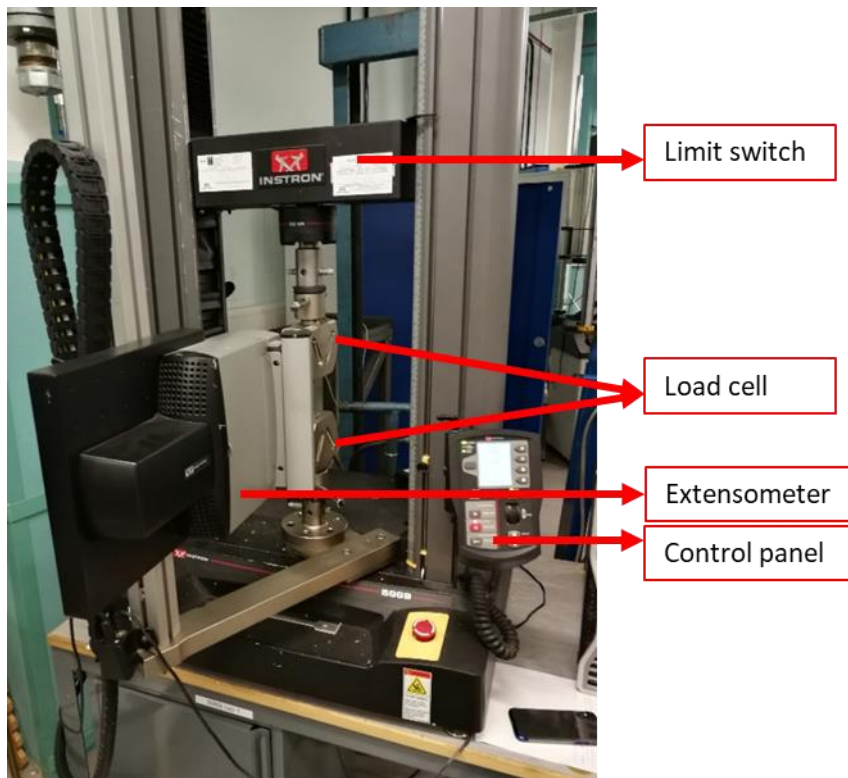
Figure 3-5 Instron 5969 used for tension test
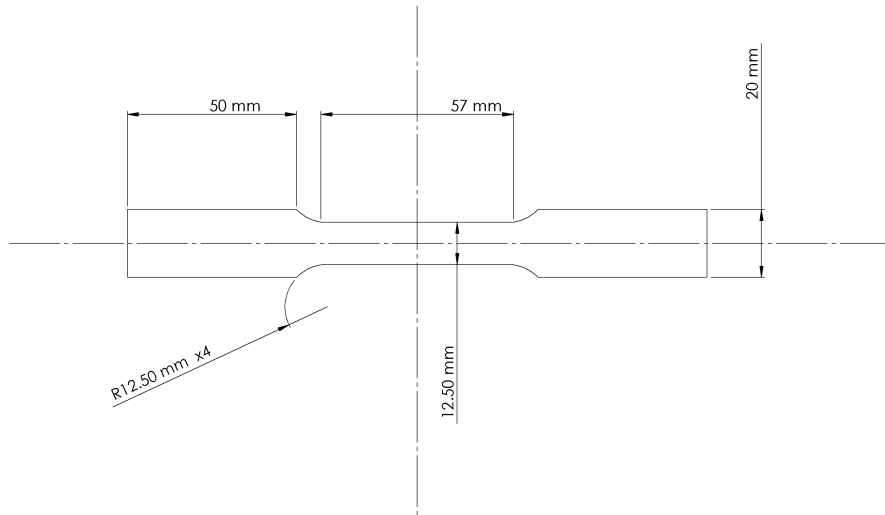
Figure 3-6 Dimensions of test samples

3.4 Results

From the test data the plotted stress-strain curve for the AA1050-H14 and mild steel are given in Figure 3-7 and Figure 3-8.

(a)

True Stress - True Strain
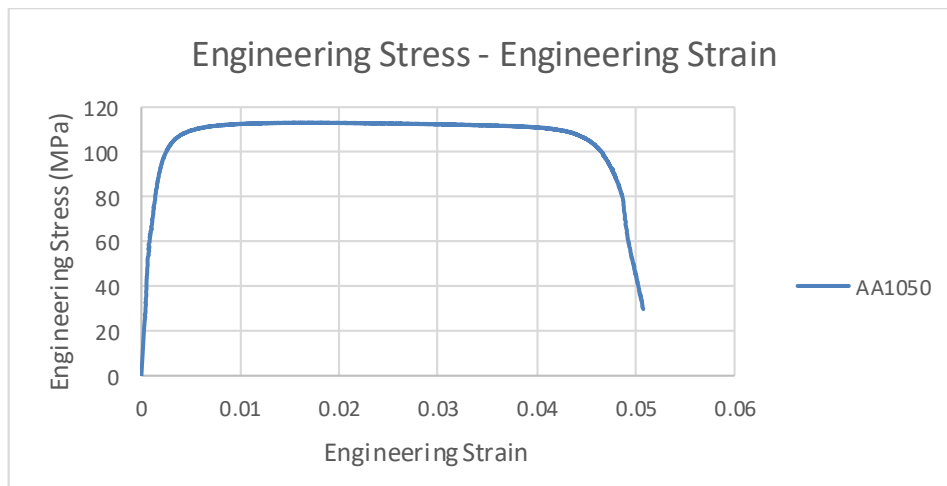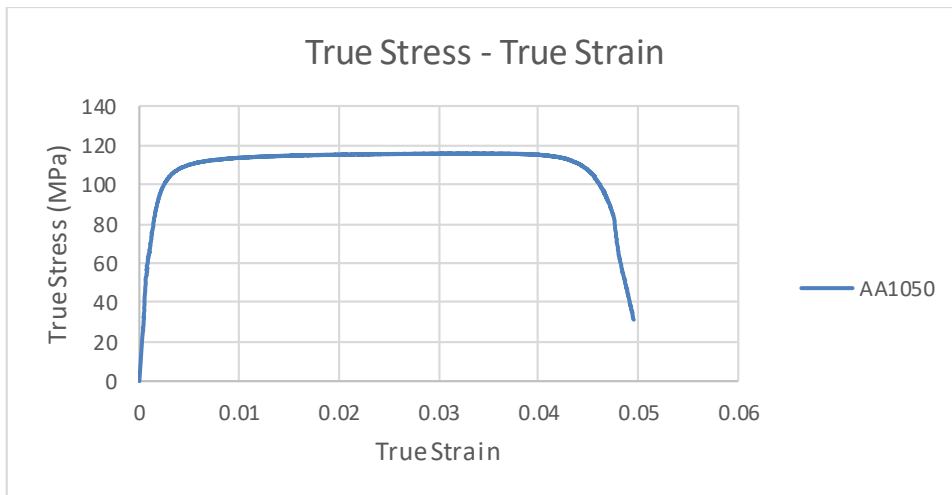
(b)

Figure 3-7 Stress-strain curve of AA1050-H14

Engineering Stress - Engineering Strain
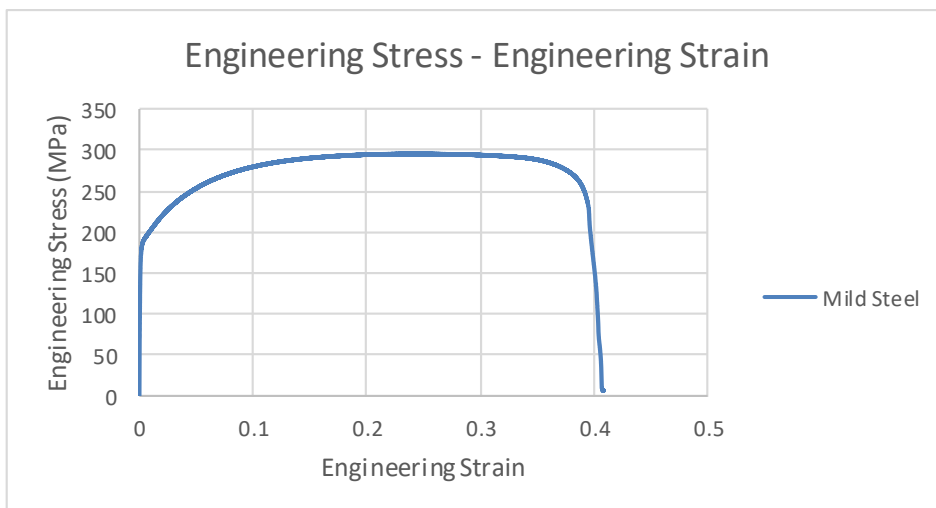
(a)
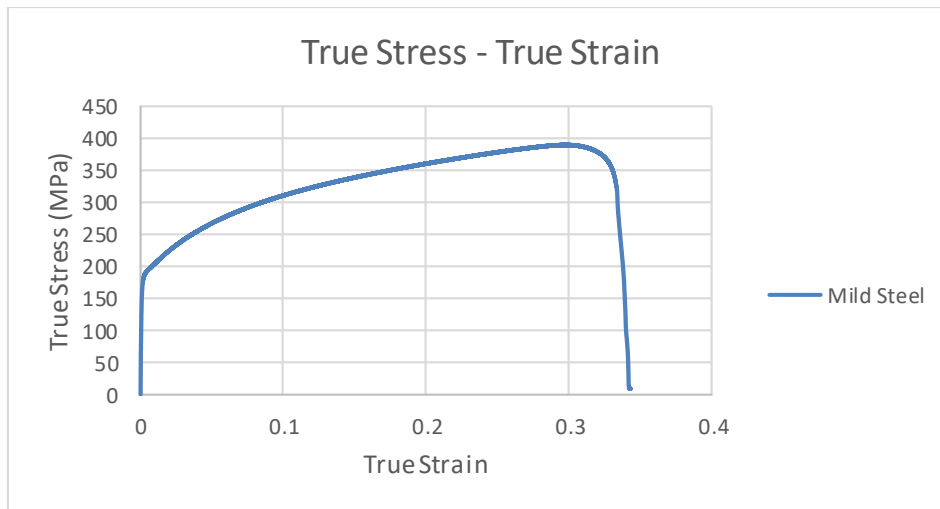
(b)

Figure 3-8 Stress-strain curve of mild steel

From the above figures a linear elastic deformation occurs first until the yield point, and then the materials reach plastic regions with continuously non-linear increasing stress due to material hardening. The yield stress, UTS and elongation of mild steel are larger than those of AA1050-H14. The mechanical values for aluminium alloy and mild steel are given in Table 3-3.

Table 3-3 Mechanical properties of aluminium alloy and mild steel

	Aluminium Alloy 1050-H14	Mild Steel DC01
Density	2710kg/m^2	7830kg/m^2
Elastic Modulus	68Gpa	212Gpa
Poisson Ratio	0.35	0.31
Yield Stress	97MPa	190Mpa

54

UTS	113MPa	295.5MPa
Max Strain	0.03	0.3

The plotted stress-strain curves for AA6082 are shown as follows
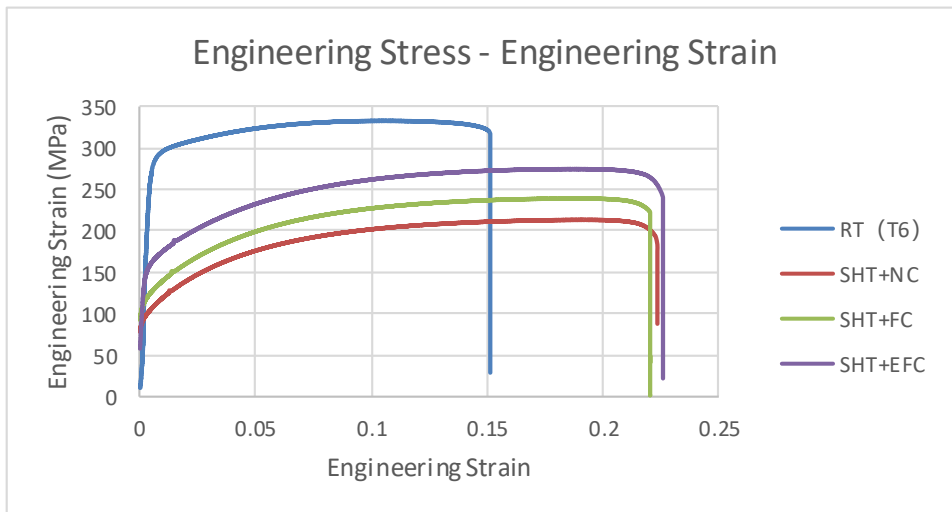
(a)
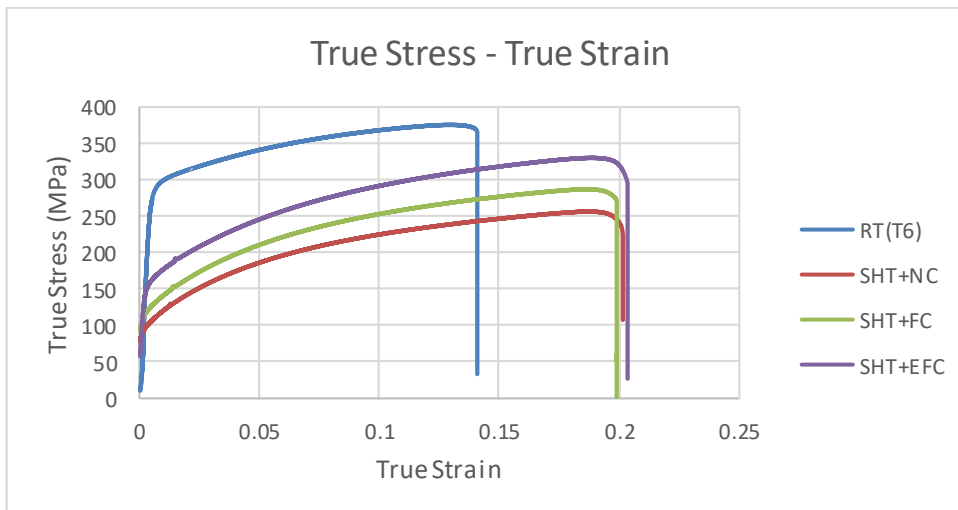
(b)

Figure 3-9 Stress-strain curve of AA6082

From the stress-strain curves in Figure 3-9, there is a large decrease for both yield stress and UTS but an increase for elongation at break when the samples are solution heat treated and cooled, which improves the formability and extends the tool life. The UTS for samples with RT, SHT+NC, SHT+FC, SHT+EFC are 332.8MPa, 213.4MPa, 239.1MPa and 274.7MPa. There is little difference in maximum elongation under different cooling rates, however, the UTS increases along with cooling rates. This proves the influence of cooling rates on material mechanical formability. Based on these obtained results of mechanical properties, numerical and experimental forming tests are performed in the following chapters to study the effect of cooling rate on forming limit using the developed fast cooling methods. The mechanical values for AA6082 are given in Table 3-4.

Table 3-4 Mechanical properties of AA6082 under different heating and cooling methods

	RT	SHT+NC	SHT+FC	SHT+EFC
Density	2710 kg/m²	2710 kg/m²	2710 kg/m²	2710 kg/m²
Elastic Modulus	68Gpa	68Gpa	68GPa	68GPa
Poisson Ratio	0.35	0.35	0.35	0.35
Yield Stress	263MPa	90.7Mpa	110.5MPa	133.8MPa
UTS	332.8MPa	213.4MPa	239.1MPa	274.7MPa
Max Strain	0.13	0.185	0.18	0.183

3.5 Summary

This chapter describes the uniaxial tensile tests setup to determine the mechanical property of materials used in this research. Aluminium alloy

1050-H14 and low carbon steel sheets with the thickness of 1mm were selected for cold deep drawing with multi-point tooling due to their good ductility and machinability at room temperature. The large differences in ultimate tensile strength and elongation at break made them comparable when studying the effect of working material selection. Commercialised high-strength aluminium alloy 6082-T6 sheets with 1.5mm thickness were tested for hot stamping with fast contact-cooling. These AA6082 test pieces were heated up by the electrical furnace and subjected to intermediate cooling prior to the tensile testing. Different cooling rates, such as 5°C/s, 50°C/s and 100°C/s were achieved and their effects on the mechanical performance has been investigated.

All test pieces were cut in the 'dog-bone' shape following ASTM E8 Standard in three different angles to the rolling path and their average values were selected. After gripping each side of the work piece, tensile displacement increased at a speed of 0.9 mm/min until fracture. By analysing the force and displacement recorded and transferring to relative stress and strain parameters, their relationship can be obtained.

The stress-strain curves from all test pieces include an elastic and a plastic region. The yield strength, ultimate tensile strength and elongation of low carbon steel are much larger than those of AA1050-H14, which helps with the following comparison of the effect of material properties on surface performance. The tested yield strength and ultimate tensile strength of AA1050-H14 are in the range given from an existing database, while the elongation at break tested is 0.03, which is smaller than that of 0.08 from the database. All the tested properties of low carbon steel are consistent with the relative data range available commercially. From the tested stress-strain curves of AA6082-T6 it is believed that the high strength can be greatly reduced after heating and fast-cooling, with the elongation largely increased. Increasing the cooling rate can increase the ultimate tensile strength while the extended elongation is maintained. This could lead to a

significant improvement in the material formability at a critical area, while the forming force requirements are reduced as appropriate. The test results are important for this research since this kind of data is not available commercially. All these data can be used in the numerical simulation in the following chapter and are able to help with an illustration of experimental performance of the forming limit improvements in this study.

Chapter 4 FE Analysis of Deep Drawing with Multi-Point Tooling

4.1 Introduction

Finite element modelling is a robust tool in industry because the cost in time and money can be reduced greatly by changing the process parameters directly in the software. In this chapter Abaqus 3D finite element modelling was employed for the study of shape performance of deep drawing with multi-point tooling. A multi-point model with 23 tightly packed pins on each side was developed by using the commercial software Abaqus, with investigation of the influencing factors, such as the depth of forming curvatures, working materials, holding force, surface lubrication, and thickness of rubber cushions, all in a quantitative manner at room temperature. From the numerical results, the internal stress distributions from the process can be obtained and analysed since these cannot be measured from experimental test parts. A further step is set to investigate the forming limit improvements on samples after being solution heat treated and cooled using high strength aluminium alloy 6082, in order to feasibly explore the possibility of the multi-point hot forming process since no one has done this in this area.

In Section 4.2 a numerical simulation of the cold multi-point tooling deep drawing process is conducted by introducing to the model geometrical and material definitions, modelling techniques and effect variables. A parametric study is conducted on the main variables to qualify the final shape performances. Abaqus has no units built into it, there the units chosen must be self-consistent. In this research SI units are employed for the model geometries, so the units of the simulated results can be clarified accordingly. Then in Section 4.3 modelling of multi-point tooling deep drawing of heat-treated and cooled blanks are explained with a comparison

59

of the fracture performance at the critical section in order to explore the formability resulting from different cooling rates in a heat treated and cooling process.

4.2 Modelling of cold multi-point tooling deep drawing

4.2.1 Geometrical model

In this research, a finite element model with 23 tightly packed pins and 4 blank holders on each side of the MPF system was developed to study the multi-point tooling deep drawing process. The plate is clamped by blank holders and covered by elastic cushions to reduce wrinkles and indentations. Figure 4-1 presents the finite element model built in Abaqus with some simplification.

The pin heads are hemispherical but the tightly packed hexagon columns are changed to cylinders as a simple sketch as shown in Figure 4-2 and the movement of each pin is independent of others. The initial positions of the pins were placed according to the calculation from the 3D printed surfaces in Figure 4-3. A curve depth of 16mm was taken as the basic profile, but the position can be easily changed to other profiles by moving the pins in the ram direction. The blank sheet is set as 200 mm * 200 mm with 1 mm thickness and constrained by blank holders at each edge, so the formed area of the blank sheet is 125mm * 112mm. There is a small angle of approximately 45° along the thickness of the blank holder in the inner edge to avoid a sharp cut to the blank sheet. Rubber was placed at each side between the pins and the blank sheet to reduce force concentration and there is a small gap with the blank holder.

Dynamic explicit analysis is employed for the simulation to achieve better convergence because this method does not require a large computational

cost. Coulomb friction model was assumed and the friction coefficient was set as 0.02 for a lubricated condition and 0.17 for a normal dry condition [123] [131].
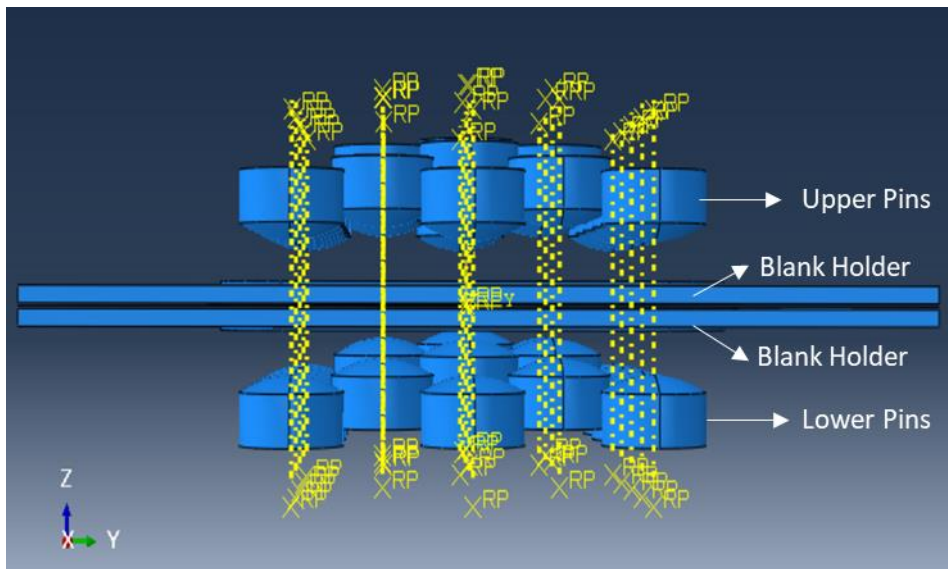
(a)
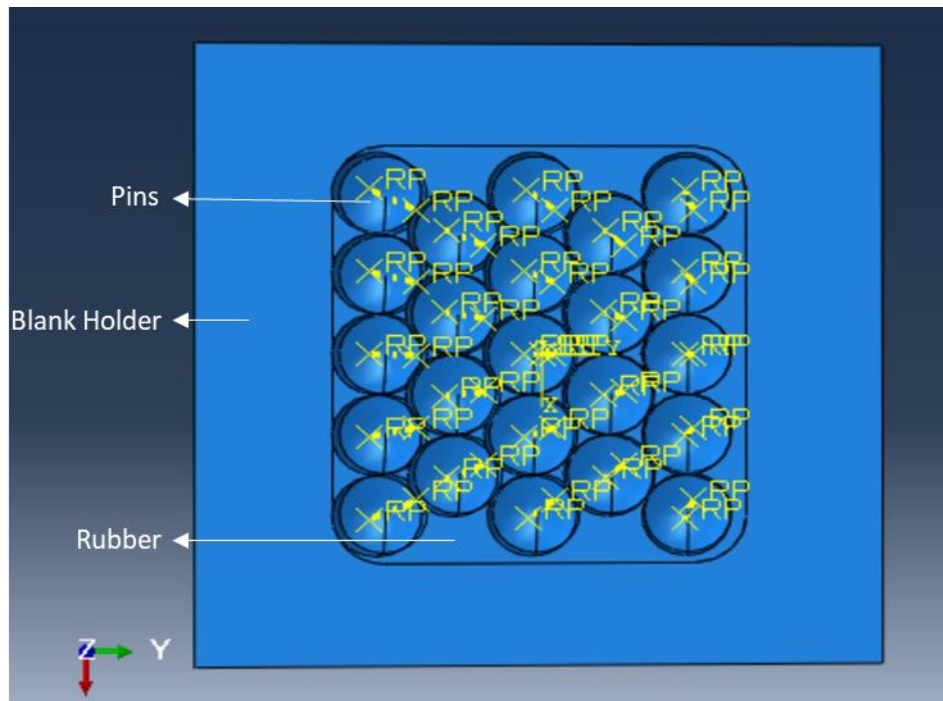
(b)

Figure 4-1 Abaqus finite element model of 23 pins MPF: (a) front view
and (b) top view
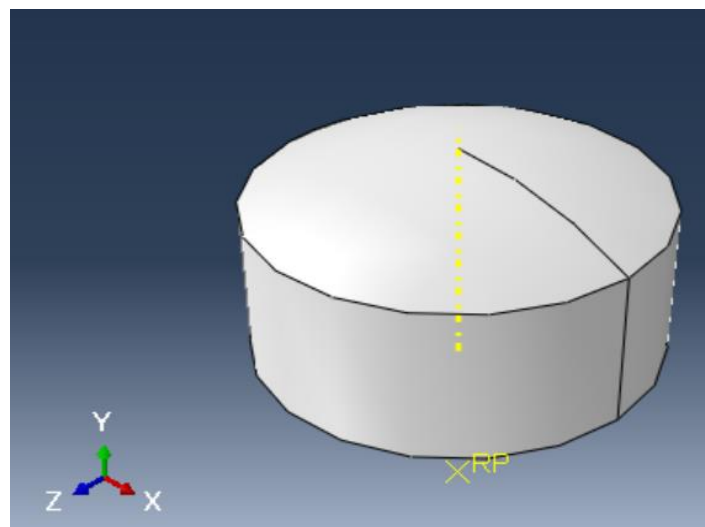
Figure 4-2 Simplified pin head
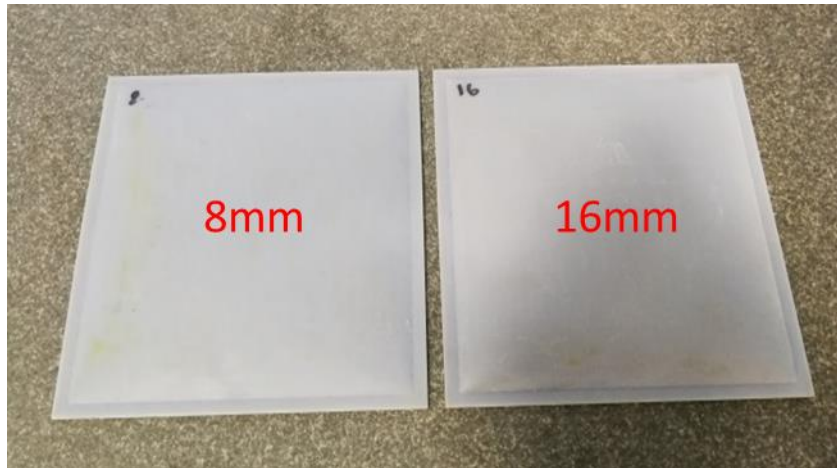
Figure 4-3 3D printed dome-like surfaces

4.2.2 Material definition

The blank materials used in the simulation for cold multi-point tooling deep drawing are aluminium alloy 1050-H14 and mild steel DC01 square sheets with 1 mm thickness whose mechanical properties were tested from tensile tests as described in Chapter 3 with some main parameters presented in Table 3-3

Both materials are regarded as Von Mises material with isotropic hardening involving elastic and plastic behaviour. The linear elastic region follows the theory of Hook's law and for plastic modelling, the tested stress and strain data can be input into the material property definition. It is assumed that the maximum elongation is 0.03 and 0.3 for AA1050-H14 and mild steel before fracture, although there is a small range of steady decrease of stress during tests.

The cushion used is Polyurethane which is mainly non-linear hyper-elastic and it is assumed to be isotropic and incompressible. The constitutive behaviour of Polyurethane is usually derived from the polynomial strain energy function (SEF). To determine the mechanical nominal stress-strain property, mostly a uniaxial test, volumetric test, planar shear test and biaxial test are used [205]. In Abaqus several hyper-elastic material models are available, or the test data can be input directly. The test data provided by Aquaseal Rubber ltd. is plotted as shown in Figure 4-4
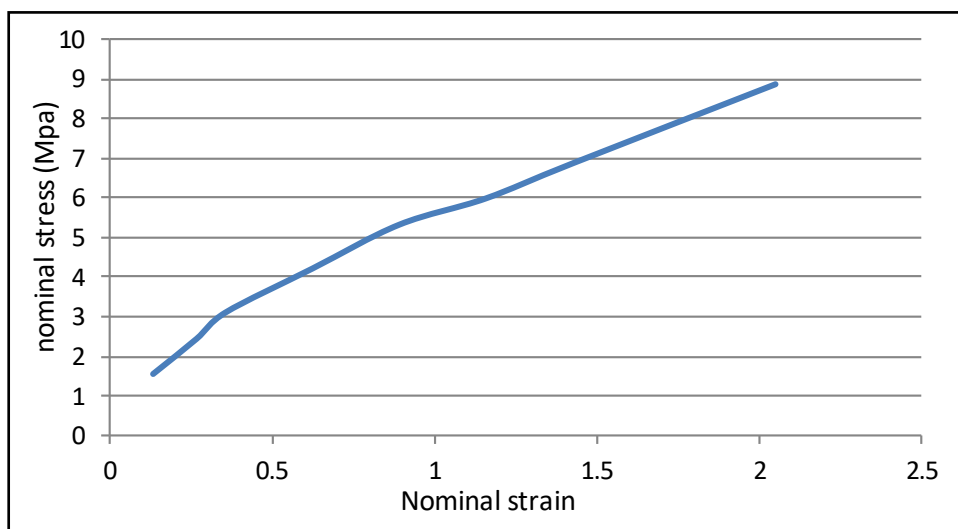
Figure 4-4 Nominal stress-strain relationship for polyurethane

4.2.3 FE model

In the FE model, the pins on both sides were set as analytical rigid bodies to save processing times. The blank holders were modelled by discrete rigid bodies with R3D4 element meshes which reduced the computation cost but maintained the key features, especially the round corners as well as the smooth angles along inner edges. Shell element S4R was applied to the thin plate to reduce calculation costs and study the section thickness, while the rubber pads were built up through deformable solid parts with C3D8R element meshes. The global mesh size of the blank sheet and

64

cushion was set as 0.005 m. So 1600 elements were generated for the blank sheet and 718 elements were generated for the rubber. Figure 4-5 and Figure 4-6 show the mesh assignment for blank sheet and cushion, which are mostly symmetric.

Different boundary conditions were set to determine the effects of process parameters including working materials, lubrication, rubber thickness, spring strength and forming geometry. The initial positions of pins were placed in advance to form different curvatures of 8 mm and 16 mm. During the forming process the lower pins were totally constrained while the upper pins moved vertically until they achieved their relative curvature displacements. The lower blank holder was supported by springs with different strengths, whose reaction forces can be applied through boundary conditions linearly from Hook's law. The lubrication condition can be realized by assuming a different friction coefficient in the sliding formulation.
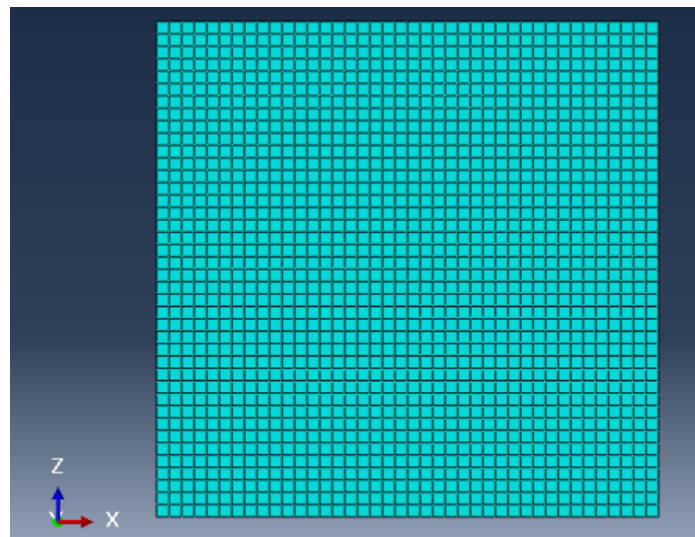
Figure 4-5 Mesh assignment for blank sheet
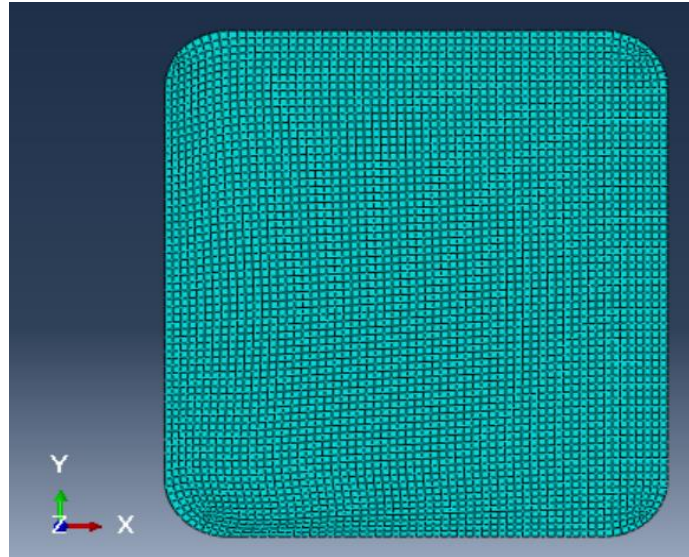
Figure 4-6 Mesh assignment for cushion

A total of six models were employed for comparison. We set the basic model as 1mm thick aluminium sheet which was lubricated and covered by 4mm thick cushions on each side. The initial positions of the pins were set following the 16mm curved surfaces. The holding force was produced by springs with a stiffness of 8.79daN/mm. Other control groups with different process parameters can be set up accordingly with details shown in Table 4-1.

Table 4-1 Overview of the modelling conditions

Test	Blank Material	Lubrication	Rubber Thickness	Spring Strength	Curved Depth
1	Aluminium	Yes	4mm	8.79 daN/mm	16mm

2	Aluminium	Yes	4mm	8.79 daN/mm	8mm
3	Steel	Yes	4mm	8.79 daN/mm	16mm
4	Aluminium	Yes	4mm	3.9 daN/mm	16mm
5	Aluminium	No	4mm	8.79 daN/mm	16mm
6	Aluminium	Yes	2mm	8.79 daN/mm	16mm

4.2.4 FE analysis

In this section investigation of the simulation results on the proposed cold multi-point tooling deep drawing is explained by comparing different variables. The main variables are selected as forming geometry, working materials, holding force, surface lubrication, and thickness of rubber cushions. The central profile of the formed parts in X and Y direction (i.e. path AB and CD as shown in Figure 4-7), pressure, thickness distribution and equivalent strain are described to qualify the shape performance.
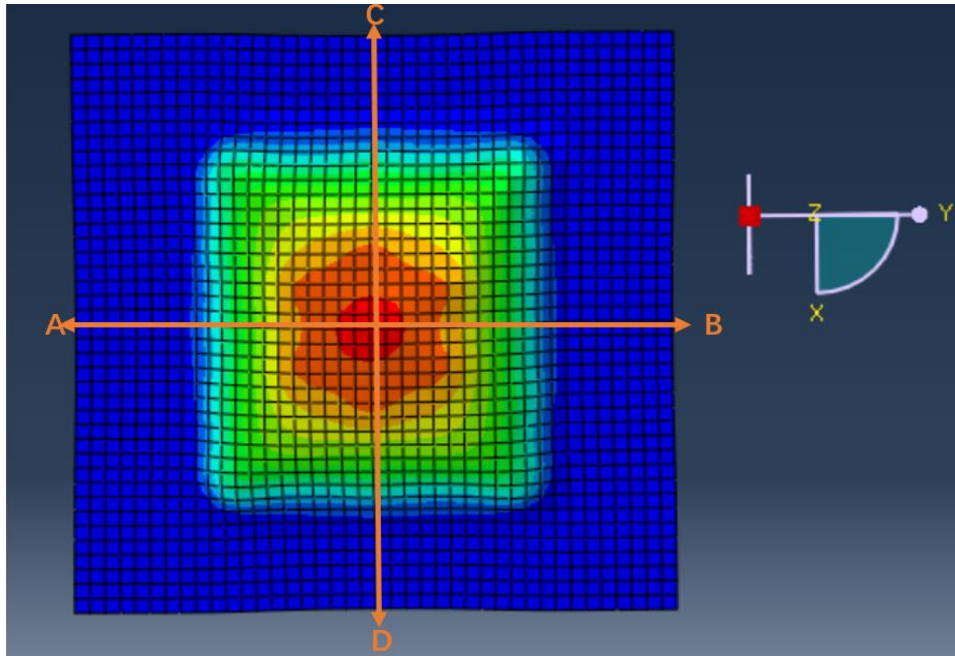
Figure 4-7 Plotted profile paths

4.2.4.1 Effect of the forming geometry

Different curvatures of the formed parts with the same dimensions determine stress and strain concentration conditions at critical areas. To study its influence, all other variables should keep constant all the time. In this study, the depths of curves were selected as 16mm and 8mm at the centre line of aluminium alloy 1050-H14 with 1mm thick. The coefficient of friction between the blank holder and the sheet blank was set as 0.02 and the thickness of the rubber cushion was 4mm on each side placed between the pins and sheet blank to avoid indentation. The holding force was the same for both models and increased along with the pressing displacement. The formed profile of the central line AB and CD is shown in Figure 4-8. The target profile was measured from the 3D printed dome-like surfaces using CMM. For both path AB and path CD, the curve profile with 8mm depth is smoother than that with 16mm depth. The small peaks on 16mm curves represent the indentations where pin heads contact with the sheet blank. It is believed that by increasing the forming depth, the

68

increased contact force makes the indentation apparent due to stress and strain concentration. The 8mm profile is much closer to its target profile line, and a larger deviation can be seen for the 16mm formed profile. The large contact force restricts the material flow of the rubber cushion and this proves that the shape accuracy of the formed parts should increase with a decreased forming curve depth. The small asymmetry of the formed profile is probably due to numerical effects caused by rounding errors during the simulation..
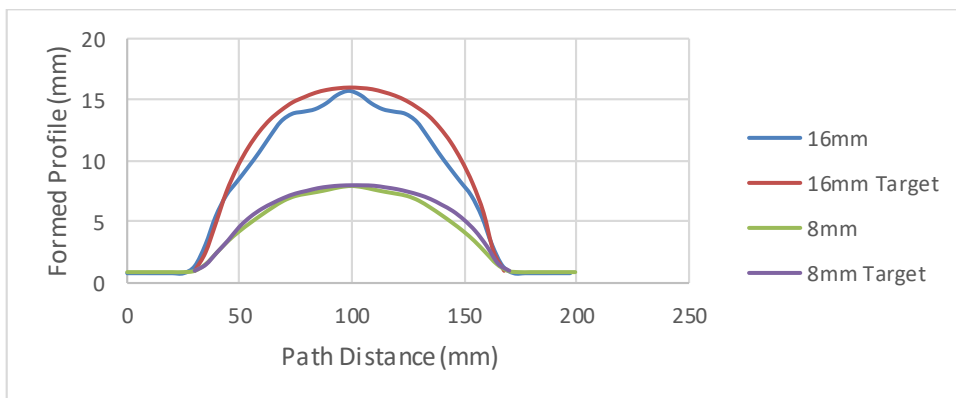
(a)
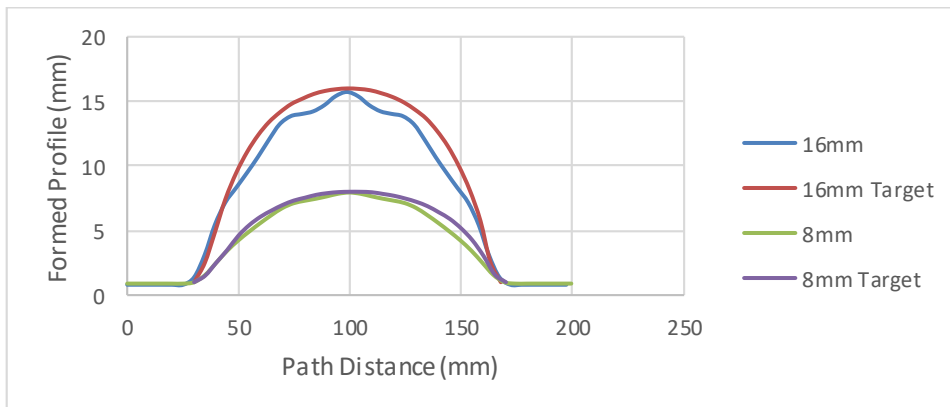
(b)

Figure 4-8 Effect of curve depth on formed profile: (a) path AB and (b) path CD

Figure 4-9 shows the equivalent pressure stress components distribution of the formed sheet blank with a curve depth of 16mm and 8mm. A positive value indicates that the stress is in tensile in that local area, while a negative value indicates compression. The equivalent pressure stress concentration spots can be clearly seen when formed to 16mm which results in large indentations on the final shape. In Figure 4-9(b) the diffused region near contact spots is believed to help with stress components distribution due to the use of the rubber cushion. In general increasing the curve depth can increase the pressure between pin heads and the sheet blank thus making indentation easy to occur.
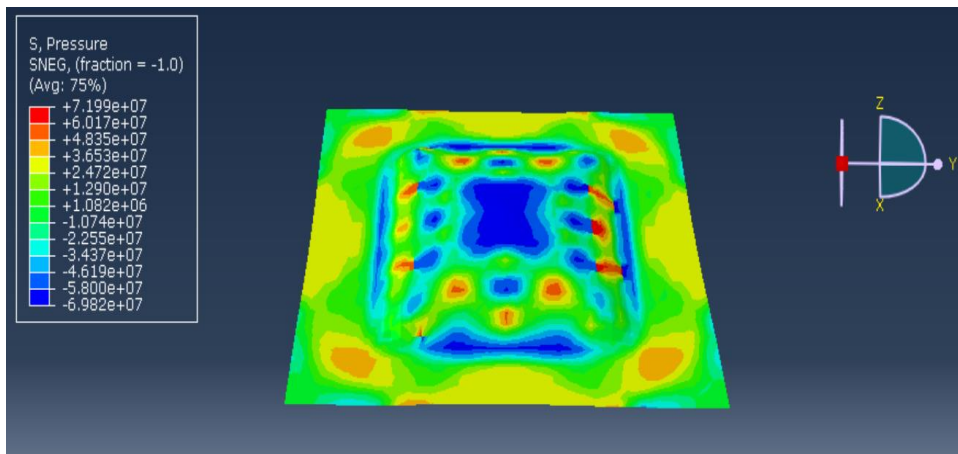
(a)
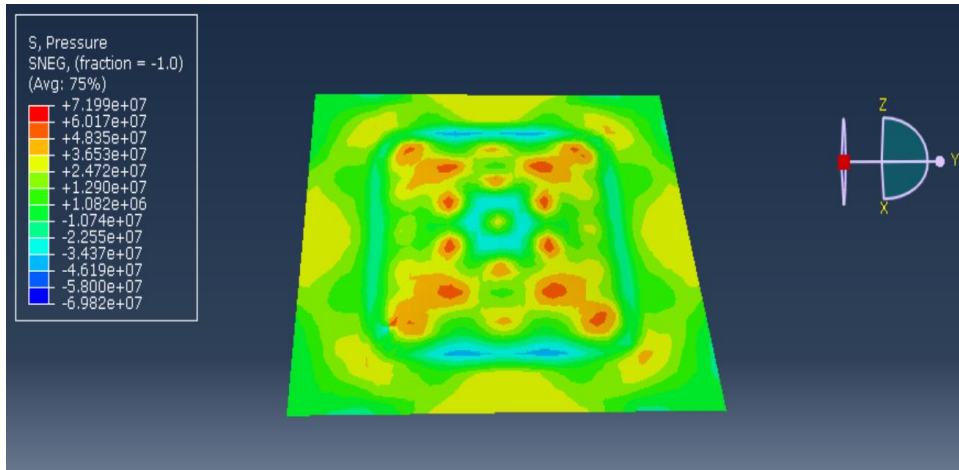
(b)

Figure 4-9 Equivalent stress components distribution (unit: Pa) of formed parts under different depth of curve: (a) 16mm and (b) 8mm

From Figure 4-10, it can be seen that the maximum equivalent plastic strain occurs at the long edge of the formed area. It should be noticed that the maximum equivalent strain value in the simulation exceeds the tensile tested value of 0.03. This is mainly because the material is strain-rate sensitive, but in simulation the strain rate effects were not considered and it is related to the press forming velocity. In addition the area near the four corners also experiences larger equivalent plastic strain. This is why a gap between the blank holder and rubber cushion is necessary. It can be proved that the equivalent plastic strain increases along with the forming curve depth.
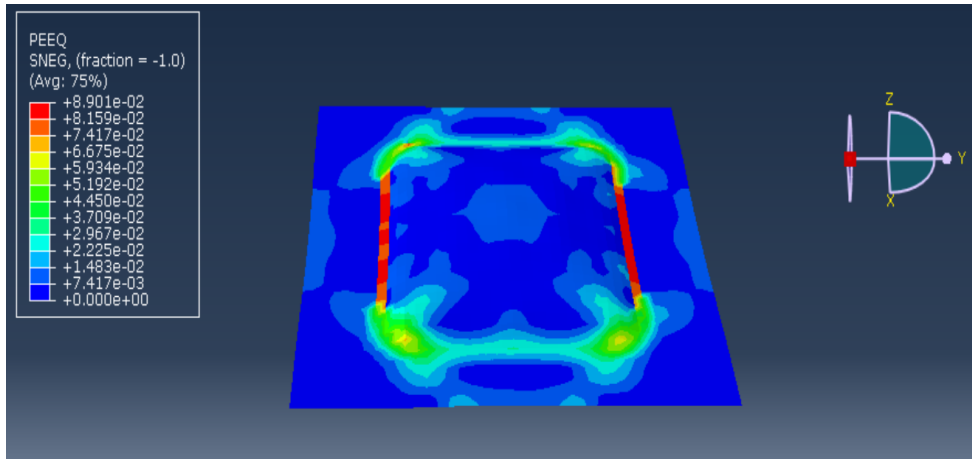
(a)
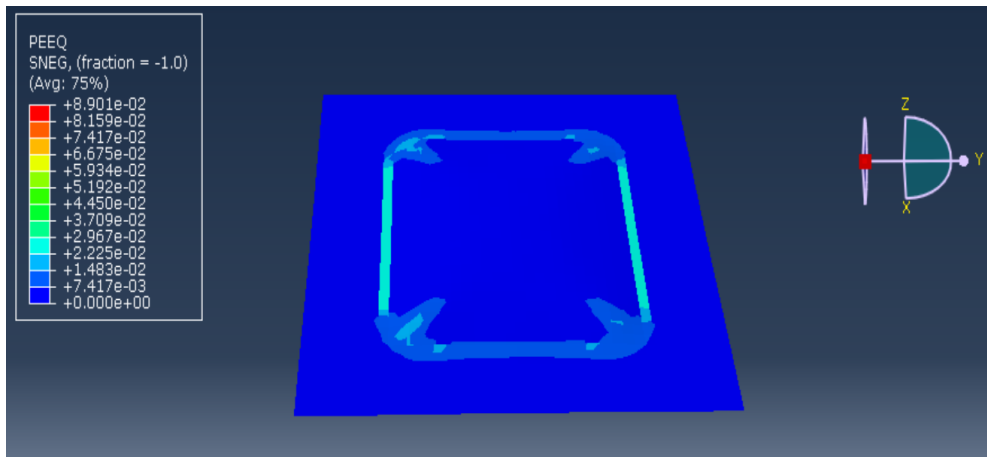
(b)

Figure 4-10 Equivalent plastic strain distribution of formed parts under different depth of curve: (a) 16mm and (b) 8mm

4.2.4.2 Effect of the working material

To investigate the shape performance of materials with different properties, AA1050-H14 and DC01 mild steel sheet blanks with a thickness of 1mm were selected due to their large differences on yield stress, UTS and fracture elongation. All the samples were formed to a depth of 16mm and constrained under lubricated conditions. The rubber thickness on each side and spring strength remained as 4mm and 8.79daN/mm. Figure 4-11

illustrates the formed profile along path AB and path CD for these two materials. In general the profiles are similar under the same forming and lubrication conditions.
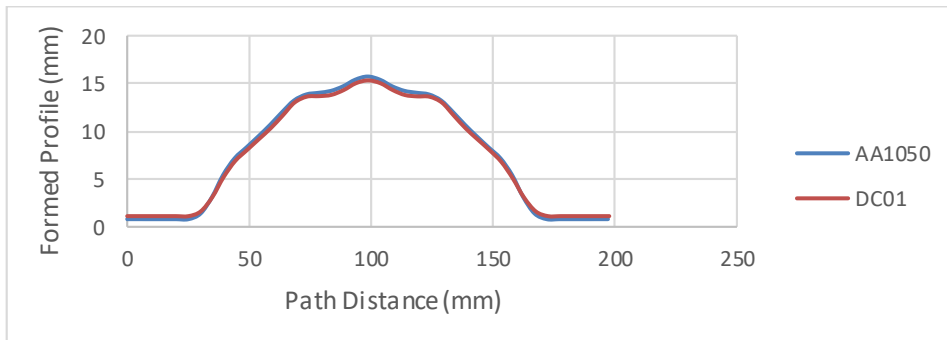
(a)
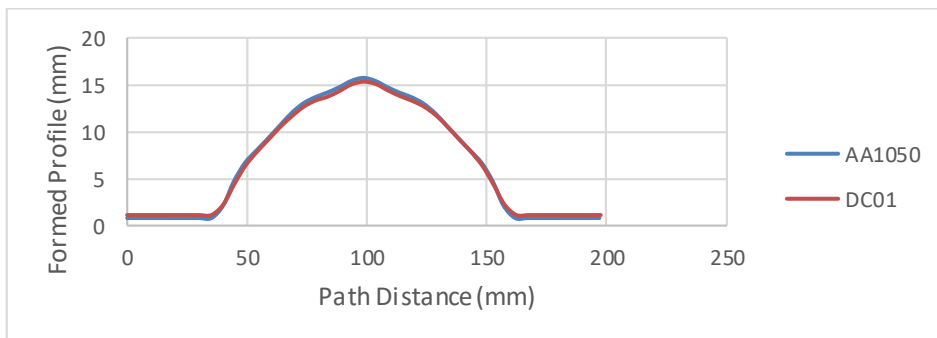
(b)

Figure 4-11 Effect of material on formed profile: (a) path AB and (b) path CD

As seen in Figure 4-12, the equivalent pressure stress components of the formed part depend on the relative mechanical properties. Since the yield stress and UTS of steel are much higher than those of aluminium alloy 1050-H14, forming of steel sheet blank to the same shape requires more force. Although the elongation of steel is larger, the effects of the different materials on the shape performance are a combined result of their properties as long as the press can provide enough force.
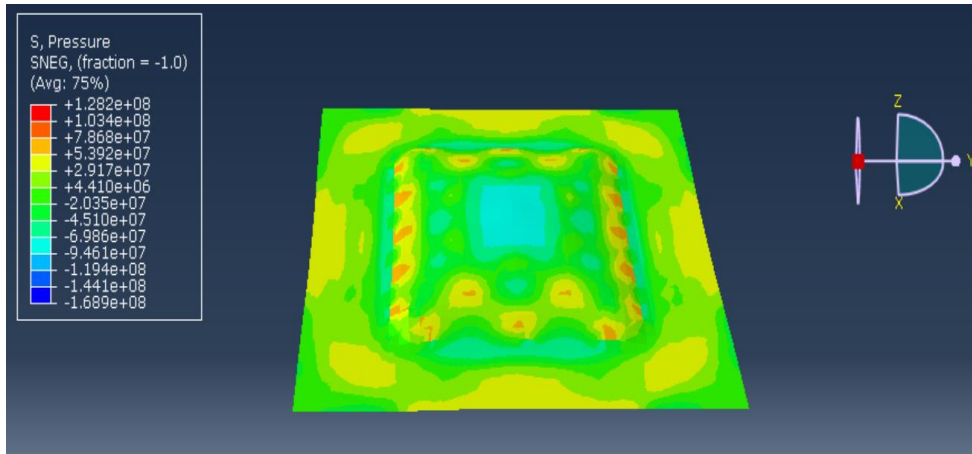
(a)
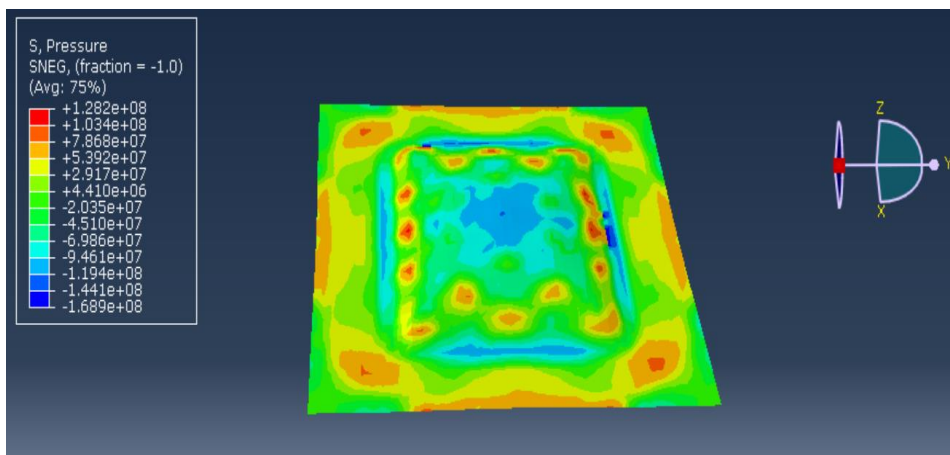
(b)

Figure 4-12 Equivalent stress components distribution (unit:Pa) of formed parts: (a) AA1050-H14 and (b) DC01

4.2.4.3 Effect of the holding force

To compare the effect of holding force on shape performance, two types of mechanical springs were selected with different stiffness (8.79daN/mm and 3.8daN/mm). During simulation the reaction force was applied to the discrete rigid blank holder and its value increased linearly following Hook's law. To control other parameters, the forming geometry, surface lubrication, rubber cushion thickness were maintained constant. 1mm thick

AA1050-H14 plate was used for the simulation. Figure 4-13 describes the simulated Mises stress distribution of samples when formed to a depth of 16mm with a maximum holding force of 2812.8N and 1216N. The slight difference on the Mises stress and the equivalent plastic strain may not be clear if the maximum and minimum limits were set the same. It can be seen that the stress on the sample with higher spring stiffness is larger. This may be due to the restriction of material flow at the edges. In this condition the increased equivalent plastic strain requires a large stress between the pin heads and formed parts as shown in Figure 4-14 without considering the strain rate effect of the material. However, the difference of stress and strain distribution is not very obvious under various holding force, which indicates the value of the appropriate holding force should be a combination of material and tooling for a specific shape. For thin sheets the balance should be carefully considered since the holding force can both restrict the material and help with wrinkle avoidance.
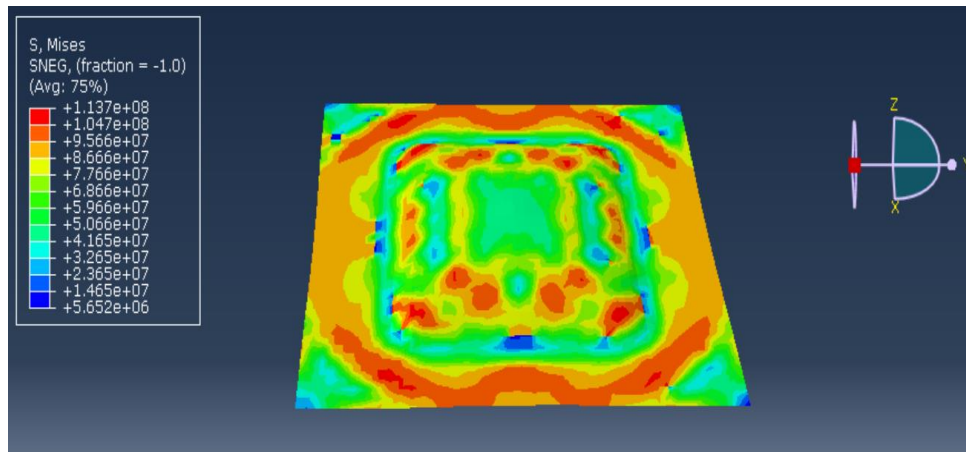
(a)
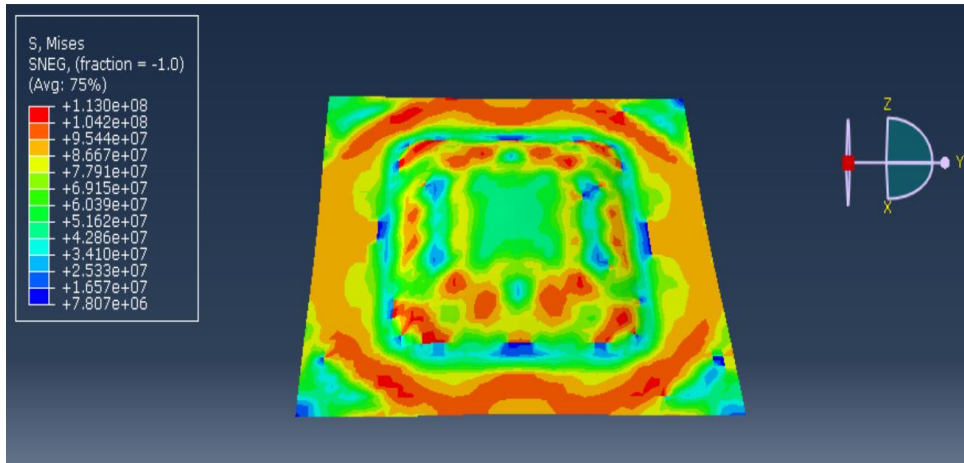
(b)

Figure 4-13 Mises stress (unit: Pa) of formed parts: (a) large holding force and (b) small holding force
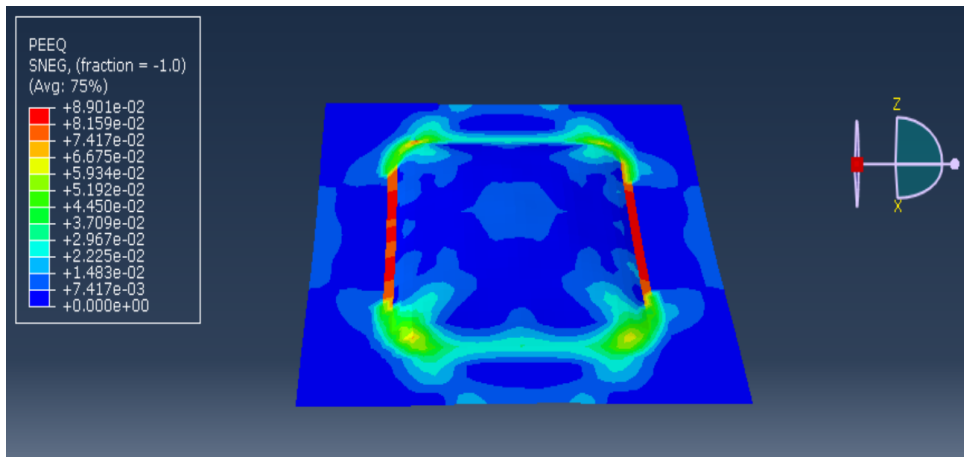
(a)
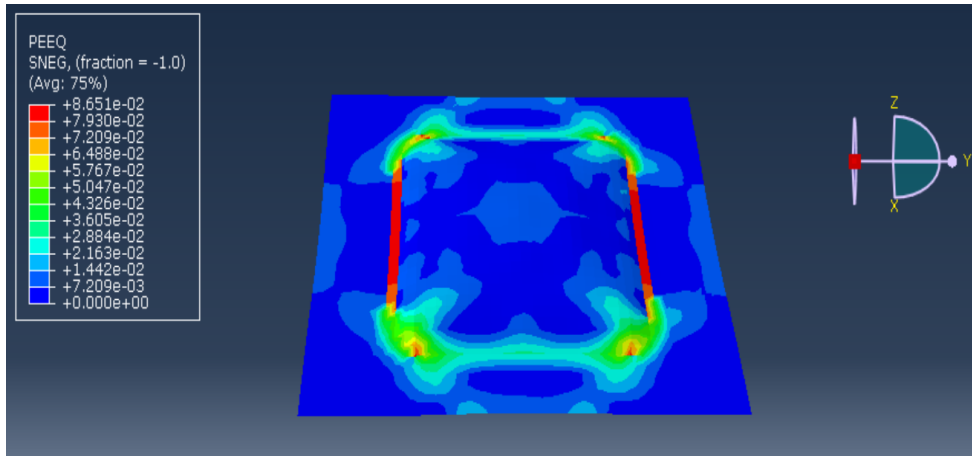
(b)

Figure 4-14 Equivalent plastic strain distribution of formed parts under different depth of curve: (a) large holding force and (b) small holding force

4.2.4.4 Effect of the surface lubrication

The surface lubrication is a major factor affecting the material flow, stress and strain distribution of formed parts apart from the holding force. It is determined by the coefficient of friction of contacting surfaces. To investigate its effect on the shape performance, two different coefficients of friction were assigned as contact properties in simulation, whose values are set as 0.02 for lubricated surfaces and 0.17 for unlubricated surfaces [132] [124]. Other parameters were kept constant for the aluminium alloy 1050-H14 sheet blank with a forming depth of 16mm, a spring stiffness of 8.79daN/mm and rubber thickness of 4mm on each side. Figure 4-15 shows that the increase of the coefficient of friction can reduce the sliding of the material for large deformation, resulting in an increase of Mises stress at contact area. These increased internal stresses at the critical wrinkle and indentation area may cause the sheet blank to crack more easily.

77
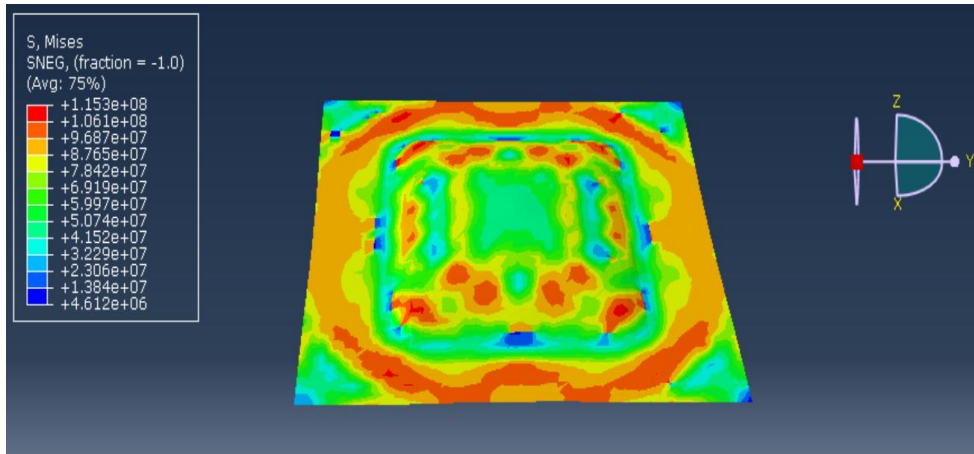
(a)
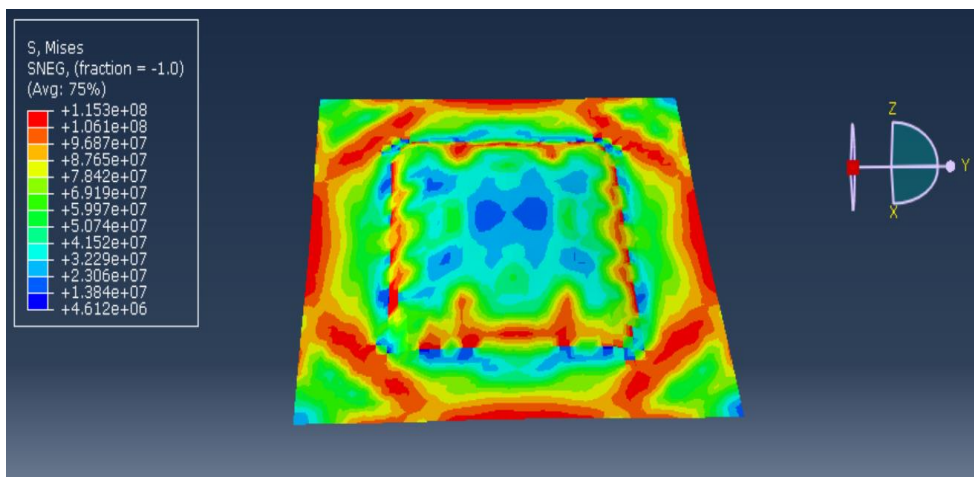
(b)

Figure 4-15 Mises stress (unit:Pa) of formed parts: (a) coefficient of
friction 0.02 and (b) coefficient of friction 0.17

Figure 4-16 shows the equivalent plastic strain distribution under different
lubrication conditions and the results prove the Mises stress distribution.
When the lubrication oil is applied, the reduction of the equivalent plastic
strain may be due to a more uniform force distribution on the blank. These
variations may affect the indentation of the formed parts and the
lubrication oil should work with the correct holding force. The simulated
equivalent strain is also larger than the tested material maximum
elongation due to the strain rate sensitive effects.
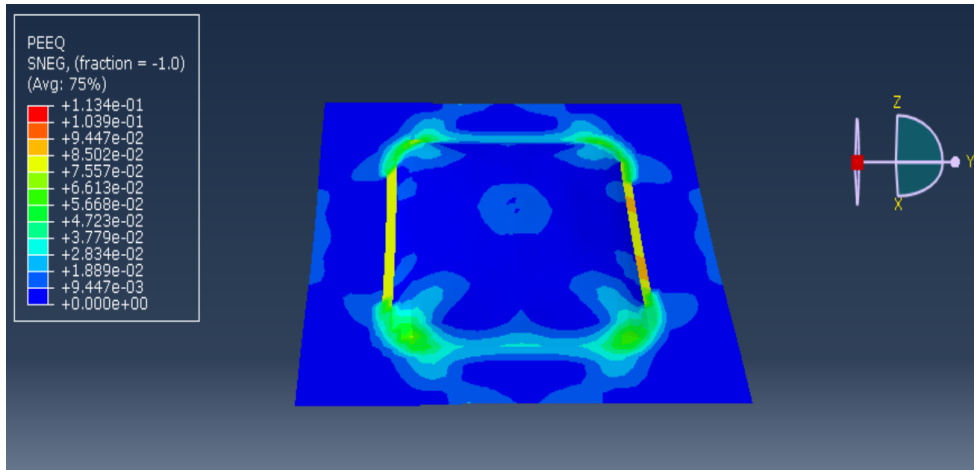
(a)
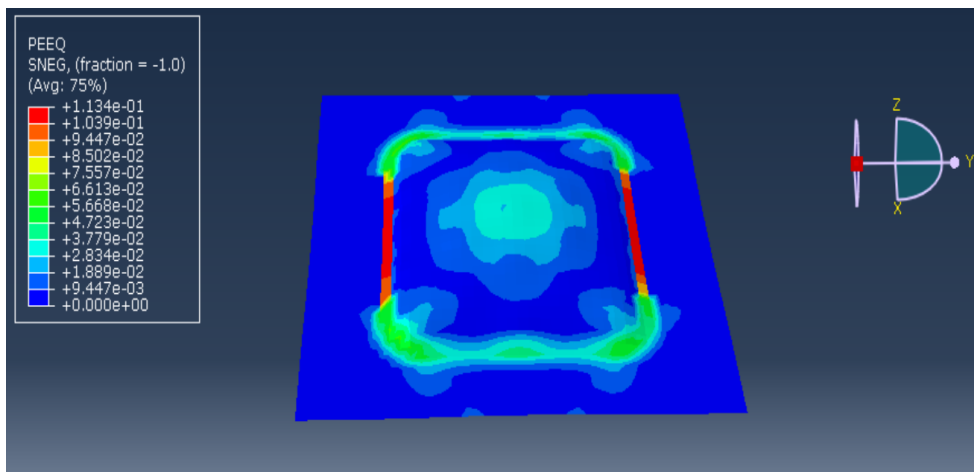
(b)

Figure 4-16 Equivalent plastic strain distribution of formed parts: (a) coefficient of friction 0.02 and (b) coefficient of friction 0.17

4.2.4.5 Effect of the rubber cushion

The rubber cushion is used between the pins and sheet blank formed area to enable a dimpling elimination through a uniform force distribution. This section investigates the effect of rubber thickness, i.e. 4mm and 2mm, on the shape performance. Since there are two sets of pins along the ram

direction of the proposed multi-point tooling, both sides of the sheet blank should be covered by rubber cushion. Figure 4-17 and Figure 4-18 show the variation of equivalent pressure stress components distribution and equivalent plastic strain on the formed parts. It can be seen that the stress components can be reduced by applying a thicker rubber cushion, especially at the critical contact spots between pins and sheet blank, although the effect of rubber thickness on the equivalent plastic strain is not significant. This proves that increasing the rubber thickness can help with a more uniform force distribution and improve dimpling problems.
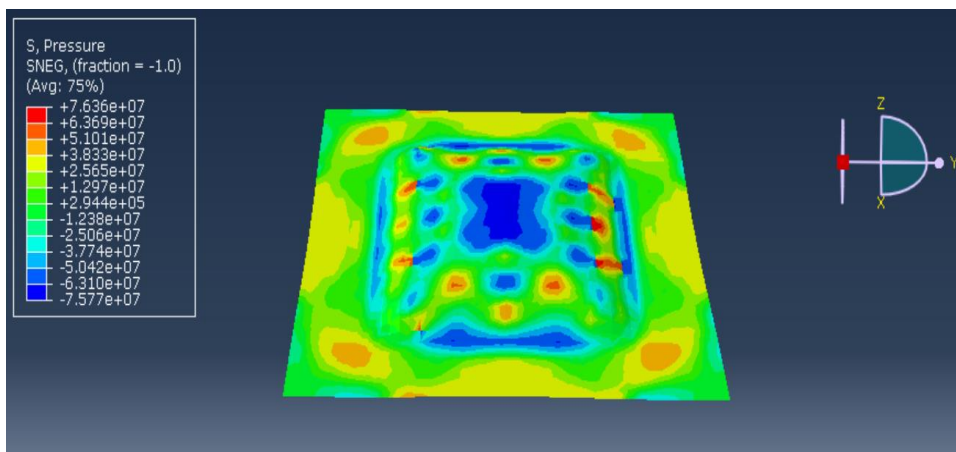
(a)
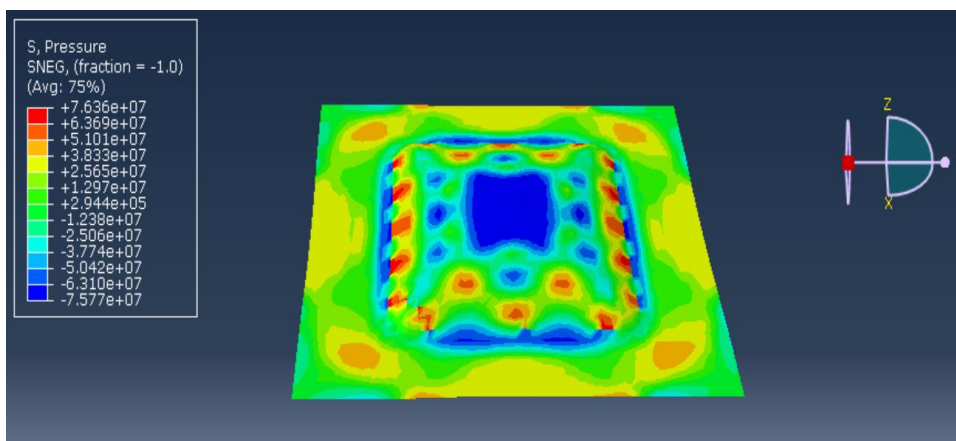
(b)

Figure 4-17 Equivalent stress components distribution (unit: Pa) of formed parts: (a) rubber thickness of 4mm and (b) rubber thickness of 2mm
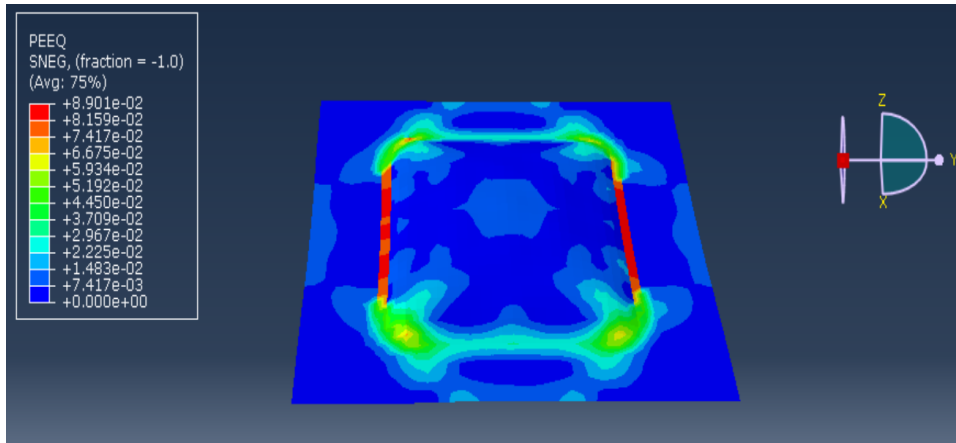
(a)
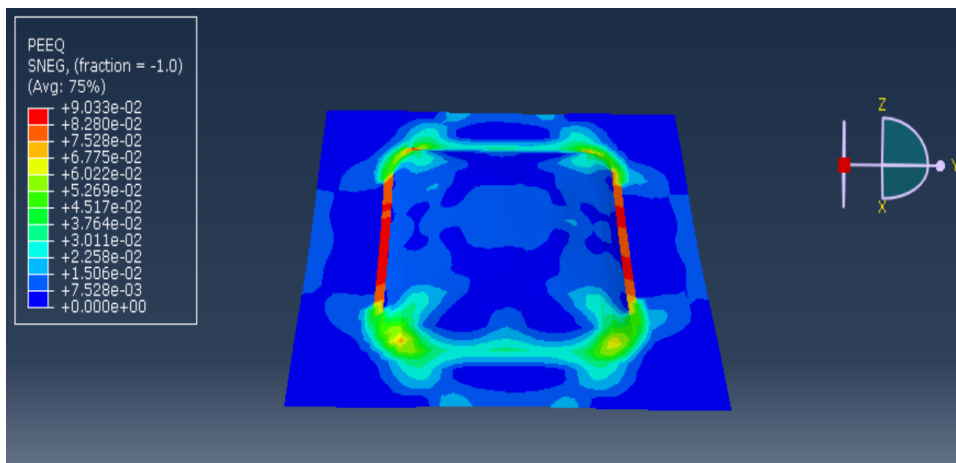
(b)

Figure 4-18 Equivalent plastic strain distribution of formed parts: (a) rubber thickness of 4mm and (b) rubber thickness of 2mm

The thickness distribution of formed parts using a rubber thickness of 4mm on each side is more uniform than those using a rubber thickness of 2mm, especially for the contact spots, as revealed in Figure 4-19. In this condition fewer indentations can be observed on the final shape. Since the cover range of the rubber cushion is only the forming area, wrinkles can still occur at the constrained edges.
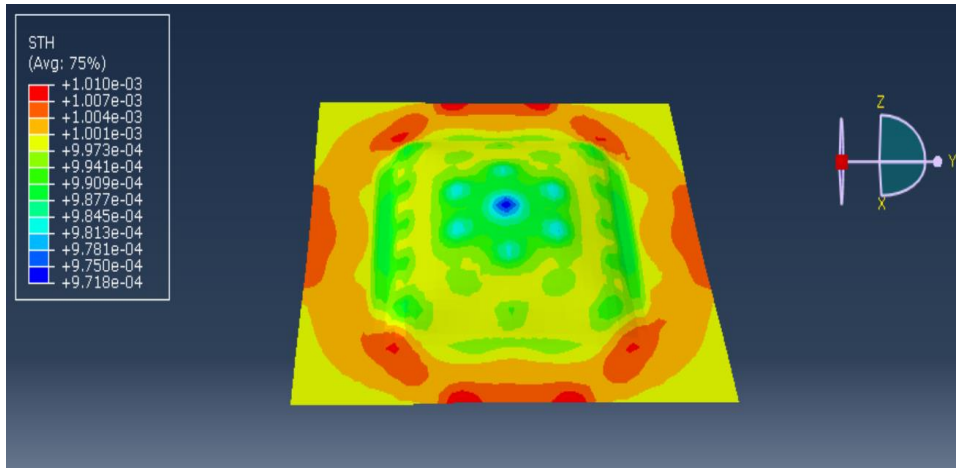
(a)
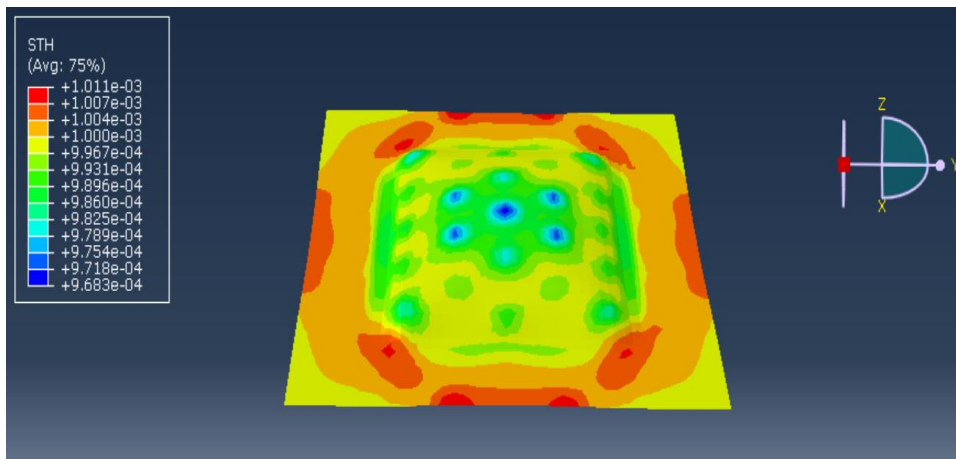
(b)

Figure 4-19 Thickness distribution (unit: m) of formed parts: (a) rubber thickness of 4mm and (b) rubber thickness of 2mm

4.2.5 Discussion

In this section finite element modelling was employed for the cold multi-point tooling deep drawing to investigate the effect of different parameters on shape accuracy. By comparing the results of the formed profile, stress, stretch, pressure and thickness distribution, the importance of forming curve depth, material properties, blank holder holding force, lubrication condition and thickness of rubber cushion was explored in order to guide

the experiment setup in the following chapter. An optimal combination of these process parameters should be considered together for a better performance.

4.3 Modelling of multi-point tooling deep drawing of heat-treated and cooled blanks

Although modelling of cold multi-point tooling deep drawing proves its superiority as a flexible forming technology at room temperature, for high strength materials it may require large press forces and may damage the tool before forming to the desired shape. Since hot forming has proven to be an efficient method for improving the formability of such high strength alloys, we would like to employ the multi-point tooling with heated sheet blanks. To study the formability improvements, a finite element modelling of multi-point tooling deep drawing using heat-treated high strength materials was introduced in this section. These high strength sheet blanks were heat-treated and cooled with different cooling rates and numerical simulations of deep drawing were conducted for room temperature. A feasibility investigation of formability improvements of high strength alloys was conducted for further experiments.

4.3.1 Material properties and damage definition

The blank material is set to be aluminium alloy 6082-T6 with a dimension of 200 mm * 200 mm * 1.5mm in terms of length, width and thickness, whose mechanical properties from tensile tests can be found in Chapter 3. Different heating and cooling procedures were applied to the sheet blanks to investigate the effect of cooling rate on the material formability. Figure 4-20 shows the mechanical property of AA6082 in terms of stress and strain in three groups, i.e. SHT and NC, SHT and FC, SHT and EFC. The sheet blank was first heated to 480°C and maintained for 10 minutes for solution heat treatment, afterwards it was transferred and cooled to about

350°C. NC, FC and EFC refers to natural cooling, fast cooling and extra fast cooling, where the difference is cooling rate, varying from 5°C/s, 50°C/s to 100°C/s. This contributes to the differences in yield stress and UTS, which may affect the formability of AA6082 on multi-point tooling deep drawing of hot blanks.
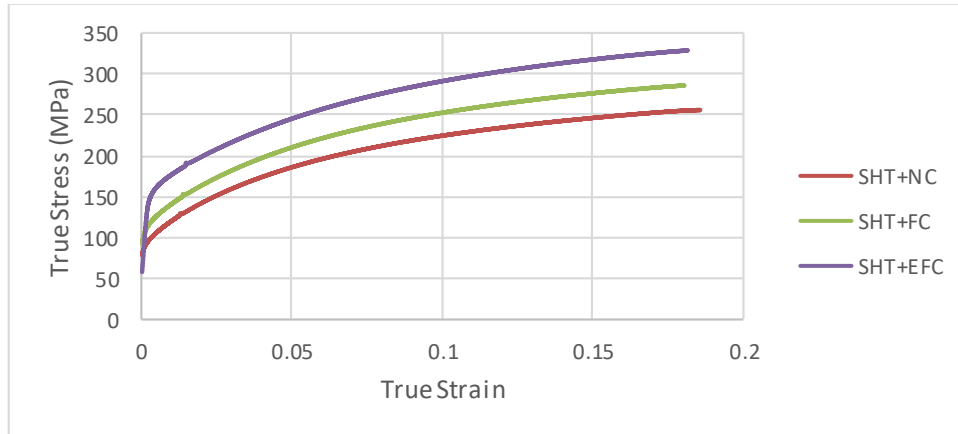
Figure 4-20 True stress-strain curve of AA6082 with different heating and cooling procedures used for finite element material definition

In Figure 4-21 the plotted forming limit diagram (FLD) of heated AA6082 is given [206]. The test was conducted by Shao and other researchers at hot stamping conditions using a novel biaxial testing system. Although there is slight difference with our simulation conditions, this can provide a guidance on the formability performance of heat treated and cooled sheet blanks. In simulation the data from the plotted curve in Figure 4-20 was input into the property definition table in Abaqus, together with the data of the forming limit diagram (FLD), to investigate the effect of cooling rate on sheet blank formability.
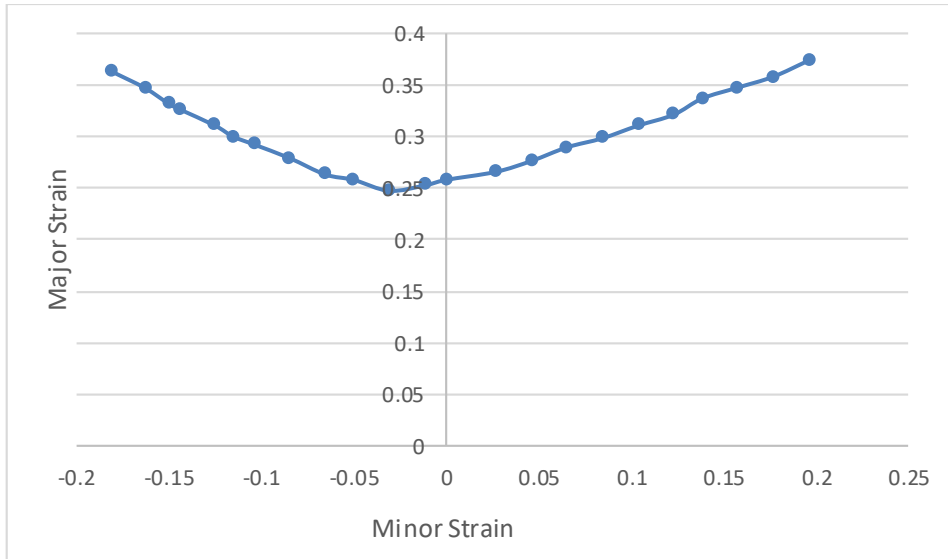
Figure 4-21 Forming limit diagram (FLD) of AA6082

4.3.2 Model procedure

The assembly of the 23 tightly packed pins model is similar to the one in the previous section but without the use of rubber cushions, in order to investigate the performance at the critical section. The pin height was set the same on each side for this model instead of the dome-like shape, to make the four corner edges as the critical area in which to observe the fracture. A 20mm forming depth was selected which was enough to see the damage initiation. Figure 4-22 presents the global FE model in Abaqus where the pins, blank holders and blank sheet were specified as an analytical rigid body, discrete rigid body and deformable solid elements respectively. 1600 S4R (4-node doubly curved thin shell with reduced integration) elements were generated for the blank sheet. The coefficient of friction between contact surfaces was 0.02. Boundary conditions of the system were the same as the cold deep drawing system in previous section. The maximum and minimum in-plane principal strain can be output for fracture investigation. The analysis was set as dynamic explicit so that better convergence can be achieved.

85
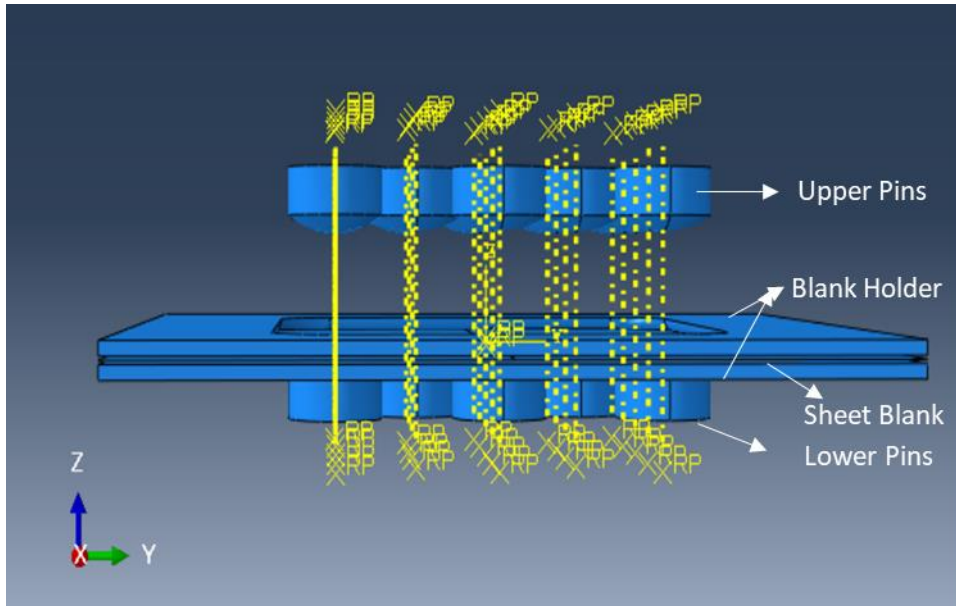
(a)
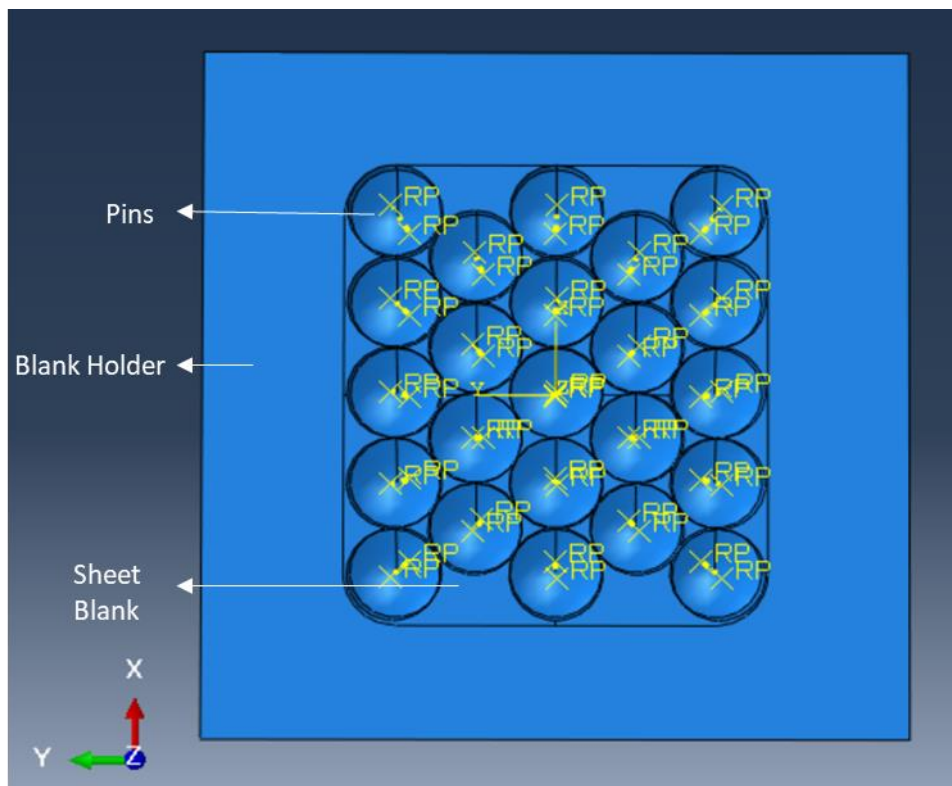
(b)

Figure 4-22 Model setup for the square plate formability test: (a) front
view and (b) top view

4.3.3 Numerical results and discussion

4.3.3.1 Equivalent pressure stress distribution of the formed parts

Figure 4-23 shows the equivalent pressure stress components distribution on the formed parts and it is believed that the four corners and edges of the formed region are the most critical section for blank sheets with any cooling rate. Although the maximum tensile and compressive stress increases with the increased cooling rate due to the tested yield stress and UTS, they are much smaller than those in T6 condition. So there is little influence on the tool life under different cooling rates, but the effect of cooling rate on formability should be illustrated through a damage initiation parameter.
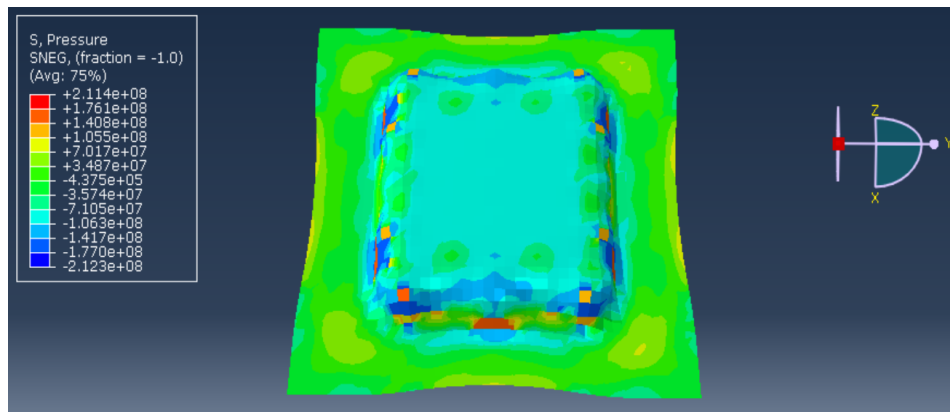
(a)
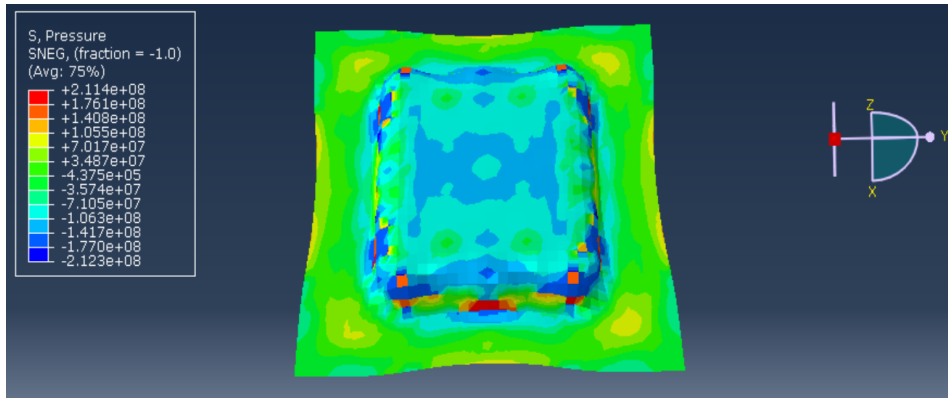
(b)
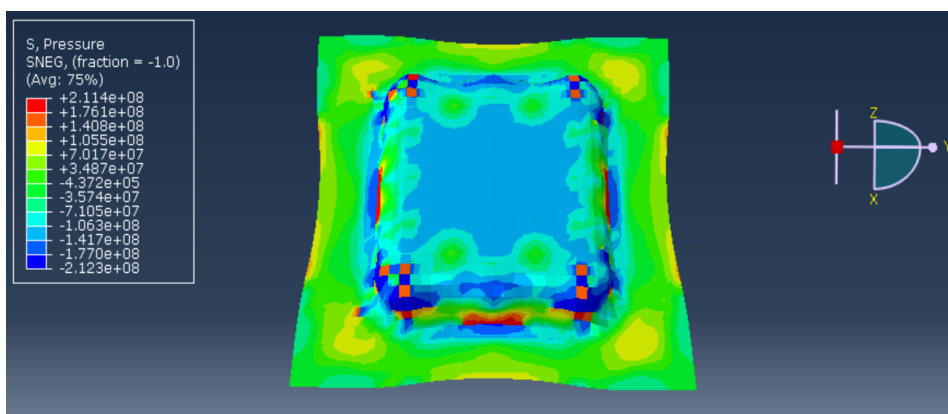
(c)

Figure 4-23 Equivalent stress components distribution (unit: Pa) of
formed parts: (a) SHT+NC, (b) SHT+FC and (c) SHT+EFC

4.3.3.2 Forming limit diagram and damage initiation criterion

In Figure 4-24 FLDCRT is the maximum value of the FLD damage initiation criterion which is intended to predict the onset of necking instability in sheet metal forming. It refers to the ratio of the current major principal strain to the major limit strain on the defined forming limit diagram to present the deformation state. Generally a value of 1 or greater for output variables associated with a damage initiation criterion indicates that the criterion has been met. If damage evolution is defined to be associated with the FLD damage initiation criterion, the value of maximum

FLDCRT is limited to 1. Otherwise, the criterion for damage initiation will continue to be computed beyond the point of damage initiation; in this case the output variable can take values greater than 1, indicating by how much the initiation criterion has been exceeded. In this modelling we mainly focus on the initiation condition of formed parts with different heating and cooling methods. But it should be noticed normally for stretch loading, much greater strains can be achieved than those marked on the forming limit diagram.
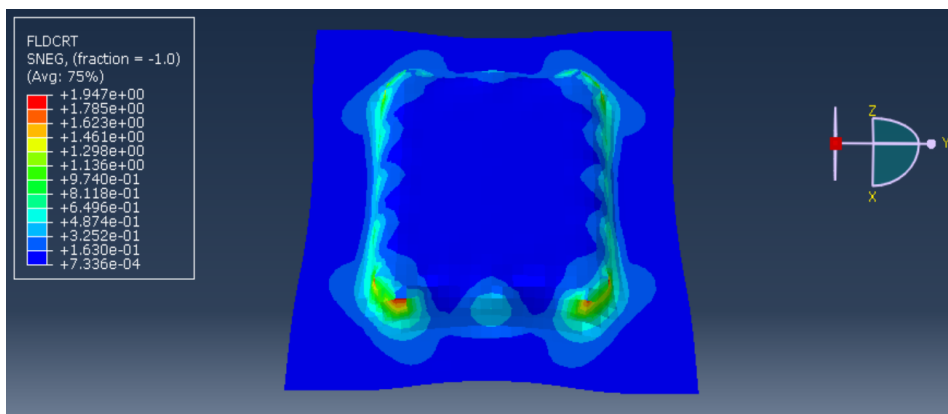
(a)
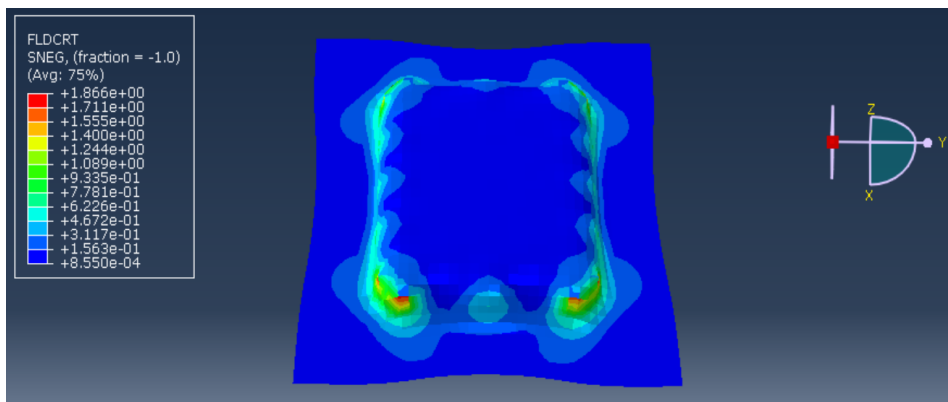
(b)
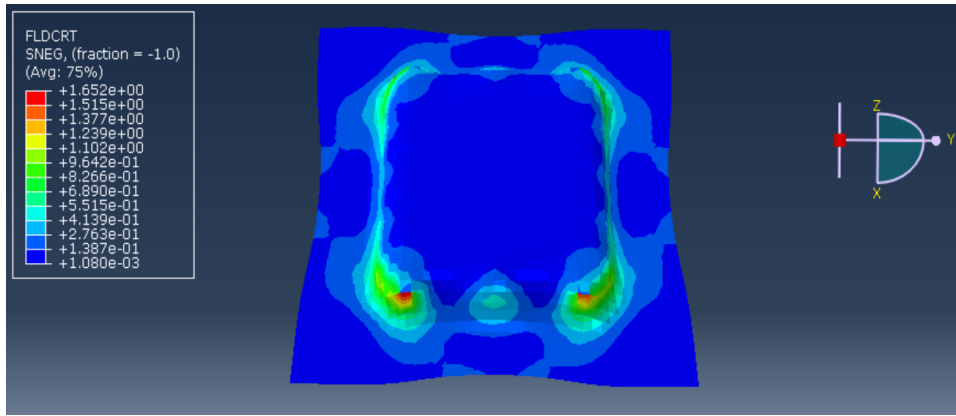
(c)

Figure 4-24 Maximum value of FLD damage initiation criterion at the
final shape: (a) SHT+NC, (b) SHT+FC and (c) SHT+EFC

Figure 4-24 illustrates the extent of damage initiation after forming to a depth of 20mm. By comparing the FLDCRT values, it is realized that the excess of the damage initial criterion is reduced with increased cooling rate. This can provide guidance that under the same forming conditions, samples treated with an extra fast cooling method (cooling rate 100°C/s) have the best formability performance, although the pressure is the largest.

Figure 4-25 shows the FLDCRT of samples with different cooling rates at the time step when the natural cooling sample meets the damage initiation criterion. At this moment the FLDCRT value for fast cooling and extra fast cooling samples do not exceed 1, which means they do not start to damage at the critical area. However, damage is easier to initiate for samples treated with fast cooling if the forming process continues. This illustrates that increasing the cooling rate can improve the formability of hot stamped sheet blanks for complex and large deformation.
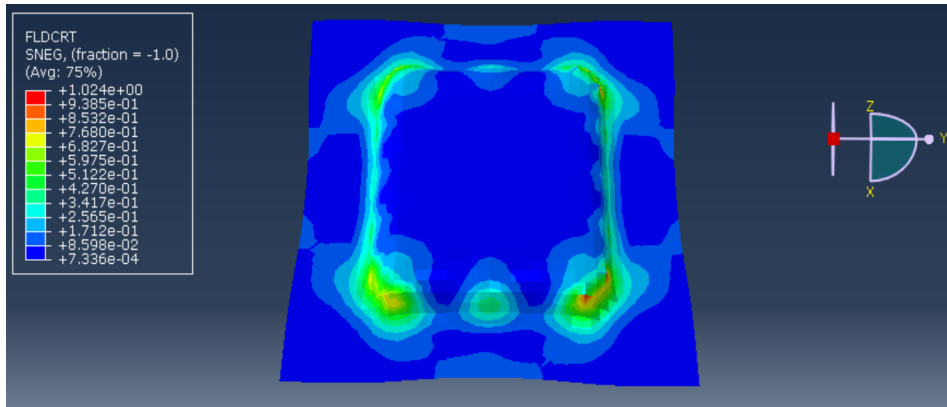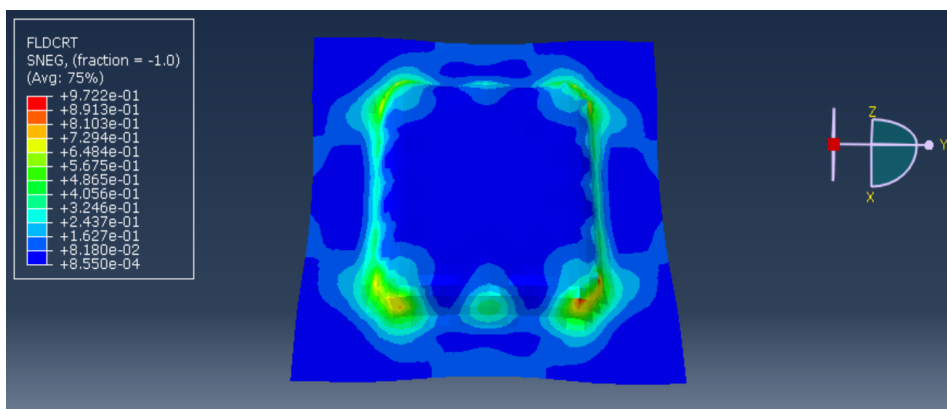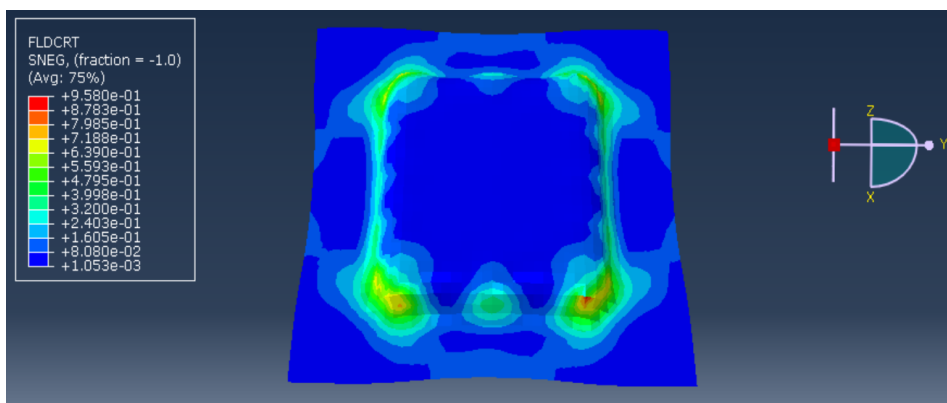
Figure 4-25 Value of FLD damage initiation criterion at a time step of 0.8: (a) SHT+NC, (b) SHT+FC and (c) SHT+EFC

4.3.3.3 In-plane principal strains at the critical section

Since the stress and strain distribution from four corners of the formed area are most critical, Figure 4-26 shows a path with 100 nodes selected at one corner whose maximum and minimum principal (in-plane) logarithmic strains at any specific time step are plotted in the forming limit diagram.
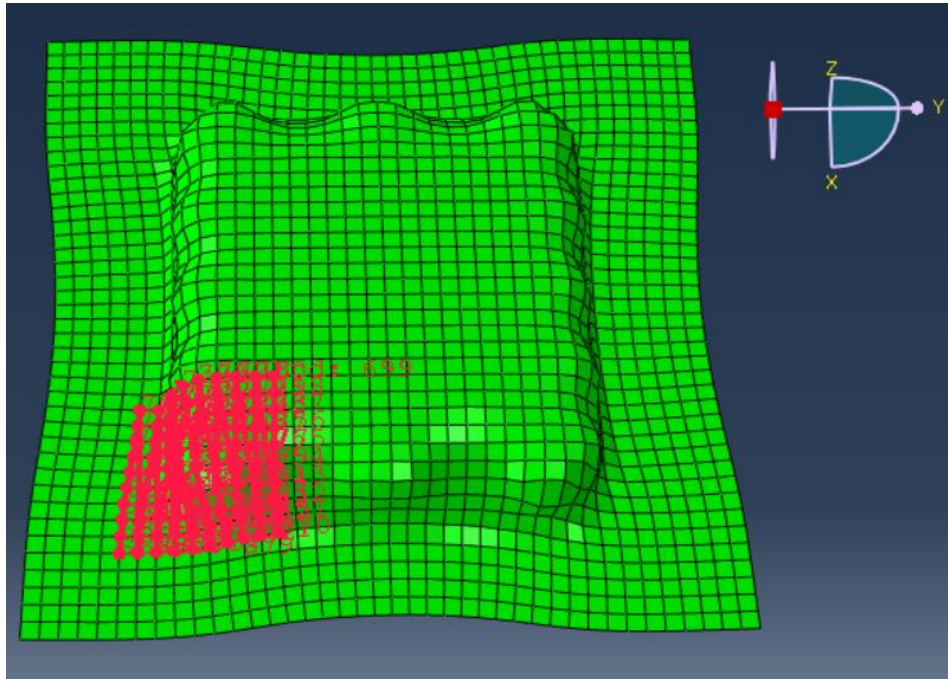
Figure 4-26 Path of nodes selected for strain output

(a)
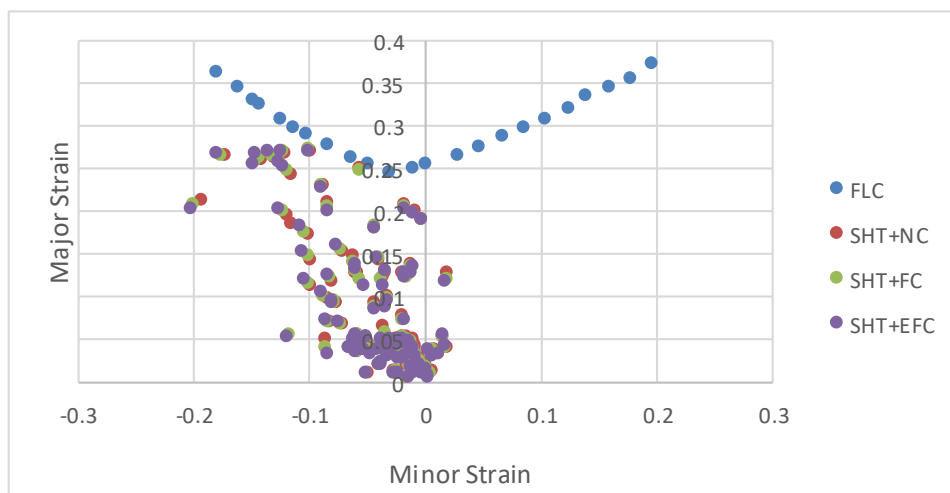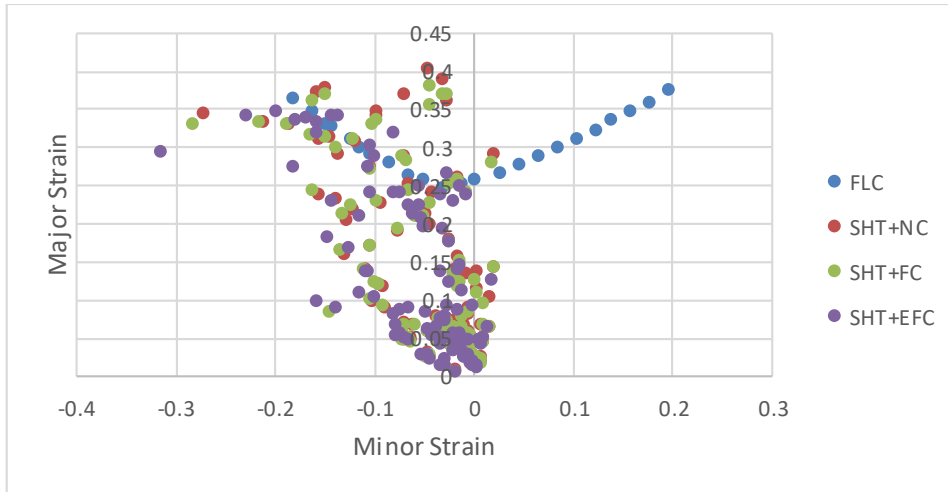
(b)

Figure 4-27 Deformation state of selected nodes in forming limit diagram: (a) forming depth of 17mm and (b) forming depth of 20mm

In Figure 4-27, the position of each selected node is plotted in the forming limit diagram in terms of minor principal strain and maximum principal strain. The principal strain of some plotted nodes are larger than the maximum defined elongation (0.2) because of the strain rates sensitivity effect of the material which is related to the press forming velocity. The blue dots represent the forming limit curve obtained from literature [206]. When the sheet blank is formed to a depth of 17mm, damage starts to initiate for some nodes, although all the nodes locate in the safe region. When formed to the final shape, damage occurs on all samples. However, it can be seen that for all the nodes in the damage region, damage is more severe with decreased cooling rate.

4.4 Summary

In this chapter a finite element method was employed in two forming processes using multi-point tools. Firstly a cold multi-point forming model of dome-like samples was proposed to investigate the effects of factors such as forming depth, sheet blank material, holding force, coefficient of

93

friction and rubber thickness, on the final shape performance. By comparing the simulated variables, it was found that reducing the coefficient of friction and increasing the holding force properly can help with the wrinkling avoidance, while increasing the rubber thickness promotes a reduction in indentations. However an optimal combination plan of all factors is necessary for each specific test group according to the required formed shape and sample material. Then due to the formability limitation of high strength material, a modelling of multi-point tooling deep drawing was conducted using AA6082 sheet blanks which were heat treated and cooled with an innovative 'fast cooling' process design. The cooling rate varies from 5°C/s, 10°C/s to 100°C/s so that the formability improvements can be observed and discussed. It is believed that increasing the cooling rate can help with the formability performance before damage initiated and can also save sheet blank preparation time. Although the model simulates the forming at room temperature which is separated from the fast cooling process, it is able to provide guidance for experiment setup, combining hot forming with multi-point tools, and using our proposed 'fast cooling' concept. During experiments the formability should be better because rubber is used with a thermal insulation layer and the sheet blank is hot formed using the multi-point tools.

Chapter 5 Cold Multi-Point Tooling Deep Drawing Experiment

5.1 Introduction

The need for a sheet forming process with adjustable dies has grown rapidly due to flexible operations and different surface requirements. Many studies have been conducted on the superiority of MPF. However, wrinkles and cracks may appear if the loading and holding pressure is not appropriate, the focus of this work is examination of a multi-point forming process for the forming of miniature sized components when they are applied to deep drawing. A finite element analysis has been conducted before setting up experimental tests. In this chapter a deep drawing operation with a multi-point tooling test rig was developed for the study. During the experiments a simple variable method was used to study the influences under different variable conditions, i.e. variations of the depth of curvatures, sheet metal selection, holding force, surface lubrication, and use of rubber as cushions. The formed parts were measured with a coordinate measuring machine (CMM) and the indentations were observed so that a relationship to the process variables can be established. The process of the experiments is described and the results are presented, being followed by describing the measurement method and the analysis carried out.

In Section 5.2 the MPF equipment is introduced with a detailed setup and pin configuration. Then related parameters containing material, influence factors and measurement methods are illustrated in Section 5.3. Those influence factors are classified into groups for comparison. After comparing the experimental formed profile with simulation results, in Section 5.4 the relationship between these factors and surface quality are given on the trend, together with comments for further investigation.

5.2 Experimental equipment

Figure 5-1 shows a multi-point forming test rig which is newly developed in the University of Strathclyde to study possible material and process variations and associated quality and control when thin sheet metals are drawn into various cap shapes, being focused on small sized components. This MPF system was designed using the commercial software SolidWorks and assembled in the university lab. This system consists of 23 tightly packed adjustable dome-like pins with an hexagon cross-sectional area column for each of top and bottom punch-set, with detailed arrangement shown in Figure 5-2. The bottom punch is fixed to the base, while the movement of the top punch is controlled by hydraulic force in the vertical direction along the guide pillars. The heights of the pins can be adjusted by a screw thread and using a spanner. Further the movements of these vertical pins can be controlled numerically. Four blank holders are attached to the top punch-set to control the sliding of the sheet metal along the surface of the die-plate during the forming process.

When the system is pressed down, the equivalent reaction force is provided by two changeable springs, which limits the distance range of the top punch movement. From the design sketch, the diameter of each dome head projection image is 26 mm, so the area of deformed sheets covered by the pins in this system is about 125 mm * 112 mm. All the tests below are conducted with this multi-point tooling system.
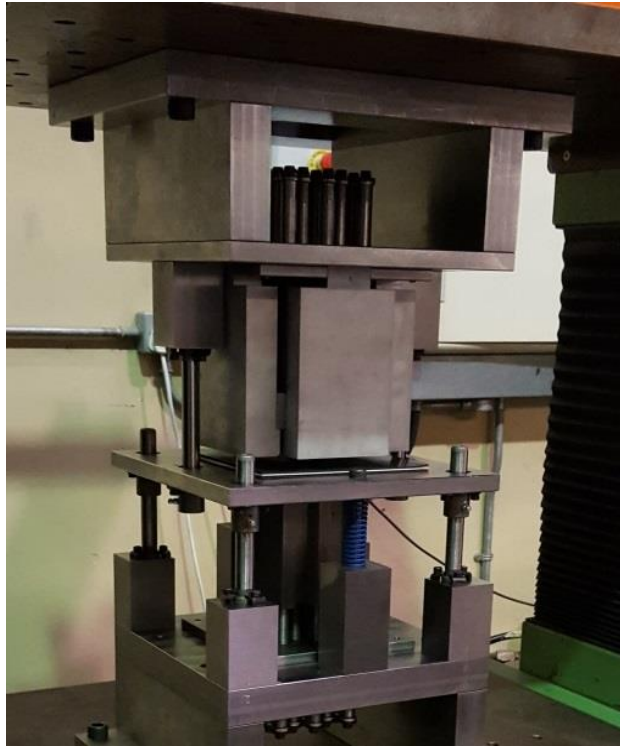
Figure 5-1 The MPF used for the experiment reported
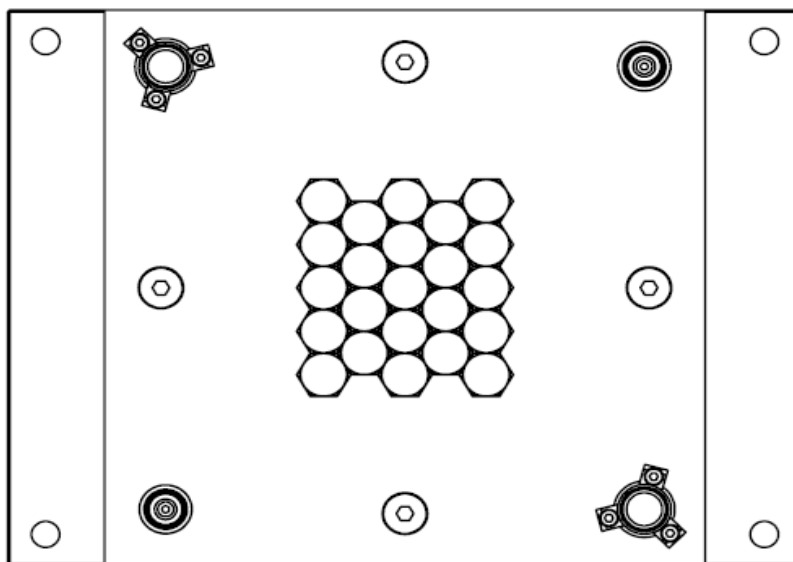
Figure 5-2 The arrangement of the movable pins for each punch-set

5.3 Design of experiment

5.3.1 Materials preparation

In this experiment, effects of sheet material and geometry, lubrication condition, thickness of rubber cushions, holding force to the test sheets, and curvatures to be formed, on the formed component geometry and surface quality, have been investigated to quantify their influences on the final finished sheet metal parts.

For the experimental materials, aluminium alloy 1050-H14 and low carbon steel sheets with the thickness of 1 mm were used as raw materials, each being cut into the size of 200 mm * 200 mm. The choice of thickness considered the balance between surface quality as well as formability. In this case there is enough area to be held down by the blank holders during the forming process without affecting the deformation area. The mechanical properties of these two materials can be obtained through tensile tests for material selection analysis and computer simulation, details of the tensile test results were explained in Chapter 3. Those sheet metal cap parts were formed with two different dome-like finish curvatures, the depth of which at the centre were taken 8 mm and 16 mm respectively, considering the movement range as well as deformation effects. The holding force was varied by varying the holding springs, with the spring strength of 8.79 daN/mm and 3.8 daN/mm respectively used to distinguish wrinkle effects during the process. It should be noted that the holding force is not constant but increased with the press springs. A type of multi-purposes cutting oil was applied to the interfaces between the blank and the die-plate for lubrication. Polyurethane with thickness of 2 mm and 4 mm was chosen for the elastic cushions due to its good hyper-elastic property. Because both sides of the sheet plate were contacted by the pin heads, they were both covered by the cushions. For a better contrast

between the main variables and to avoid confusion when conducting the experiment, symbols of plus and minus are used as shown in Table 5-1.

Table 5-1 Main material/process/tool variables in MPF

Blank Material	Lubrication	Rubber Thickness	Spring Strength	Curved Depth
[+] Aluminum	[+] Applied	[+] 8 mm	[+] 8.79 daN/mm	[+] 16 mm
[-] Steel	[-] Not Applied	[-] 4 mm	[-] 3.8 daN/mm	[-] 8 mm

Before the test, the machine was set to the pre-defined stroke ensuring that depth of the curved surface was controlled to enable the specific curvature finish to be achieved. After each test the formed parts were ejected from the system and labelled for further recognition. Lubricating oil was cleaned after each test to ensure the similar surface contact condition for each test trial. When the tests finished, the formed sheet metal parts were measured with a coordinate measuring machine (CMM) and the indentations on the surface were observed with a high resolution camera to obtain the displacement profile as well as wrinkle conditions. The Mitutoyo 5-axis CNC CMM used in this experiment is shown in Figure 5-3. Any analysis later is based on these test results.

Figure 5-3 Mitutoyo 5-axis numerical control CMM

5.3.2 Tool setting

Since there are two different combinations for each of the five kinds of material, tooling and processing variables, a simple variable method is necessary to make the comparison reasonable. Taking the test marked as test 1 with all process variations with 'plus' remarks, i.e. a combination of 16 mm curved surface depth aluminium alloy sheet at the centre with lubrication oil applied, a total thickness of 8 mm rubber cushions with each side half covered, under the large holding force supplied by springs with a stiffness of 8.79 daN/mm, as the base model for each comparison group. The unique test number is labelled on every test piece for easy configuration. Thus a total of 32 experimental tests have been conducted. The variable arrangement for each test number is shown in Table 5-2.

Table 5-2 Variable setting arrangement plan

Test Piece	Blank Material	Lubrication	Rubber Thickness	Spring Strength	Curved Depth
1	[+]	[+]	[+]	[+]	[+]
2	[-]	[+]	[+]	[+]	[+]
3	[+]	[-]	[+]	[+]	[+]
4	[-]	[-]	[+]	[+]	[+]
5	[+]	[+]	[-]	[+]	[+]
6	[-]	[+]	[-]	[+]	[+]
7	[+]	[-]	[-]	[+]	[+]
8	[-]	[-]	[-]	[+]	[+]
9	[+]	[-]	[+]	[-]	[+]
10	[-]	[+]	[+]	[-]	[+]
11	[+]	[+]	[+]	[-]	[+]
12	[-]	[-]	[+]	[-]	[+]
13	[+]	[+]	[-]	[-]	[+]
14	[-]	[+]	[-]	[-]	[+]
15	[+]	[-]	[-]	[-]	[+]
16	[-]	[-]	[-]	[-]	[+]

17	[+]	[+]	[+]	[+]	[-]
18	[-]	[+]	[+]	[+]	[-]
19	[+]	[-]	[+]	[+]	[-]
20	[-]	[-]	[+]	[+]	[-]
21	[+]	[+]	[-]	[+]	[-]
22	[-]	[+]	[-]	[+]	[-]
23	[+]	[-]	[-]	[+]	[-]
24	[-]	[-]	[-]	[+]	[-]
25	[+]	[+]	[+]	[-]	[-]
26	[-]	[+]	[+]	[-]	[-]
27	[+]	[-]	[+]	[-]	[-]
28	[-]	[-]	[+]	[-]	[-]
29	[+]	[+]	[-]	[-]	[-]
30	[-]	[+]	[-]	[-]	[-]
31	[+]	[-]	[-]	[-]	[-]
32	[-]	[-]	[-]	[-]	[-]

In order to make pre-adjustment of the pin heights more convenient, two 3D printed sample parts were used as reference surfaces to align the pin heights. These parts were designed to fit the dimensions of the test system

102

as smooth surfaces whose depths at the centre were 8 mm and 16 mm respectively as shown in Figure 4-3. With this method, it is economic and fast to match representing surface contours when pre-setting the pin heights. The depth of the pin movements needs to be confirmed before testing because when the press is lowered beyond the pre-set position the test piece will change or damage regardless of the blank holders, rubber or lubrication. A scale should be drawn on the shoulder screw to allow the press to reach the same depth every run.

5.3.3 Parts measurement and inspection

After sheet blanks were formed under different conditions, the surfaces were measured using CMM. 19 * 19 evenly distributed points which covered the whole sheet area. They were measured consecutively along each side in a straight line with a space of 5mm and the coordinates on specific lines were plotted smoothly in Excel to illustrate the surface curvatures. Wrinkles and indentations were observed from the photos taken by the high resolution camera, indicating the relationship of these to the influences from different process and material variables. To make the comparison efficient and clear, taking test 1 as the base with all 'plus' marks, 5 more tests with only one 'minus' mark were chosen to study the influences of every variable, i.e. test 2, 3, 5, 11 and 17. Their Z-axis coordinates across the centre line profile of X-axis and Y-axis were plotted to investigate the largest surface deformations in a clear way.

Taking the ideal 3D printed dome-like surface in Figure 4-3 as a reference surface, in each group the shape error z_{error} is used to determine the difference at every contact point of the centre line contour, integrating the average shape error value E_{error} for each metal sheet. These parameters are defined as follows, being similar to that reported in [127] [156] [129]

$$z_{error} = z_{3Dtest} - z_{exp} \tag{5.1}$$

By calculating the root mean square value of the shape error above between the 3D printed dome-value and the test piece surface with different thickness, the average shape error value, E_{error}, can be given as

$$E_{error} \tag{5.2}$$
$$= \sqrt{\frac{1}{N} \sum_{i=1}^{N} \left(z_{i3Dtest} - z_{iexp}\right)^2}$$

Where N represents the total number of the measured points. It should be noticed only the values of deformed parts from adjustable pins are calculated, because the shape error of edge parts pressed by blank holders can be affected by the wrinkles. The indentation is compared based on observation.

5.4 Experimental results and discussion

5.4.1 Comparison with FE simulation

The experimental formed parts from MPF system were compared with the finite element model. The experimental profiles of sheet shapes in Z-axis along the central line of X-axis and Y-axis were plotted and compared with the simulated profiles under different process parameters, shown in the following figures. From Chapter 4 and Chapter 5, the process parameters

are specified as blank material type, lubrication condition, rubber thickness, holding force and deformed curve depth. An example of 'test piece 1' in Table 5-2 is selected as shown in Figure 5-4.

Figure 5-4 Picture of formed test piece 1
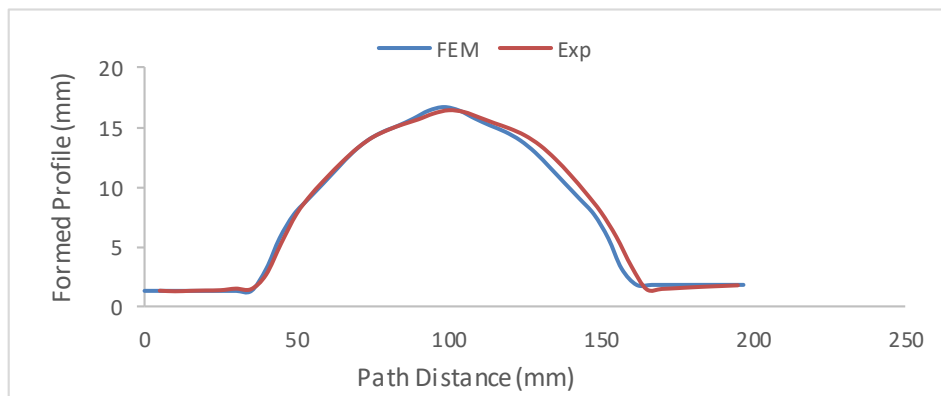
(a)
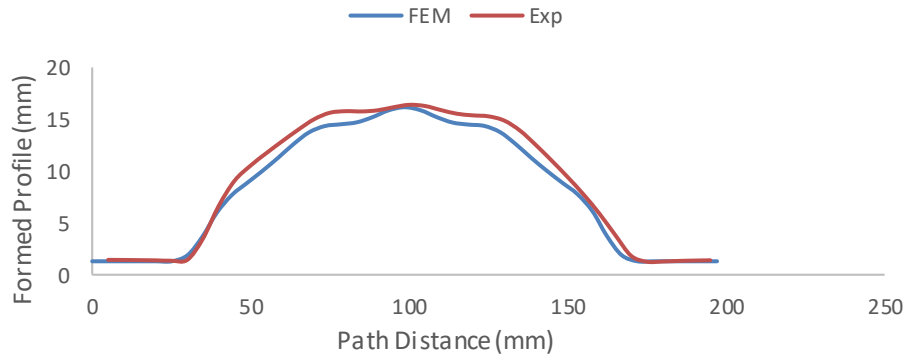
(b)

Figure 5-5 Final profile comparison on Test 1: (a) along central X-axis
and (b) along central Y-axis

Figure 5-5 shows the final profile curves of simulated and measured sheet blanks along two central lines and good agreement is made with few differences. This proves the feasibility of simulation results.

The wrinkle conditions on the edges of MPF metal sheets can be reviewed through the equivalent strain distribution as shown in Figure 5-6, and indentations pressed by the pin heads can be observed on pressure contour plots from finite element analysis, which is illustrated in Figure 5-7. The changes in equivalent strain reflect deformation on the edge, which is captured from Figure 5-6. The red regions in Figure 5-7 reveal the indentation areas where stress instability occurs because of sheet surface contraction under the actions of pin heads.
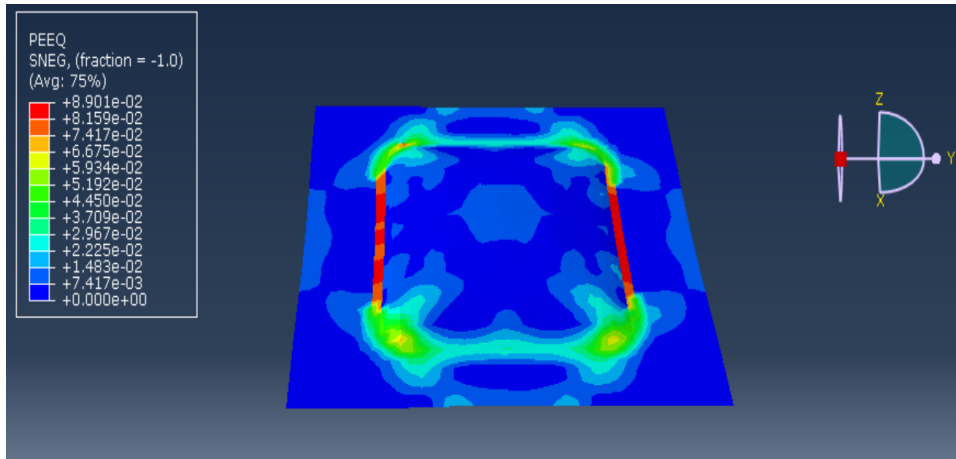
Figure 5-6 Equivalent strain distribution of test piece 1
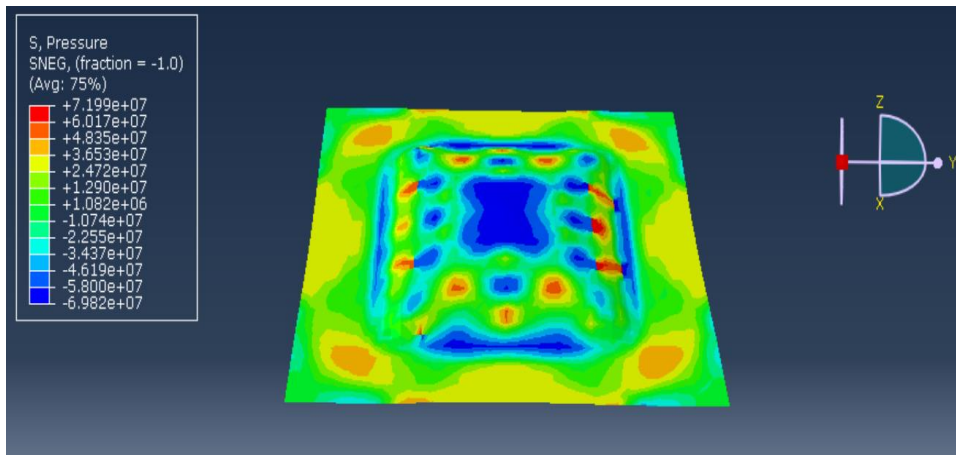
Figure 5-7 Equivalent stress components distribution (unit: Pa) of test piece 1

5.4.2 Effect of the test materials

To study the effect of material properties, the experiment was conducted using commonly seen aluminium alloy and steel sheets with a thickness of 1 mm, under the same conditions. Two formed metal sheets are shown in Figure 5-8. More wrinkles and indentations can be found in steel sheets as seen in Figure 5-8(b), while aluminium sheets provide smoother surfaces.

These may be related to the differences of the material's mechanical properties, such as plasticity, yield strength, UTS, etc, and hence, the drawing ability of those two materials. These are revealed from tensile test results conducted in Chapter 3.

(a)   (b)

Figure 5-8 Formed test pieces: (a) aluminium-test piece1 and (b) steel-test piece 2
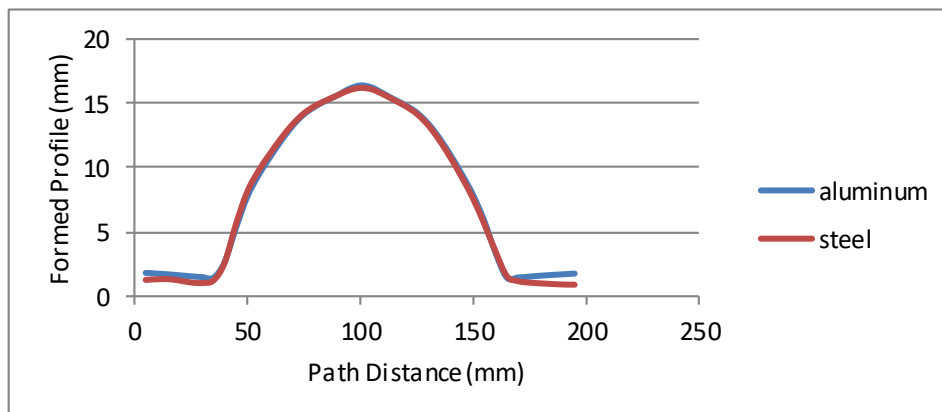
(a)
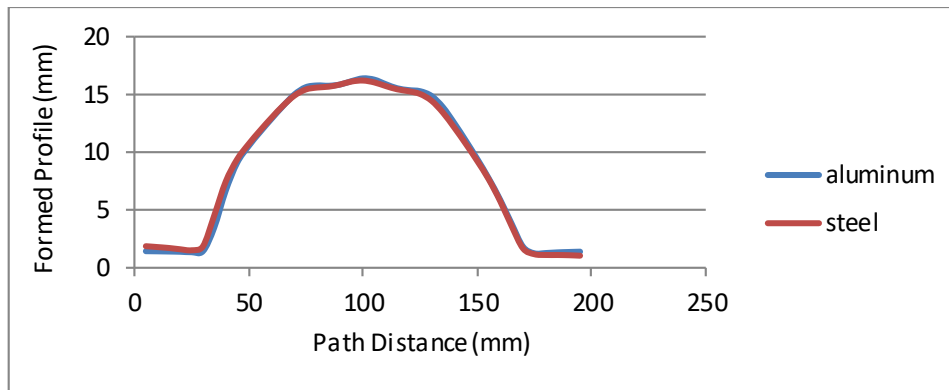
(b)

Figure 5-9 Z-axis direction measured profile of aluminium and steel
parts: (a) along X-axis and (b) along Y-axis

Figure 5-9 presents the surface profiles drawn based on the points
measured in the vertical direction along the centre line of X-axis and Y-
axis respectively. The two profiles are similar, due to similar plastic
deformation enabled during the experiment which follows the profiles set
by the pins. The calculated average shape error values for aluminium
sheets in the central line are 1.085 mm and 0.775 mm along X-axis and Y-
axis respectively, while these are 1.105 mm and 1.005 mm for steel sheets.
In general these are similar, but the steel parts have more shape errors,
which may be accounted for by combined effects from the materials' yield
strength, Young's modulus as well as deflection amount of the tooling due
to the forming force difference, etc.

5.4.3 Effect of the lubrication condition

A multi-purpose cutting oil was used to perform lubrication between the
blank and die-plate. The pictures of the formed test pieces are shown in
Figure 5-10. It appears that the wrinkles could be slightly reduced at the
edge due to using the lubricant, which may be due to a more uniform

109

holding force applied to the blank. Another influencing factor is the surface quality of the blank improved by introducing a lubrication oil. From the coordinates profile shown in Figure 5-11, the influences seem not to be too significant in the deformed dome area since no lubrication oil is applied to that area. The average shape error value is similar but slightly reduced under lubrication conditions, from 1.143 mm to 1.085 mm in the x direction and from 0.982 mm to 0.775 mm in the y direction, which may be due to the reduction of the forming force when the lubrication oil is applied. From above the lubrication oil mainly deals with wrinkle problems at the edges where pressed by the blank holders.

(a)   (b)

Figure 5-10 Formed test pieces: (a) lubrication oil applied-test piece 1 and (b) lubrication oil not applied-test piece 3
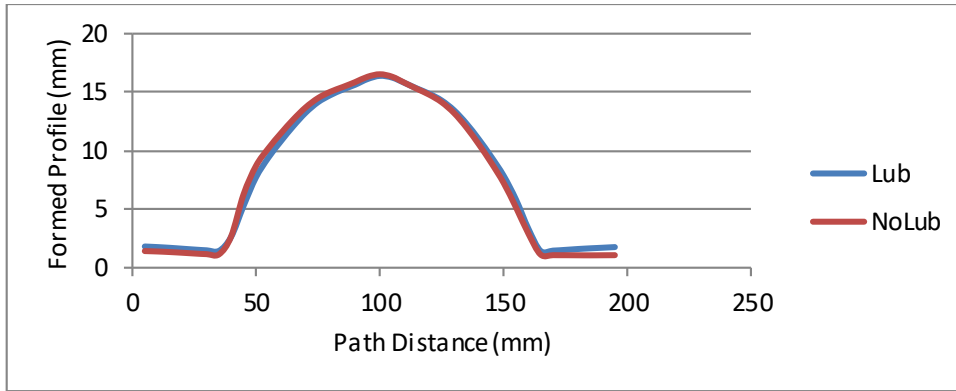
(a)
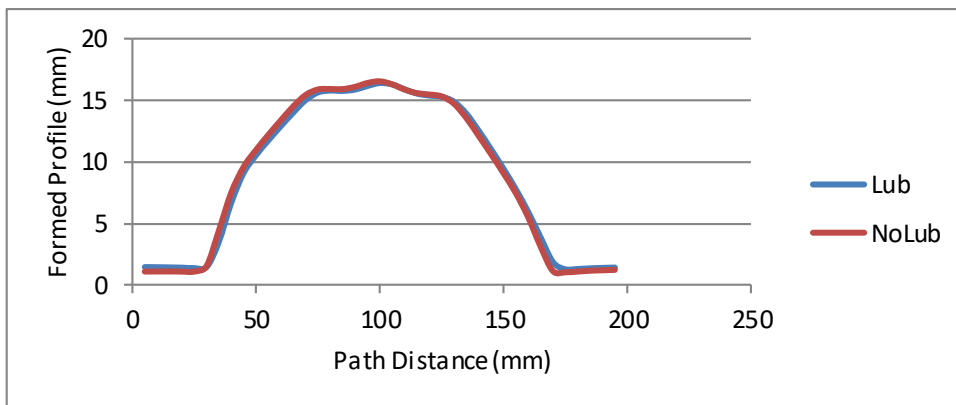
(b)

Figure 5-11 Z-axis direction measured profile with and without lubrication oil: (a) along X-axis and (b) along Y-axis

5.4.4 Effect of the thickness of rubber cushion

During the multi-point forming process, elastic rubber has been used between the pin tools and the sheets to reduce the dimples and indentations. More indentations can be observed for the sheet part with a total of 4 mm thick cushions, as shown in Figure 5-12(b), comparing to that with 8 mm thick cushion (shown in Figure 5-12(a)), which shows that increasing the

111

thickness of the cushion could reduce the occurrence of surface indents. Nevertheless, shallow wrinkles are still found on both sheet parts, since the cushions do not cover the blank-holding areas. Figure 5-13 also illustrates that the profile off the centre line that corresponds to the 8 mm thick cushion is slightly larger than that with the 4 mm cushion, which may be due to a larger forming force applied to achieve a similar shape when the cushions are thicker. Another factor is that the thickness takes up some spaces of the press stroke. This results that the test pieces do not reach the ideal shape when the press reaches the pre-defined depth for every run, thus an error compensation should be considered when the pin heights are pre-set initially.

(a)   (b)

Figure 5-12 Formed test pieces: (a) 8 mm thick rubber-test piece 1 and (b) 4 mm thick rubber-test piece 5
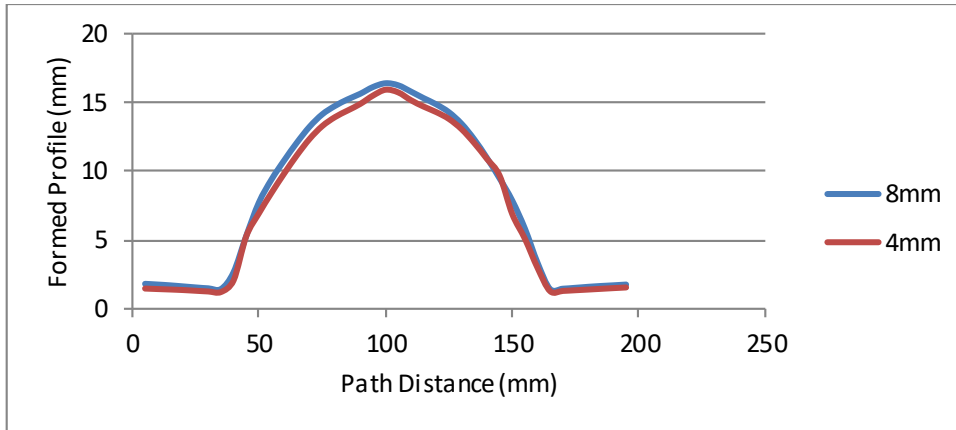
(a)
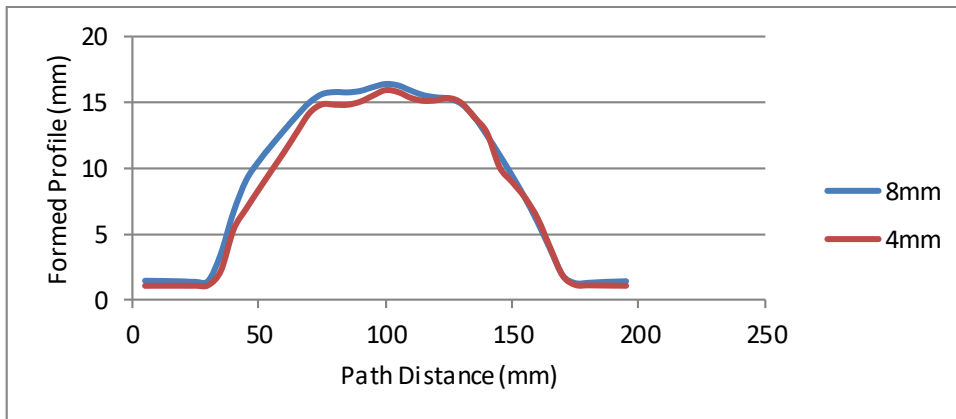
(b)

Figure 5-13 Z-axis direction measured profile for two different rubber thickness: (a) along X-axis and (b) along Y-axis

5.4.5 Effect of the holding force

The effect of the holding force is examined through the reaction force on the supporting springs with different stiffness values. The sliding of the

blank material was controlled during the forming process in order to achieve drawn parts with different surface finish. The photos shown in Figure 5-14 demonstrate the importance of using a correct holding force to reduce or eliminate the occurrence of wrinkles along the flanges of workpiece while the surface quality of the drawn parts could also be improved. (Figure 5-14 and Figure 5-15). At the same time, overstretching of the sheet metal should be avoided in order to reduce fracture development in the indented areas, if the cushion to be used is too thin. This shows that an optimal combination of the material, tooling and process parameters is needed for a particular part to be formed. It is especially the case for forming of thinner sheet metals and with relatively large pin-tool sizes when miniature components are to be formed. The pin-size reduction will be restricted so as to be not too small as manufacture and assembly has to be considered, even if the part-size is required to be small.
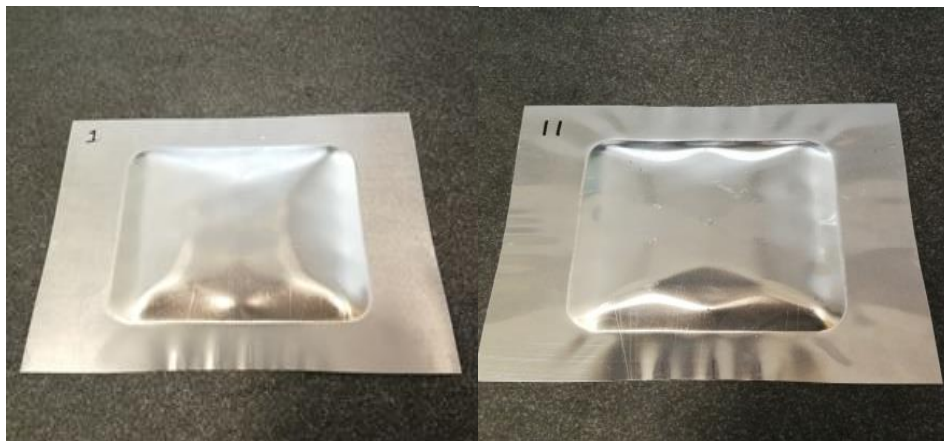
(a)   (b)

Figure 5-14 Formed test pieces: (a) spring stiffness of 8.79daN/mm-test piece 1 and (b) spring stiffness of 3.8 daN/mm-test piece 11
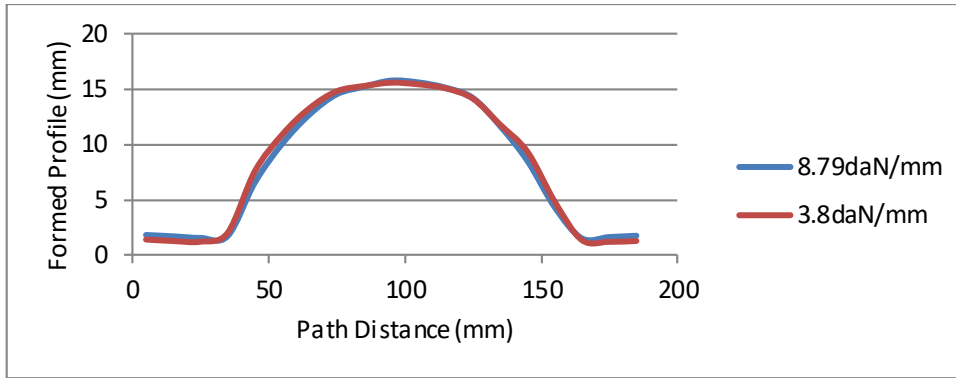
(a)
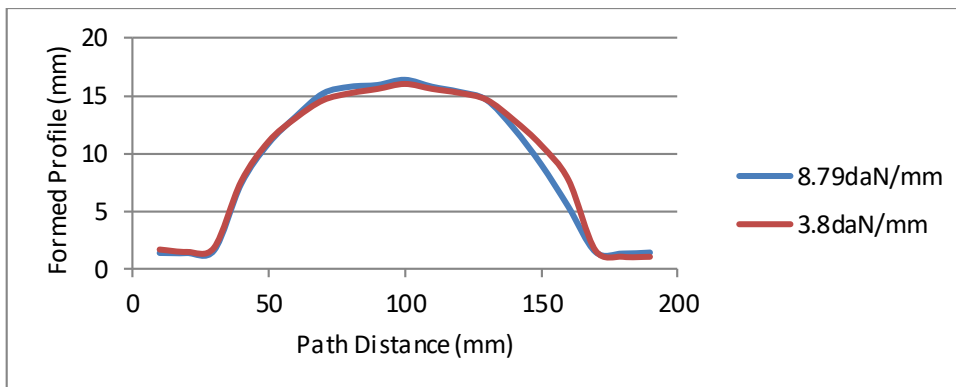
(b)

Figure 5-15 Z-axis direction measured profile with different spring stiffness values: (a) along X-axis and (b) along Y-axis

5.4.6 Effect of the depth of curvature formed

Figure 5-16 shows the formed aluminium sheet parts with a curvature depth of 16 mm and 8 mm respectively. The one with 8 mm depth shown in Figure 5-16(b) has a better finish surface, regarding both wrinkles as well as indents, because more force and deformations are applied to the sheet with the deeper curvature. The average shape error value confirms this by giving 0.804 mm and 0.4 mm at the central line in the x direction

and y direction respectively for the test piece 17, where these are 1.085 mm and 0.775 mm for the test piece 1 respectively, as illustrated in Figure 5-17. Careful attention should be paid when deeper and steeper surfaces are to be formed in multi-point forming, especially at the force concentration areas.

(a)   (b)

Figure 5-16 Formed test pieces: (a) 16 mm depth curvature-test piece 1 and (b) 8 mm depth curvature-test piece 17
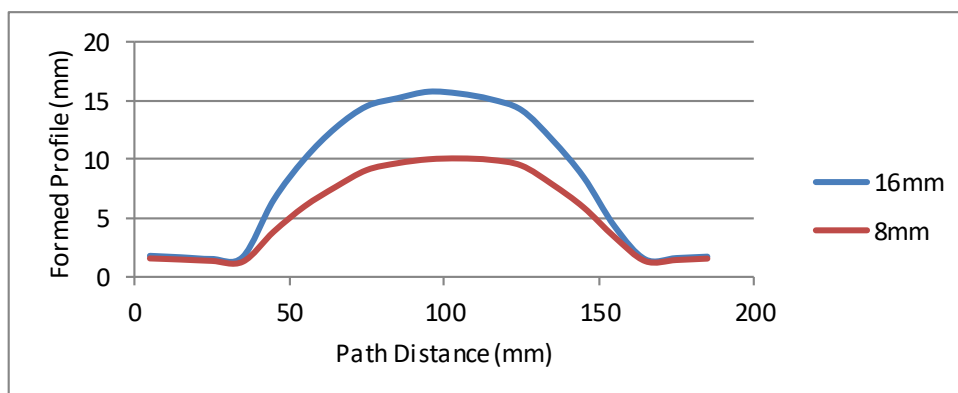
(a)
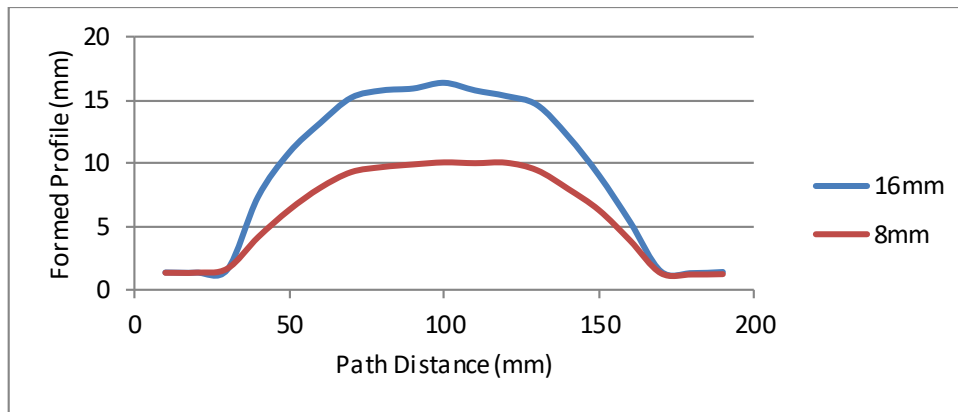
(b)

Figure 5-17 Z-axis direction measured profile with different curvature
depths: (a) along X-axis and (b) along Y-axis

5.5 Summary

The combination of deep drawing and multi-point tooling has been tested
for the forming of miniature sized, thin metal parts with a view to
extending the merits of the multi-point forming technique for sheet metal
forming. The following conclusions may be drawn from the study
described above:

- Combining multi-point tooling into a deep drawing process could
  potentially bring benefits for process and tool flexibility for deep
  drawing. However quality control has to be addressed as an important
  issue since the sheet metal deformation mechanism becomes more
  complex.

- For the process configuration tested, under the similar conditions, a
  better surface finish was achieved for the aluminium sheets, compared
  to that for the steel sheets. This may be due to drawing force applied

117

through the multi-punches used for the forming of the aluminium sheets was smaller than that for the steel sheets.

- Using lubrication could help to improve the material flow and to reduce the forming force requirement. The test cases showed that an average shape error value of 0.058 mm and 0.207 mm reduction was obtained along the two central lines for the 16.0 mm depth curved surface formed when a lubrication oil was introduced, compared to that with non-oil used.

- Using cushions is extremely important for forming thin sheet metal parts when multi-point tooling is used, and is even more important when it is used in deep drawing due to the deeper curvatures being formed, compared to simple bending and low-level deformation stamping involving multi-point tooling.

- A correct holding force is important for deep drawing. It can, nevertheless, be said to be crucial for ensuring a high quality product, considering that the contacts between the punches and the sheet metal are not uniformly distributed, even when the cushions have been used, which leads to more complex stretching and local deformation mechanisms.

- The depth of the curvature to be formed has a significant effect on the surface finish, i.e. wrinkles and indents may occur where large or steep deformations take place. The average shape error value was reduced significantly from 1.085 mm and 0.775 mm in X and Y axis direction respectively, when 16.0 mm curvature depth was formed, to 0.804 mm and 0.400 mm respectively, when 8mm depth formed

- Using 3D printing to create a model sample part to help pre-setting the multi-point tooling is an efficient approach for practical use for multi-point forming.

Finally, the results mentioned above show that careful control of process parameters and machine setup for the forming of thin sheet metals for a particular type of material and geometry is needed prior to multi-point forming. Further tests on hot forming under different geometries and compared variables can be conducted, with a focus on the thinner sheet metals and small sized components.

Chapter 6 Hot Multi-point Tooling Deep Drawing Experiment

6.1 Introduction

The influence of various factors on the surface performance using cold multi-point tooling deep drawing has been studied numerically and experimentally in Chapter 4 and Chapter 5 for materials of lower yield strength as well as UTS. However, using the same tooling, there are significant challenges when forming ultra-high strength aluminium alloy at room temperature. To solve this problem, the Centre for Precision Manufacturing (CPM) in the University of Strathclyde has been working on enhancement of Al-alloy hot forming technology with a fast cooling process for many years. This allows structural parts that have been previously manufactured from cold-formed aluminium to instead be produced from hot-formed high strength aluminium alloy. This can contribute to a reduction of material thickness and component weight, and at the same time the strength of the material and impact safety are improved. The idea of the fast cooling system is to realise an intermediate 'fast cooling' step between solution heat treatment (SHT) and forming in the existing production line. A prototype production line combining fast heating and cooling with multi-point tools was developed and it was further upgraded with improved process control, reliability, repeatability and system robustness. In this chapter the working principle of the proposed idea is illustrated first. Then an overview of the prototype line is given followed by a detailed illustration of each part, especially the design of the intermediate cooling system. To conduct a better cooling and forming performance with enhanced control and measurement, some key improvements and modifications are introduced. Several forming tests of square plates are conducted to investigate the formability improvement using the proposed prototype production line.

6.2 Working principle

The basic work principle of the hot forming is solution heat treatment and intermediate cooling and forming, as shown in Figure 6-1. High strength aluminium alloy is first heated to about to about 480 °C (SHT temperature) in a furnace and held there for a while (10 minutes usually), then the hot blank is transferred to the contact cooling plate for a short time to perform the fast cooling from approx. 480 °C to 350 °C under various cooling rates, before it is formed in the multi-point tools to the desired shape when in-die quenching occurs. Subsequent washing and artificial aging processes can be applied for final products.
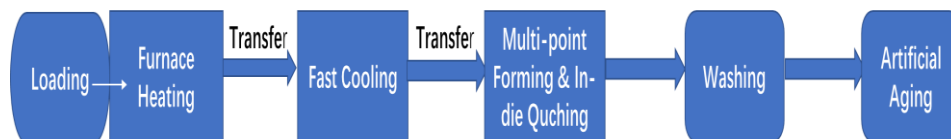
Figure 6-1 Flow chart of the working principle

The temperature profile of the process chain is given in Figure 6-2. The temperature increases to the solution heat treatment temperature in a short time (usually 7 to 10 mins) and is maintained for a while. A fast intermediate-cooling step is used to enable the preservation of the obtained optimal micro-structure during solution heat treatment, this cooling should be fast and controllable. Cooling rate can be controlled by changing the initial setting temperatures on the contact plates. The temperature will also drop when formed in the multi-point tools, but there is little damage to the tool during the process because the heat can be exported quickly. It should be noticed that there is a small temperature drop during transfer so it must be quick to minimise this.
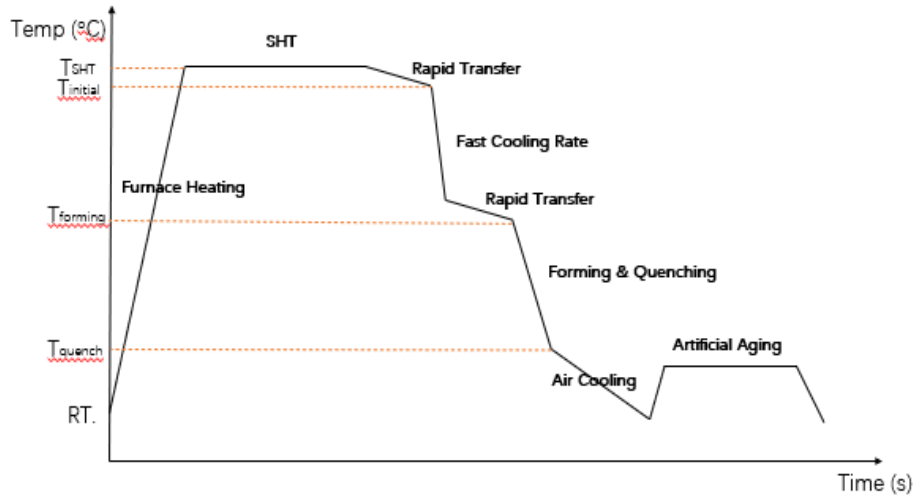
Figure 6-2 Temperature profile of the process chain

6.3 Equipment updating for hot forming

The multi-point tooling hot forming with fast cooling system consists of a furnace box, a control and measurement panel, and an integrated hydraulic press with a fast cooling tool and a multi-point tooling system, which is shown in Figure 6-3. Table 6-1 gives the tool specification of the integrated hydraulic press.
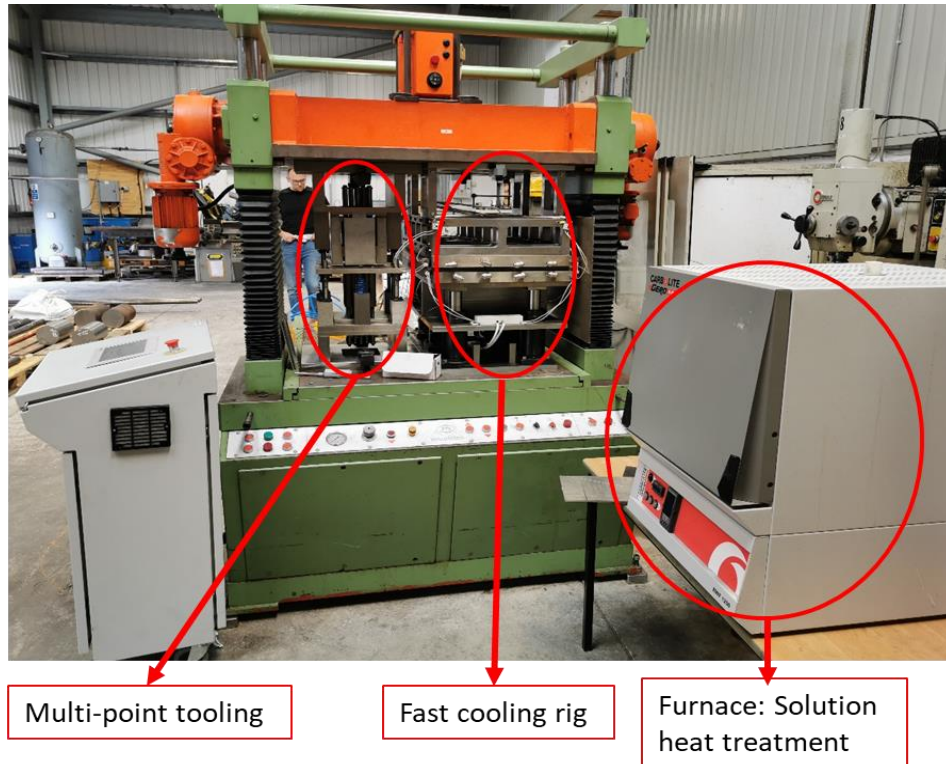
Figure 6-3 Multi-point hot forming with fast cooling system developed by the University of Strathclyde

6.3.1 Workpiece heating furnace

Figure 6-4 shows the Carbolite furnace for heating the blanks to the solution heat temperature before fast cooling takes place. From the control panel, the heating temperature can be set to any specific value up to 1000 ℃, then auto-temp recording and stabilization can be achieved. Before heating a blank, the furnace should be pre-heated to maintain a constant temperature. Since the actual temperature of the blank is lower than the air temperature in the furnace, the real-time temperature profile of the blank itself needs to be measured separately. Thermocouples are good choices by mounting one side in the corner of each test sample and connecting the other side to the Omega thermocouple/voltage input data acquisition module. Instantaneous temperature can be read directly from a

laptop through the portable USB and relative time and temperature data can be saved for future use.

Figure 6-4 Carbolite RWF 1200 furnace

6.3.2 Fast cooling system

Shown in Figure 6-5, a contact fast cooling system with a dedicated control unit has been developed. Cartridge heaters and thermocouples are used to obtain a variable die temperature. To optimise the system reliability, both software and hardware were amended many times before it was employed for the process chain. Before experiments the contact fast cooling system was firstly pre-heated to the desired working temperature through the control and measurement panel. Afterwards the temperature on the blank should increase then maintain steady through the cartridge heaters. The

temperature of the fast cooling station was constantly monitored and adjusted by an automatic control system in case a temperature difference occurs. Ideally during cooling the heat transfer from the hot blank to the fast cooling tool and the heat loss on the tool should be equalised, thus a minimal cycle time can be achieved.
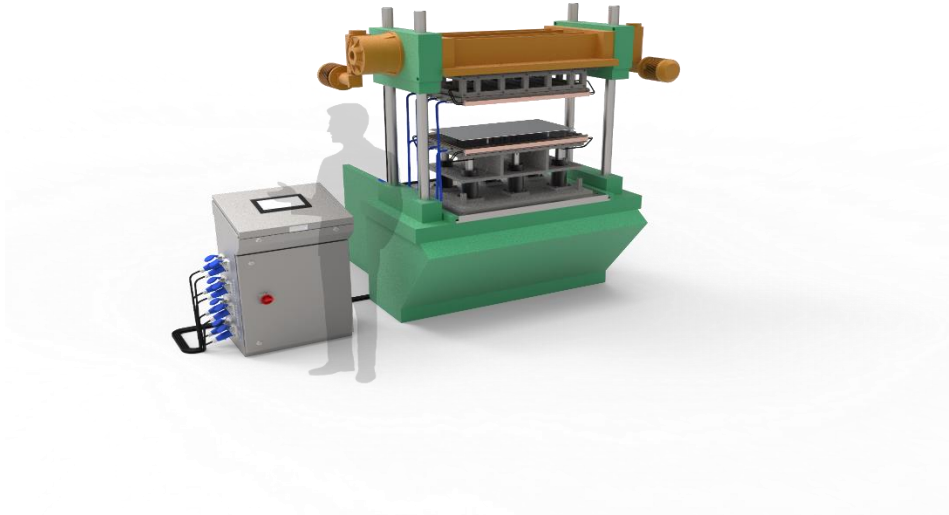
Figure 6-5 Model of the contact cooling system

6.3.2.1 Contact cooling station design

The cooling station is separated to an upper and lower die with its own cooling plate. Both dies are mounted with the movable hydraulic press and connected to the control cabinet. They are identical for a better heating and cooling performance. Figure 6-6 shows that damping components and sprung pins are designed for the lower die to lift the blank for an automated robot. The tool design allows the contact material to be changed to obtain a variety of thermal conductivities in order to achieve different heat transfer and cooling rates. In this process copper is employed for all tests due to high thermal conductivity which allows for high cooling rates. The sub-frame is thermally isolated from the cooling plate for each die in order

to reduce the thermal mass and ensure that the only hazardous components of the tool are the contact plates. The tool specification is illustrated in Table 6-1.
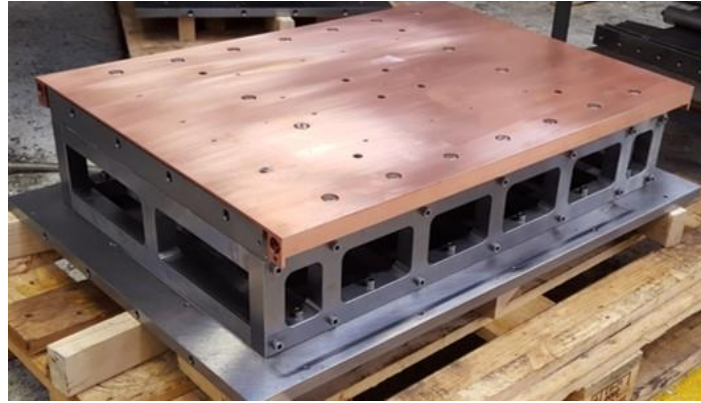
(a)

(b)

Figure 6-6 Design of contact cooling dies: (a) upper and (b) lower

Table 6-1 Tool specification

	Specification
Tool dimensions	H = 680mm; L = 870mm; W = 620mm
Maximum blank	800mm x 430mm
Maximum force	270kN
Maximum tool temp	400°C
Weight	Upper = 250kg; Lower = 350kg
Control	Automatic or manual
Catridge heaters	8 x 2kW
Thermocouples	16

Heating: Both dies feature four 2kW heating cartridges fixed within the copper contact plate. Although the plates can be pre-heated up to 400°C, the most likely temperature required would be 150-250°C and that takes around 30 minutes. The upper and lower plates are always in close contact during pre-heating to speed up the heating procedure. As the areas near the heaters will reach higher temperatures, they are situated outside of the blank cooling area preventing a reduced cooling. This is also mitigated with cascade control which will be explained in the control section.

Cooling: In the proposed process chain where the tool is in use for a sustained duration, the heat transfer from high volume stamping will begin to heat up the contact plates. Pressurized air can be channelled through the dies to cool the contact plates. When the temperature across the plate reaches the set limit, the process will engage automatically.

Damping: A number of gas springs are designed to be included in the lower die in order to provide a homogenous contact pressure distribution, whilst also reducing the impact from a faster industrial press. A maximum of six gas springs can be fixed and their capacity can be selected across a wide range. The gas springs also make the tool flexible for operators to use side-by-side with a forming tool, such as a multi-point forming tool in this project. Tool heights will have to be within a 70mm range of each other to ensure both dies can close.

6.3.2.2 Temperature measurement and control unit

The control cabinet shown in Figure 6-7 situated adjacent to the tool is designed for temperature control and data recording. It can be used either in a manual state, or in an automatic state which can meet industrial requirements. A maximum of sixteen thermocouples can be connected to the cabinet to measure live temperatures. All measured data and controlled functions can be displayed on the main operating screen in Figure 6-8 or sent to a server through ethernet. Cascade control is used by the software under an automatic state and six thermocouples integrated within each cooling plate can regulate the heating cartridges according to a set temperature. This ensures each cartridge is independently controlled for a homogenous temperature distribution across both plates. Then the cartridge can be cut off automatically once the temperature at the heating cartridge reaches its limit. However, it is designed to reduce the power gradually but not shut off completely if only the centre of the cooling plate is approaching the limit but the heating cartridge is under the limit. A further four thermocouples are integrated within sprung pins to record the temperature throughout the process.

Figure 6-7 Control unit of the fast cooling system
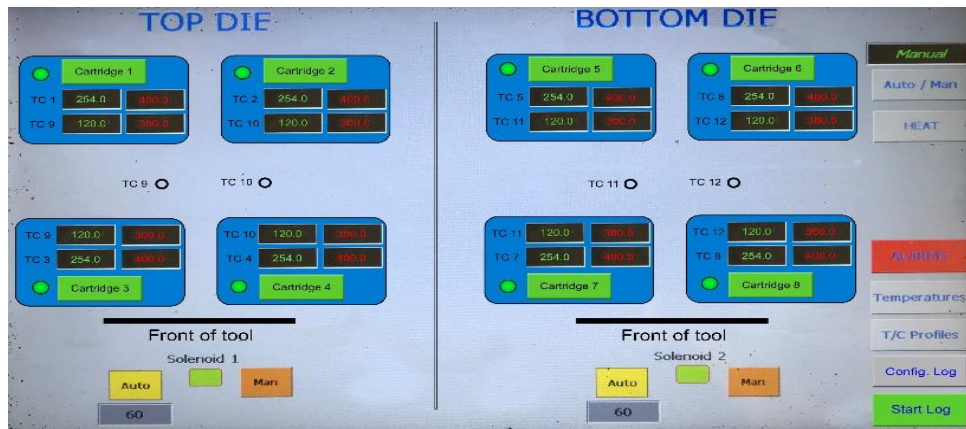
Figure 6-8 Main operating screen for the control cabinet

Safety measures to avoid overheating are also considered and included in the software. In one aspect, the power output of the cartridge heaters is slowly reduced as the temperature reaches the desired level. On the other hand, in the case of a control thermocouple failure, the cartridge heater

allocated to that thermocouple will shut off so that the operator can be notified.

6.3.3 Multi-point tooling for hot forming

The multi-point tool used in this process chain is the same as the 23 pin one mentioned in Chapter 5. It is situated adjacent to the fast cooling station and fixed to the same hydraulic press as shown in Figure 6-9, so the balance of these two tools needs to be considered. When the fast cooling station is heated, the performance of the multi-point tool is not affected significantly due to heat transfer. During forming the movable matrices with dome-like heads enable a smooth surface of the target sheet metal part to be achieved. The heights of the pins can be adjusted for different dome curvatures, or for simulating different process setups, such as bending, stretching, and deep drawing.
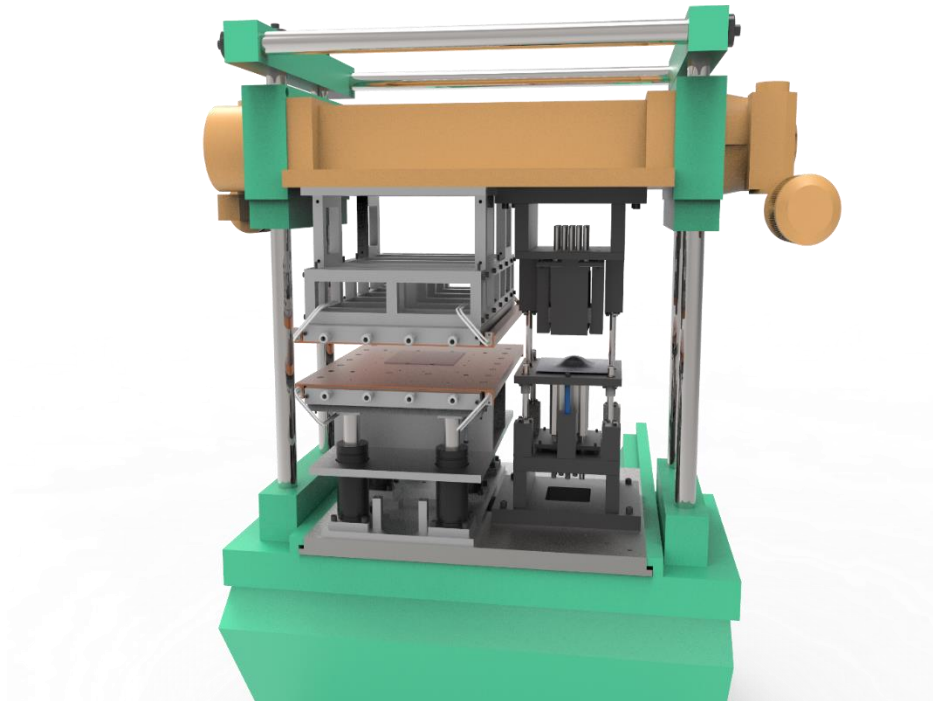
Figure 6-9 Fast cooling station and multi-point tool fixed to the same hydraulic press

Based on trial tests, some improvements and modifications have been made for a better cooling and forming performance, which will be addressed and explained in Appendix A.

6.4 Hot forming experiment results and discussion

6.4.1 Experiment setup

To further investigate the forming capability for industrial application, it is necessary to combine multi-point tooling with hot blanks after they are solution heat treated and cooled. The material (AA6082-T6) is cut into 200mm * 200mm square plates 1.5mm thick. Thermocouples are mounted at the edge of all blanks to monitor the temperature change during the whole heating, cooling and forming process. As all four edges are constrained for the square plates, the stress and strain conditions can represent the most universal industrial applications.

A polyurethane pad is used as the elastic layer to homogenise the force distribution as it is assumed to be isotropic and incompressible. In order to avoid the heat conduction to invalidate rubber performance and damage the pins, Calcium-Magnesium Silicate thermal insulation sheet 2mm thick whose thermal conductivity is 0.07 W/m.K. at 400°C is employed between the hot blank and polyurethane rubber, as shown in Figure 6-10. Also a very thin Silica and Vermiculite cloth with high tensile strength, good temperature and abrasive resistance is placed between the blank and the rubber cushion since the ductility of the thermal insulation sheet is low.
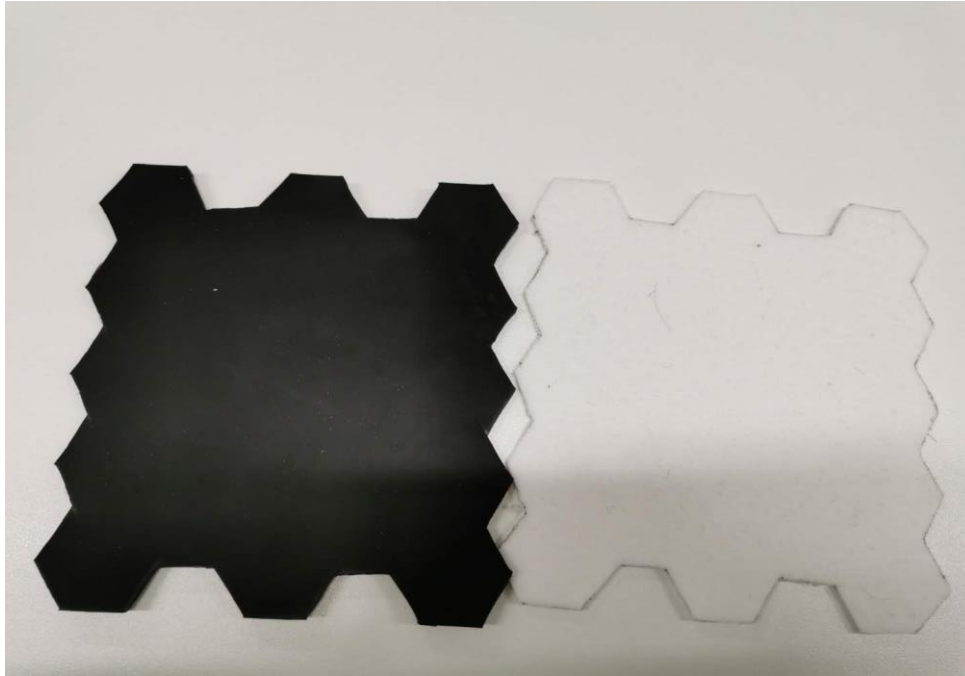
Figure 6-10 Polyurethane pad and thermal insulation material

A heavy-duty anti-seize spray is used as the lubricant for multi-point hot forming since it has an operating temperature of -30 °C to +900 °C. Before each forming cycle the lubricant is uniformly applied to the tools whose area contacts with the hot blank edge. During the forming tests, the maximum force of the hydraulic press is set constant and the stroke of the press is set by a mechanical stop.

6.4.2 Results and Discussion

A total of nine groups of square samples were formed as shown in Figure 6-11 and these were classified in three general categories with the label '1,2 and 3', which represented an increased pressing stroke of 20mm, 22mm and 24mm. Details can be found in Table 6-2. In each category three samples are presented, i.e. SHT+NC, SHT+FC and SHT+EFC, which are cooled at a rate of 5°C/s, 50°C/s and 100°C/s before being formed using the multi-point tools. These samples are shown from Figure 6-12 to Figure 6-14 together with an enlarged view.

132

Table 6-2 Overview of test groups for the hot formed square plate

Group Category	Formed depth	Heat-treatment Method
1-1	20mm	SHT+NC
1-2	20mm	SHT+FC
1-3	20mm	SHT+EFC
2-1	22mm	SHT+NC
2-2	22mm	SHT+FC
2-3	22mm	SHT+EFC
3-1	24mm	SHT+NC
3-2	24mm	SHT+FC
3-3	24mm	SHT+EFC

Figure 6-11 Square Samples from hot multi-point forming with cooling process
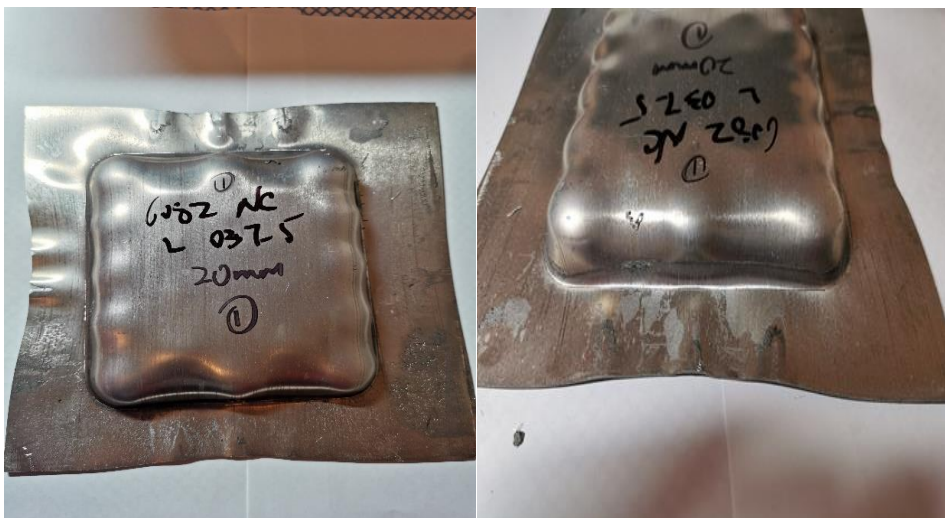
(a)
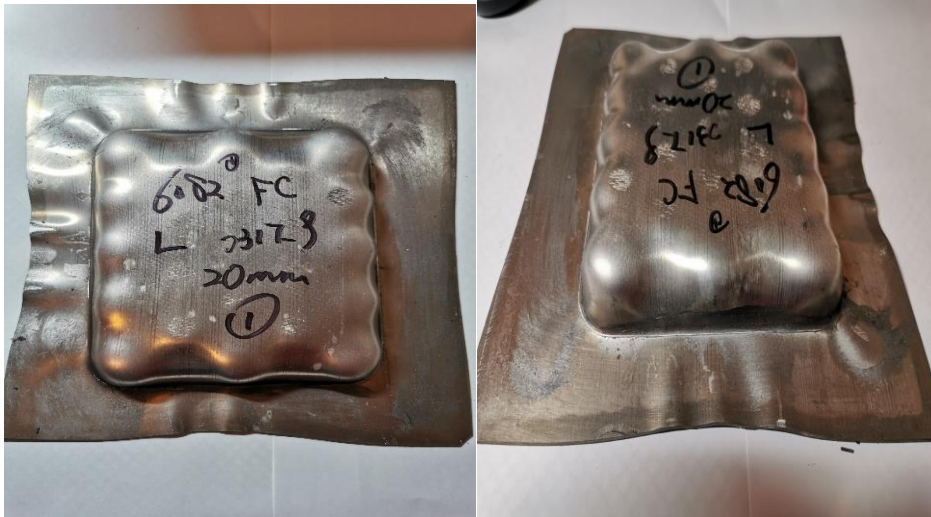
(b)

(c)

Figure 6-12 Square samples with formed depth of 20mm: (a) SHT+NC, (b) SHT+FC and (c) SHT+EFC

(a)
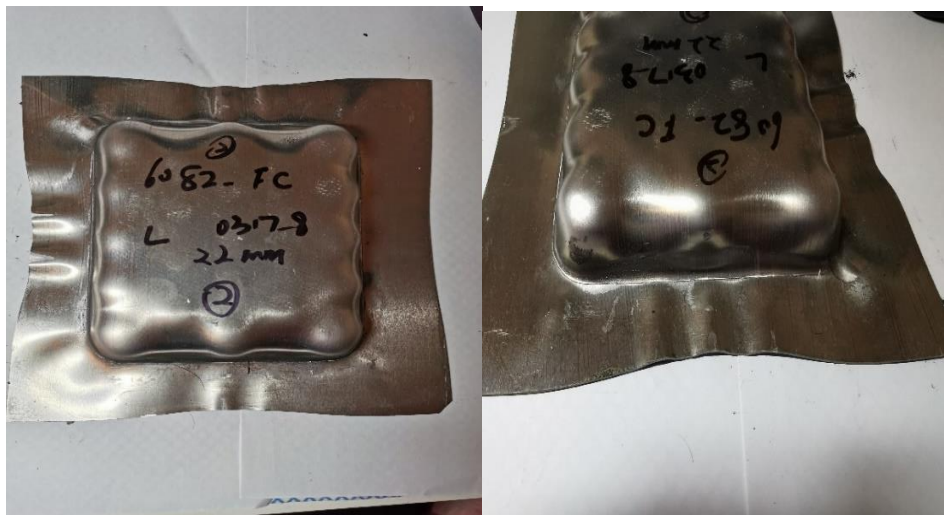
(b)

(c)

Figure 6-13 Square samples with formed depth of 22mm: (a) SHT+NC, (b) SHT+FC and (c) SHT+EFC

(a)

(b)

(c)

Figure 6-14 Square samples with formed depth of 24mm: (a) SHT+NC,
(b) SHT+FC and (c) SHT+EFC

The four corners of the formed plate are the most critical areas which are
going to crack first due to the stress concentration on the four pins at the
corners. Since the target formed shape is designed to be severe enough to
investigate the crack initiation and propagation, wrinkles on the holding
edges and dimples on the formed surface can be clearly seen. The
discussion in this section refers to level of deformation, initiation of defects,

extent of the damage, influence by the cooling rate, comparison with the FE simulation, etc.

When formed to the same depth, there is little difference of the final shape of the sample parts with different cooling rates. This is partly due to the similar Young's modulus and maximum elongation under different cooling rates. Nevertheless, a reduced wrinkle can be observed for the sample parts that were cooled at a higher cooling rate, especially shown in Figure 6-12. Together with Figure 6-13 and Figure 6-14, large transverse shrink on the edge of the sample parts can be seen that were naturally cooled. This can be due to the restriction of a lower UTS of aluminium alloys with a decreased cooling rate. There is little difference for the dimples on the formed surface where the outer pin heads contact with the blank sheets. The possible reason is that under this severe formed shape, once the strength is beyond the critical tensile strength, sheet metal thinning and crack may occur.

When the sample parts were formed to a depth of 20mm, thinning begins to occur for sample parts with a cooling rate of 5°C/s, defined as natural cooling. At this time there is no damage on other two groups of sample parts with larger cooling rates as presented in Figure 6-12. Figure 6-13 when the sample parts were further formed to 22mm, obvious cracking can be seen on the edge of sample parts in the group of SHT+NC. But at the same formed depth, thinning has just started on sample parts with a process of solution heat treatment and fast cooling whose cooling rate is 50°C/s. There is still no damage seen for the sample parts with solution heat treatment and extra fast cooling. When the sample parts were formed to 24mm, cracking continues to propagate and a large opening can be seen for the sample parts in the group of SHT+NC. In the meantime, thinning turns to cracking for sample parts with solution heat treatment and fast cooling, but the cracking is still better than the samples with natural cooling. For sample parts in the group of SHT+EFC, thinning finally occurs. When formed to the same depth, the different shape performances show that formability can be improved by increasing the cooling rate and

139

prove that our promising hot multi-point stamping process with a fast cooling method is able to form large and severe shapes using high-strength aluminium alloys.

The pressure distribution from FE simulation in Figure 4-23 proves that four corners of the formed plate are most likely to fail during stamping. Following the forming limit diagram damage initiation value in the simulation, the extent of damage can be reduced with an increased cooling rate under the same forming conditions. In this hot forming experiment the shape performance of the tested sample parts matches the simulated results and proves that sample parts under solution heat treatment and natural cooling always damage earlier than those under solution heat treatment and fast cooling. In addition, the simulated values of maximum and minimum principal logarithmic strains were output and their ratio on selected nodes were plotted in the forming limit diagram. The plotted results illustrate that damage is more severe with a decreased cooling rate, which is proven by the extent of crack propagation on the sample parts. The simulated results show damage starts from a forming depth of 17mm for naturally cooled sample parts, but during experiment the thinning starts when formed to around 20mm. This is because the simulation does not employ the rubber cushion between the pins and blank sheets and the resulting increased stress concentration makes the sheet blanks easier to damage. Another reason is because of the improved formability at elevated temperature during the experiment, while in the simulation the forming process was modelled without temperature related setup. In this aspect the experiment proves that use of a rubber cushion is important for the formability improvement.

Table 6-3 Final shape edge performance of square samples

Curve depth	Heat treatment and cooling status	Final shape edge performance
20mm	SHT+NC	Thinning
	SHT+FC	No damage
	SHT+EFC	No damage
22mm	SHT+NC	Crack
	SHT+FC	Thinning
	SHT+EFC	No damage
24mm	SHT+NC	Propagated crack
	SHT+FC	Crack
	SHT+EFC	Thinning

Table 6-3 illustrates the final conditions of the edges as shown in the enlarged figures. It can be seen that the cracking propagates along with the increasing formed depth. Also cooling rate is of importance to the final shape condition and for AA6082-T6, the formability can be improved by increasing the cooling rate. In this case samples under solution heat treatment and extra fast cooling perform the best. One possible reason, from the tensile test results, is the strength differences under different cooling rates. Based on the HFQ concept proposed by Lin et. al, the underlying reason is that when aluminium alloy is heated close to solution heat-treatment temperature, the material is very soft, ductile and easy to deform because the crystalline particles become the unstable supersaturated solid solution, which are desirable for high post-form strength. However, a fast cooling is necessary to obtain the optimal mechanical properties by freezing the supersaturated solid solution and

maximizing the effect of strain rate hardening. Various cooling rate also have impacts on the forming performance. Since the material microstructure is unstable near its solution heat-treatment temperature and strain hardening effects, too much decrease of the strength may cause the material to be softer and this further makes the sample easier to damage when the elongation at the break point remains the same. So a suitable cooling rate needs to be taken with a balance between formability and ductility. Finally the production efficiency can be increased by using the contact cooling test rig, i.e. there is no long waiting time in the production line (the waiting time for extra-fast cooling takes only approximately 2s, compared with that of 25s for natural cooling). The experimental results prove the applicability of the proposed hot sheet forming technology with a fast cooling process for high strength aluminium alloys.

6.5 Summary

Lightweight technology development is one of the fastest growing markets in the world and will have a broad and fundamental impact on almost all sectors of the global economy. In this chapter an innovative idea is brought to the development of hot sheet forming technology, by introducing an intermediate 'fast cooling' step between heating and forming steps for high strength aluminium alloys to fulfil industrial needs. It also expands the applications of multi-point tools at elevated temperature for the first time by establishing a one-step industrial production demonstration line with high TRL.

Through this fundamental research (such as process configuration and forming mechanical studies) and processing with contact cooling tool development, the process chain was simplified to reduce the occurrence of human errors with an enhancement of the fast cooling system. The prototype production line was initially tested and some key improvements were made to improve the reliability and consistency. The results prove that hot forming can greatly improve the formability of high strength

aluminium alloys. Also cooling rate could affect the final material properties and is important to the final shape performance for a multi-point sheet metal hot forming process. For AA6082-T6, increasing the cooling rate can improve the material formability. The developed contact cooling test rig leads to potentially significant time saving due to speeding up the process. Meanwhile the proposed production line involving solution heat treatment, contact fast cooling and multi-point forming procedures is able to enhance aluminium alloy hot forming capability.

Chapter 7 Hot Stretch Forming with Multi-Point Tooling

7.1 Introduction

It is widely lab-proven that the formability of high strength aluminium alloy can be improved at elevated temperatures. Using the optimised prototype production line introduced in Chapter 6, several forming limit tests were conducted on the square sheet blanks to investigate the intermediate cooling rate and its influence on the forming quality and efficiency to improve the formability, shorten the cooling period and increase the productivity. The outcomes were explained and analysed for an enhanced aluminium alloy hot forming capability as well as a practical industrial demonstration. In this chapter stretch forming is conducted to study the effects of the proposed 'fast cooling' process on the forming and springback performance. This is supplementary to the formability improvement of the proposed 'fast cooling' method.

In section 7.2 the blank sheet geometry and material property definition within different cooling rates are explained. Then a finite element modelling of the stretch forming using multi-point tooling is described and discussed in section 7.3. Based on the simulation, section 7.4 describes a strip bending test by using the proposed prototype line in this research. The deformation profiles of the strips were plotted to illustrate the effect of heating and cooling methods on the shape formed as well as the springback.

7.2 Specimen dimensions and material properties

Strips are formed to a flat surface with a depth of 24mm in this test, which means the height for each pin is kept constant. The material (AA6082-T6) is cut into 200mm * 45mm rectangular strips 1.5mm thick. These strips are

placed at the centre along the longer line of formed area as shown in Figure 7-1. The position of each pin can be obtained from the CAD file, and the 45mm width enables the long edges of the strips to be contacted by the top head of the pins during forming to avoid large wrinkles of the unconstrained edges. Compared to the square plate forming process in last chapter, this stretch process is more like a uniaxial bending condition because only one direction is constrained by blank holder. The holding force is provided by two springs whose stiffness is 8.79 daN/mm each.

Figure 7-1 Rectangular strips position for bending

The strips are pre-treated with different heating and cooling procedures as explained in Chapter 3, which are room temperature (RT), solution heat treatment with natural cooling in the air (SHT+NC), solution heat treatment with fast cooling (SHT+FC) and solution heat treatment with extra fast cooling (SHT+EFC). RT means that the samples are tested directly from T6 condition without any further treatment. In other heat-treated and cooled groups, the cooling rate is varied as 5°C/s, 50°C/s and 100°C/s after solution heat treatment. Temperature of all samples were planned to drop to around 350°C before being formed, so the cooling time may vary within various cooling rates. The stress-strain data obtained from the tensile tests are used for material definition for numerical simulation as shown in Figure 7-2.
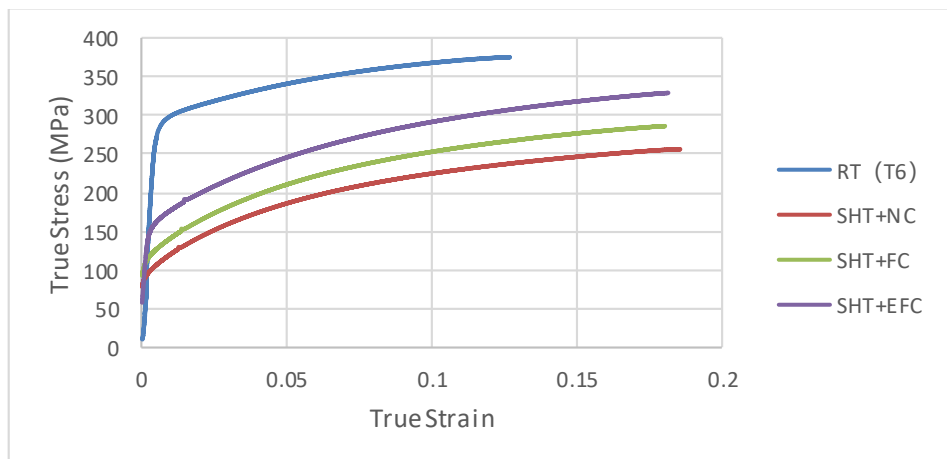
Figure 7-2 True stress-strain curve of AA6082 from tensile tests under different heating and cooling methods

7.3   FE analysis of stretch forming

7.3.1 FE model

Figure 7-3 shows the model setup for stretching. The model is the same as the tooling setup of square plate forming. Only the square sheet blank is replaced by the strips. Top pins are hidden for a clear view. No rubber

cushion was used for simulation. The coefficient of friction between blank holder and strip was 0.02 under lubrication conditions. Abaqus/Explicit was used for the forming step to avoid convergence problems, and a static step with Abaqus/Standard was employed to study the springback of the formed parts. The strip was modelled as shell element and 400 meshes were generated for the analysis. Analytical rigid body and discrete rigid elements were used for the pins and blank holder to reduce computation time.

During simulation the bottom pins are fixed, only top pins move vertically along with blank holders. A boundary condition is applied to central line movement of the strip in the X or Y direction. The process is modelled at room temperature, and the only variable is the material property under different heating and cooling methods.
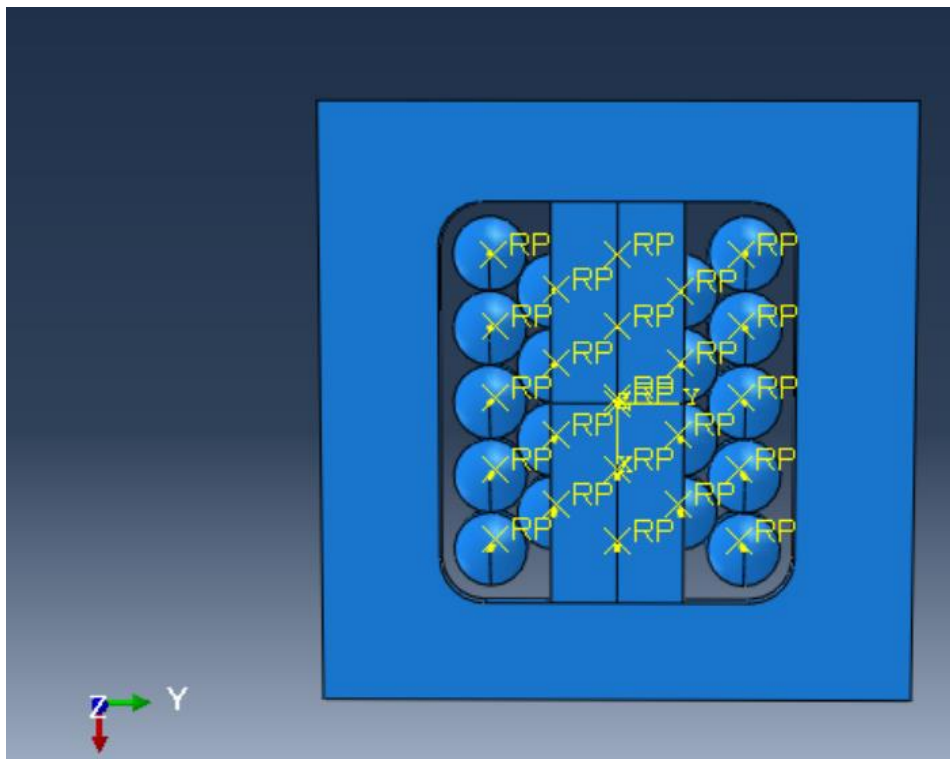
Figure 7-3 Model setup for stretching

7.3.2 Simulation results and discussion

In multi-point forming springback is the main defect apart from wrinkling and dimpling. In this section the springback improvements of the proposed intermediate fast cooling process are investigated. Although the simulation models forming at room temperature, it can provide guidance for the experimental work.

7.3.2.1 Stress distributions

The Mises stress distribution of the formed parts after springback is shown in Figure 7-4. Although the value of stress depends on the material mechanical properties, it can be seen that the stress distribution at the edges of the formed area and contact spots between pins and strips for cold stretching (RT) is less uniform than those of strips under the heating and cooling method. Thus heat treatment with a reduced stress can help with dimpling and springback and protect the forming tools.
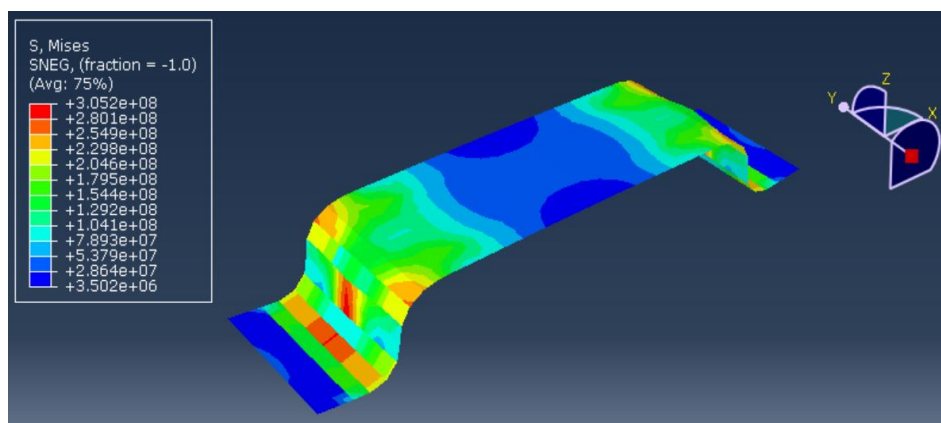
(a)
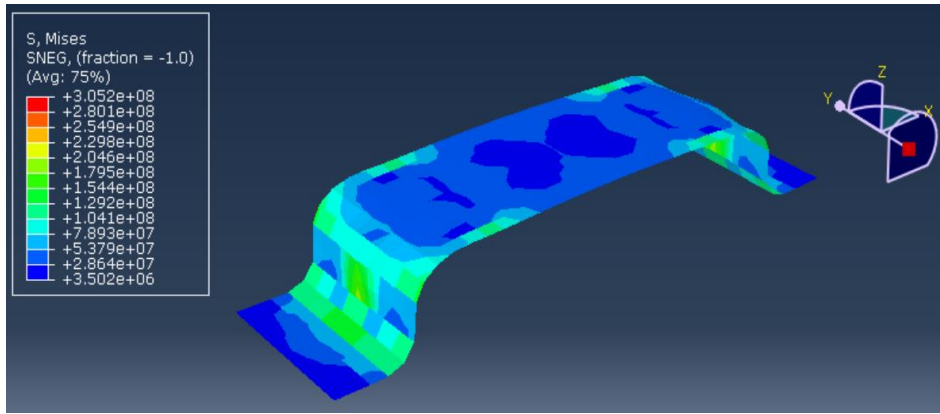
(b)
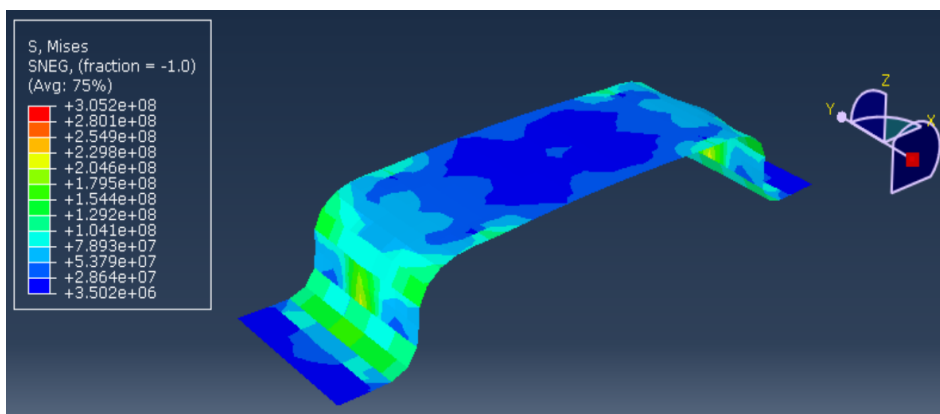
(c)
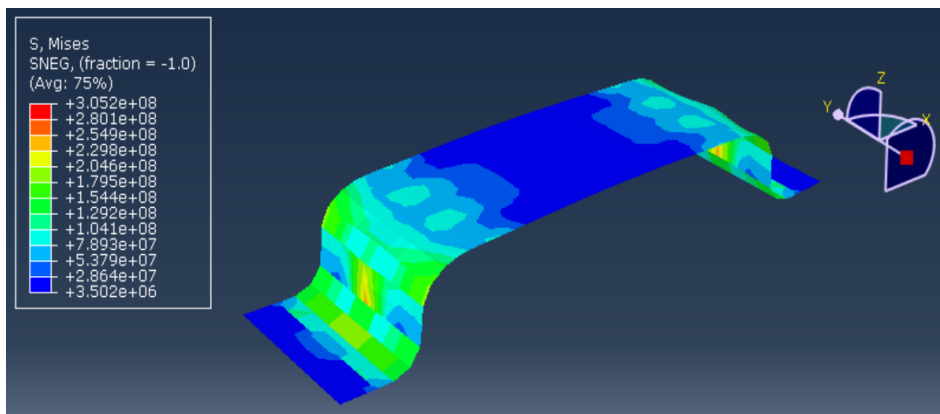
(d)

Figure 7-4 Mises stress distribution (unit: Pa) of formed strips after springback: (a) RT, (b) SHT+NC, (c) SHT+FC and (d) SHT+EFC

7.3.2.2 Springback of the formed parts

Static analysis is employed for the springback analysis. Taking the stress, strain and displacement of the formed strip as pre-defined initial field conditions, the springback in the forming direction is displayed by the variable U, as shown in Figure 7-5. The maximum and minimum limits are not the same because the difference is not significant. It is easy to compare the springback on heat treated formed strips and to study the effect of cooling rates on springback, since they have a similar springback distribution. From Figure 7-5 it is apparent that the increase of cooling rate can lead to a slight decrease in springback. More tension occurs in the strip because of the stress variations from increased cooling rate. The position of maximum springback on cold stretching strips is different with other heated treated samples. The simulated strip profiles are plotted in Figure 7-6 for a clear comparison which shows that large springback happens for high strength materials to be formed directly at room temperature, especially the flat stretching area and the area constrained by the blank holder. The springback improvements in the uniaxial stretching process with increased cooling rate are not as clear as the formability improvements of the square forming process whose stress and strain states are more complicated.
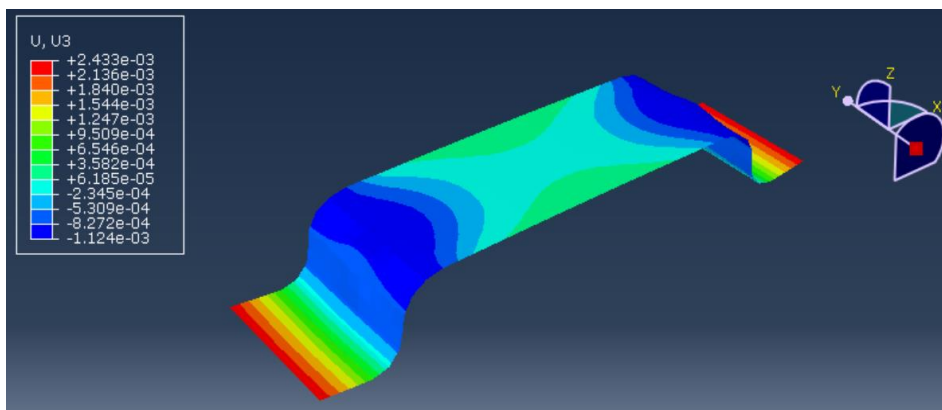
(a)
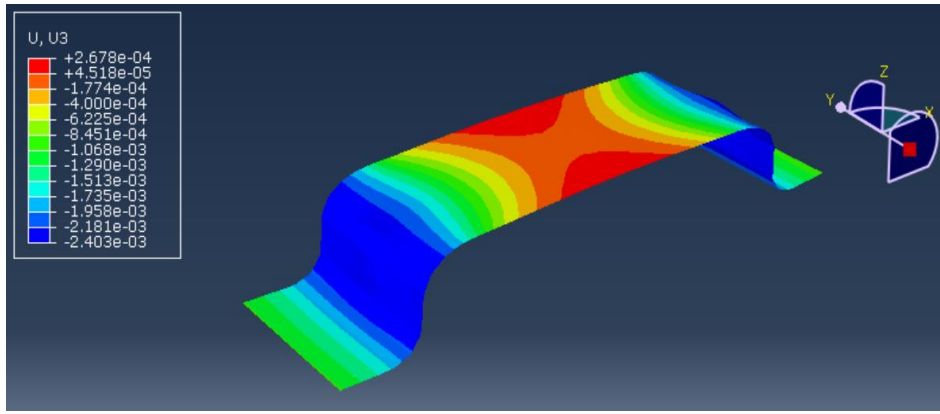
(b)
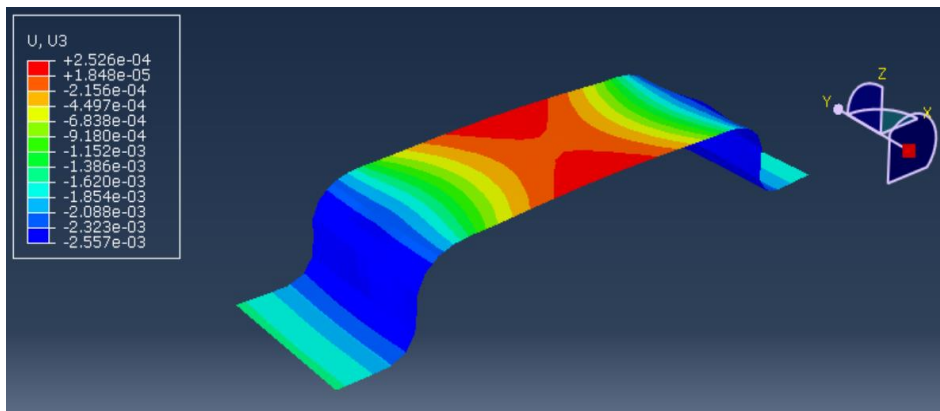
(c)
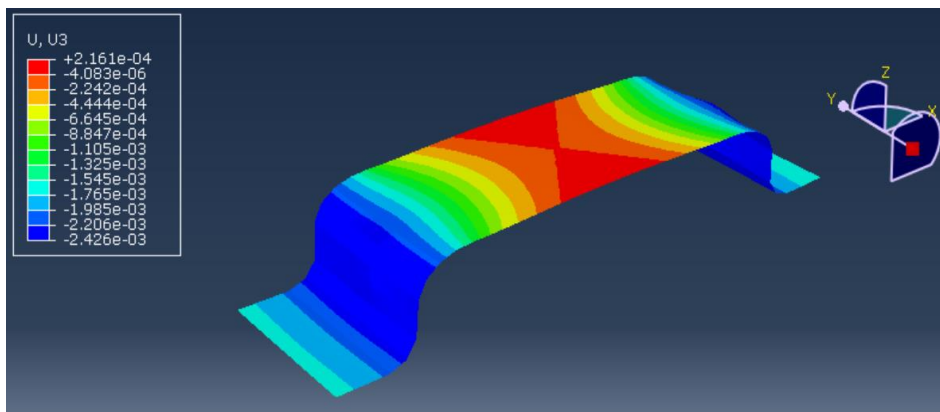
(d)

Figure 7-5 Springback (unit: m) of formed strips: (a) RT, (b) SHT+NC,
(c) SHT+FC and (d) SHT+EFC

151
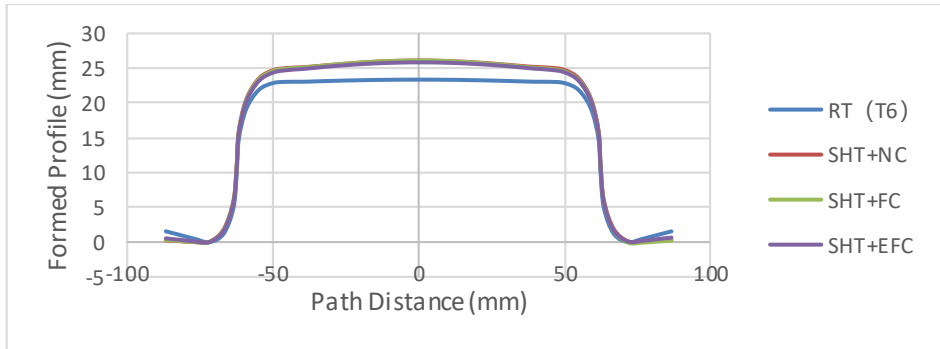
Figure 7-6 Ploted profiles of formed strips with different heating and
cooling methods

7.4 Hot stretch forming experiment, results and discussion

Following the setup in the last chapter, the same polyurethane pad was
used as the elastic layers for dimpling reduction. Since the stretching takes
place at a temperature around 350°C, the Calcium-Magnesium Silicate
thermal insulation layer was also used with the high elastic Silica and
Vermiculite cloth as explained in Chapter 6. The thermal conductivity of
the thermal insulation sheet can be 0.07 W/m.K. at 400°C and this prevents
the rubber cushion from decomposing. During the whole heating, cooling
and stretching process, the instantaneous temperature profile of the strip
was recorded continually through thermocouples mounted at the edge of
each strip. Lubricated oil, which works at high temperature, was applied to
the upper and lower blank holder before each test to help with the material
flow. During the forming tests, the maximum force of the hydraulic press
was set constant and the stroke of the press was set by a mechanical stop
to make sure the target shape is the same. With only two edges constrained,
these strips provided a simplified stress and strain distribution for
springback study.

Table 7-1 Groups of hot formed strips

Group No.	Heat-treatment method
1	RT (Not Lubricated)
2	RT (Lubricated)
3	SHT+NC
4	SHT+FC
5	SHT+EFC

The strips are classified into five sub-groups, as indicated in Table 7-1. Two cold samples named 'RT' were selected to compare with hot formed parts. The cooling rates are still 5°C/s, 50°C/s and 100°C/s for SHT+NC, SHT+FC and SHT+EFC blanks before being sent to the multi-point tool. The bended samples are given in Figure 7-7 and Figure 7-8. Their relative formed profiles are plotted in Figure 7-9 using a squared ruled pad with different colours.

Figure 7-7 Samples parts with bent profiles

153

Figure 7-8 Edge details of the sample parts
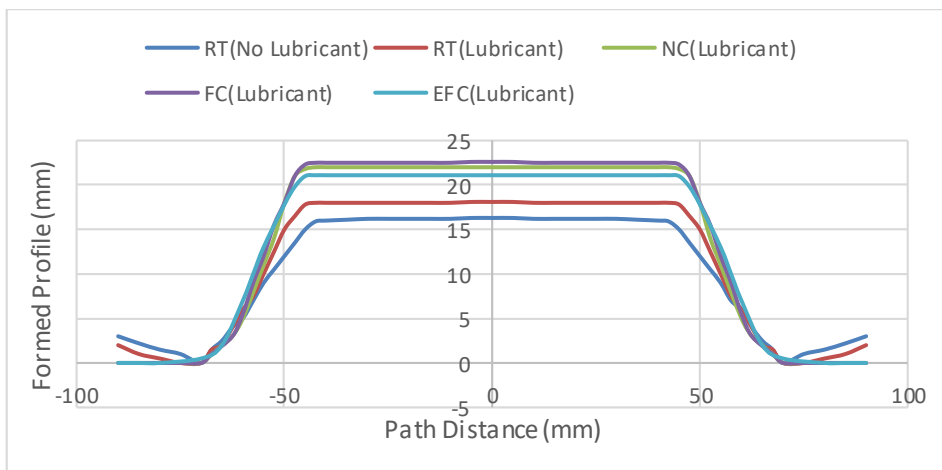
Figure 7-9 Formed profiles of the bent strips

When formed to the same curve depth (24mm), great improvements have been made on the springback and final shapes by employing the proposed hot forming configuration, comparing to that produced during the cold forming as presented in Figure 7-10. Figure 7-11 shows that lubricated condition could also help with the material flow under a large holding force of 4219.2N. Nevertheless, there is little difference in the amount of

154

springback between the hot forming samples with different cooling rates. This could be explained well by consulting the results presented in Figure 3-9 and Table 3-4 in which it is indicated that different cooling rates did not obviously influence the material's Young's modulus. Although in Figure 7-8, large dimples at the edge of the samples that were naturally cooled can still be seen, due to the relatively lower strength of the material after cooling. In theory, the different yield strengths induced by different cooling rates should reflect differences in the amount of springback of the sheet metals after unloading. Such an amount could well be seen if a larger amount of elastic deformation occurs in a forming process, such as free bending. From this point of view, the different cooling rates will have an obvious influence on the springback in hot forming when an intermediate cooling is introduced. At the same time, the production time for forming with fast cooling could be much shorter than that for forming under natural cooling conditions, which can improve the industrial efficiency significantly.

(a)

(b)

(c)

Figure 7-10 Profile comparison of hot and cold bent sample parts (cold bent sample part in front): (a) RT and SHT+NC, (b) RT and SHT+FC, (c) RT and SHT+EFC

Figure 7-11 Profile comparison of cold bent sample parts with and without lubrication (Unlubricated sample part in front)

7.5 Summary

To investigate the effect of cooling rate on springback for the trial material (AA6082-T6), a number of uniaxial stretching tests have been conducted numerically and experimentally. The results prove that hot forming can greatly improve the springback performance of high strength aluminium alloys compared with cold stretching. Although the differences on cooling rate have little effect on the springback, the developed contact cooling test rig leads to potentially significant time saving due to speeding up the process. Also the proposed production line provides a formability and springback improvement method for other high strength materials. The improved forming limit from the proposed technology would give industry opportunities to form complex geometries without failures. Although this has been proved only with a small number of tests, this is the first successful demonstration in a production line with fast cooling incorporated.

Chapter 8 Conclusions and Considerations for Future Work

8.1 Conclusions

A feasibility study on the formability improvement of high strength aluminium alloy sheets by integrating hot stamping and multi-point tooling has been conducted in this research with a newly developed fast cooling concept. This study consisted of five main parts: 1) material tests and characterisation of sheet blanks, 2) finite element simulations of stamping using multi-point tooling concerning the influence of factors on shape performance at room temperature and effect of cooling rate on formability improvement at elevated temperature, 3) experimental evaluation of cold deep drawing with the proposed 23 tightly packed multi-point tooling, 4) illustration of the prototype pilot production line combining the hot stamping of aluminium alloys and newly developed fast contact-cooling system, 5) feasibility study of the formability and springback improvements by employing the prototype production line with the two test cases – deep drawing and stretch forming. The tests conducted demonstrated that introducing a high-temperature forming configuration into a multi-point forming process with integration of fast contact-cooling is feasible, provided an enhanced aluminium alloy hot forming capability, and establishment of an industrial production demonstration line with high TRL. The main conclusions drawn from this research are as follows:

- Literature review

Aluminium alloys are one of the most popularly used lightweight materials in many industry sectors including the automotive and aerospace industries. Nevertheless, due to the poor formability of high strength aluminium alloys, there are still significant challenges to the conversion of the

aluminium sheets into complex geometries. Hot stamping is a good choice for forming high strength materials with reduced forming force requirement and springback. However, after searching the literature, there are still problems mainly associated with the forming of complex shapes, forming die conditions, air/spray cooling rate as well as high productivity requirements. Multi-point tooling can add flexibility to the test trials in relation to the different shapes/features without the need to make different sets of solid dies. Therefore, there is an opportunity for making improvements by developing a prototype pilot production line that combines the hot stamping of aluminium alloys and fast contact cooling with multi-point tooling.

- Material testing and property characterisation

Two groups of materials were classified in the tensile tests. AA1050-H14 and low carbon sheet blanks were tested directly for a comparative study of shape performance in a cold multi-point tooling deep drawing process. The high strength AA6082-T6 sheet blanks were heat treated and cooled before testing with various cooling rates via fast contact-cooling. It was found that the yield stress and ultimate tensile strength can be reduced significantly for those heat treated and cooled sheet blanks compared with those in T6 condition. The yield stress and ultimate strength increased with the cooling rate, although there was little difference in maximum elongation.

- FE modelling

The purpose of finite element modelling is to identify the stress, strain and damage performance of the formed shape. The shallow square-cup shape was formed using AA1050-H14 and low carbon steel sheet blanks to study the influencing factors of the multi-point process. Through the simulation results, the coefficient of friction and holding force had an important effect on the shape performance. Due to the homogenization of contact force

distribution, use of rubber cushions can help with the dimpling problems. Further modelling was performed on the high strength alloys, the material property was obtained using our proposed fast cooling concept with various cooling rates. It was found that the formability of AA6082 sheet blanks can be improved with the increased cooling rate. Although this process was modelled at room temperature, the results can provide guidance for the experimental hot multi-point forming integrated with the newly developed fast cooling test rig.

- Multi-point tooling and cold deep drawing

A 23 tightly packed multi-point tool was designed and built to compare with the FE results. The top punch can be moved along with the vertical guide pillars of the hydraulic press. Different shapes/features can be achieved through two sets of adjustable pins, which are able to help improve dimpling, wrinkling and formed geometry.

Aluminium alloy 1050-H14 and low carbon steel with the thickness of 1mm were used in the experiment. In each test the press down stroke was pre-defined so that a specific formed curvature can be achieved. The formed parts were further measured with a coordinate measuring machine (CMM).

The effects of factors, including variations of the depth of curvatures, sheet metal selection, holding force, surface lubrication, and thickness of rubber cushions, on formed shape performance at room temperature were investigated using a simple variable method. The selected profiles of the formed parts were compared with the 3D printed model with an average shape error value calculated. It was found that use of rubber cushions was extremely important for thin plate forming to reduce dimpling problems. Correct holding force was important for a high-quality formed shape with the help of appropriate lubrication. Although lowering the material stress can help achieve a better surface and reduce the drawing force through the multi-punches, an optimal quality control combination of all factors for a

160

particular type of material and geometry is necessary, especially for the high strength materials.

- Hot deep drawing and intermediate fast cooling

To extend the multi-point tooling available at elevated temperature in an industrial scale demonstration, a prototype pilot production line that combines the hot stamping of aluminium alloys and fast contact-cooling was developed by the University of Strathclyde. The forming was effected by the multi-point tooling instead of different sets of solid dies. The small contact-cooling test rig consists of two cooling plates, cartridge heaters and a dedicated control unit. After some initial trial tests, some key improvements were made on the production line for better cooling and forming performance. A series of square plate hot stampings were produced employing the pilot production line. These tests demonstrated that the integration of fast contact-cooling into a production process is feasible and its associated cost could be relatively low. It also demonstrated that a multi-point forming process at elevated temperature is feasible, and extends the existing process capabilities. The test results showed that proper cooling rates, which are easily achievable with the facility developed, could greatly improve the forming limits of the high strength aluminium alloys, and in general the higher the cooling rate, the better were the results obtained. At the same time, the fast-cooling configuration design could potentially lead to significant process-time saving, due to the extremely short cooling time involved. The improved forming limit from the proposed technology would give industry opportunities to form complex geometries without failures.

- Hot stretch forming with multi-point tooling

Uniaxial stretch forming with rectangular strips was conducted for the investigation of springback numerically and experimentally. It was found that great springback improvements were made on the final shape by employing the fast contact-cooling. At the same time, using high cooling

161

rate can help to reduce the waiting time between the furnace heating and following forming.

8.2 Novelty and contributions to knowledge

This thesis has made significant and novel contributions to sheet metal forming research of aluminium alloys at room and elevated temperatures, combining the multi-point forming. Sheet metal forming plays an important role in a variety of industrial applications, therein multi-point forming (MPF) is regarded as a flexible tooling technology for sheet forming. Since the first automated system proposed in 1999 [2], much work has been done to improve the formability of different sheet materials [108]. Multi-point forming techniques can solve problems with different die shapes during the process, saving time and die materials. However, some undesired surface finish features such as wrinkles and indentations may appear under different setup parameters. Therefore, an experimental machine setup has been introduced to study the influence of varied controlled conditions followed by measurements using a Coordinate Measuring Machine (CMM). A general relationship is provided to help with improving final performance.

Although the global market for lightweight materials, especially aluminium alloys, is growing fast, high strength aluminium alloys can exhibit poor ductility and formability at room temperature. The costs for producing components with large complex shapes with such materials limits the application to luxury supercars and airplanes, etc [6]. It is proved that the ductility can be improved when forming at elevated temperatures because the alloy strength is reduced when the temperature increases [93]. But for some series of high strength aluminium alloy (such as 6000 series), the desired micro-structure is not well preserved if they are directly formed after heating to a solution heat treatment (SHT) temperature as disclosed in the relative patent [207]. Thus, in this thesis a novel intermediate fast

cooling step is introduced with a controllable cooling rate before transferring material to the forming tool.

The proposed process technology for forming structural parts made out of high-strength aluminium alloys provides a high-efficient, cost-effective forming technique and opens up opportunities to manufacture lighter, larger and more complex components. Two key novelties of this research are highlighted below:

- No quantified research on the intermediate fast contact cooling for the hot-forming of high-strength aluminium alloy sheets has been conducted using a contact cooling facility viable in an industrial environment. This innovative manufacturing approach can improve the capability of hot stamping of aluminium sheets in the manufacturing industry as well as substantially shorten the production time, compared to the air/spray cooling which renders much slower cooling rates.

- No hot forming has previously been done using a multi-point tool, which means this technology develops a new application for multi-point forming. Also, compared with a solid die/mould, which is currently commonly used in industry, the multi-point tool has many advantages, especially its improvement on sustainability – i.e. lower manufacturing cost, easier and cheaper to repair, flexibility to configure different shapes, etc.

Following the guidance of the finite element modelling through Abaqus, the experimental investigation has further provided a comprehensive and precise illustration of the results found under different forming conditions.

Based on what we have achieved in this research, some key contributions to knowledge are outlined below:

- Illustrated that a comprehensive control of process parameters in multi-point forming is important for a high-quality surface finish;

- Proved that hot stamping with fast cooling can greatly improve the form limits of high strength aluminium alloys;

- Demonstrated that the cooling rate is important for the forming of the final shapes for multi-point tooling sheet metal hot forming;

- The developed contact cooling test rig leads to potentially significant time saving due to speeding up the process (the cooling time has been reduced by 90%, therefore, no long waiting time in the production line is required);

- The improved forming limit from the proposed technology would give industry opportunities to form more complex geometries without failures;

- This is the first successful attempt to demonstrate the formability enhancement via a production line with a fast contact-cooling concept.

8.3 Considerations for the future work

According to the work conducted in this research, suggestions for future work are given below:

1) Currently the heights of the multi-point pins are adjusted manually, resulting in inaccuracy in the formed shape and time costs. An alternative design of an automatic control system can be investigated through a computer-aided numerical control method and the position of each separate pin can be determined by the CAD file.

2) Only 23 tightly packed pins are designed for the multi-point tool in this research, which limits the test ability with complex geometries or

164

large deformations, especially as a part of an industrial production line. A new design with more pins can be produced in the future for the investigation of forming performance in more applications, based on the experience and principals obtained from the current multi-point tool.

3) Although some improvements have already been made on the prototype production line, accurately controlling the process parameters with good repeatability is still a challenge. Currently the transfer of solution heat treated blanks, the material handling of the fast cooling system as well as the multi-point tool, mainly depend on the person conducting the process. An automatic production line can be developed to control the time for each step precisely.

4) This forming limit study has not been able to cover a whole range of the possible component forms/geometries, with only a limited number of sample-parts and geometries being tested in this research. Modifications can be applied to the production line with more parts such as load cells and transducers to obtain more data related to the forming process.

5) The process development methodology also has potential to expand to other lightweight and high strength materials, such as titanium alloys.

References

[1]   N. Nakajima, "Research on die and electrode by steel wire bind," *Japanese Journal of Mechanical Academy,* vol. 72, pp. 32-40, 1969.

[2]   M. Li, Y. Liu, S. Su, and G. Li, "Multi-point forming: a flexible manufacturing method for a 3-d surface sheet," *Journal of Materials Processing Technology,* vol. 87, pp. 277-280, 1999.

[3]   M.-Z. Li, Z.-Y. Cai, Z. Sui, and Q. Yan, "Multi-point forming technology for sheet metal," *Journal of Materials Processing Technology,* vol. 129, pp. 333-338, 2002.

[4]   Y. Liu, Y. Liu, and J. Chen, "The impact of the Chinese automotive industry: scenarios based on the national environmental goals," *Journal of Cleaner Production,* vol. 96, pp. 102-109, 2015.

[5]   M. Kleiner, M. Geiger, and A. Klaus, "Manufacturing of lightweight components by metal forming," *CIRP annals,* vol. 52, pp. 521-542, 2003.

[6]   K. Zheng, D. J. Politis, L. Wang, and J. Lin, "A review on forming techniques for manufacturing lightweight complex—shaped aluminium panel components," *International Journal of Lightweight Materials and Manufacture,* vol. 1, pp. 55-80, 2018.

[7]   S. L. Semiatin, *Introduction to sheet-forming processes* vol. 14, 2006.

[8]   E. Ghassemali, X. Song, M. Zarinejad, A. Danno, and M. J. Tan, "Bulk Metal Forming Processes in Manufacturing," *Handbook of Manufacturing Engineering and Technology,* pp. 171-230, 2015.

[9]   K. Lange, "Handbook of metal forming," *McGraw-Hill Book Company, 1985,* p. 1216, 1985.

[10]   J. Hu, Z. Marciniak, and J. Duncan, *Mechanics of sheet metal forming*: Elsevier, 2002.

[11]   J. Ludwik and O. J. Adam, "Method of making low resistance composite corrugated welded sheath for telephone cables," *U.S. Patent 3,360,409,* 1967.

[12]   J. K. Paik, A. K. Thayamballi, and J. Che, "Ultimate strength of ship hulls under combined vertical bending, horizontal bending and shearing forces," *Trans. SNAME,* vol. 104, pp. 31-59, 1996.

[13]   J. Cho, S. Moon, Y. Moon, and S. Kang, "Finite element investigation on spring-back characteristics in sheet metal U-bending process," *Journal of Materials Processing Technology,* vol. 141, pp. 109-116, 2003.

[14]   S. Panthi, N. Ramakrishnan, M. Ahmed, S. S. Singh, and M. Goel, "Finite Element Analysis of sheet metal bending process to predict the springback," *Materials & Design,* vol. 31, pp. 657-662, 2010.

[15]   M. Zhan, H. Yang, Z.-Q. Jiang, Z. Zhao, and Y. Lin, "A study on a 3D FE simulation method of the NC bending process of thin-walled tube," *Journal of Materials Processing Technology,* vol. 129, pp. 273-276, 2002.

[16]   L. Heng, Y. He, Z. Mei, and G. Rui-Jie, "Forming characteristics of thin-walled tube bending process with small bending radius," *Transactions of Nonferrous Metals Society of China,* vol. 16, pp. s613-s623, 2006.

[17]   H. E. Theis, *Handbook of metalforming processes*: CRC Press, 1999.

[18]   F. Heislitz, H. Livatyali, M. A. Ahmetoglu, G. L. Kinzel, and T. Altan, "Simulation of roll forming process with the 3-D FEM code PAM-

STAMP," *Journal of Materials Processing Technology,* vol. 59, pp. 59-67, 1996.

[19]   Q. Bui and J. Ponthot, "Numerical simulation of cold roll-forming processes," *Journal of materials processing technology,* vol. 202, pp. 275-282, 2008.

[20]   M. Brunet, S. Mguil, and P. Pol, "Modelling of a roll-forming process with a combined 2D and 3D FEM code," *Journal of Materials Processing Technology,* vol. 80, pp. 213-219, 1998.

[21]   G. T. Halmos, *Roll forming handbook*: Crc Press, 2005.

[22]   K. Sweeney and U. Grunewald, "The application of roll forming for automotive structural parts," *Journal of Materials Processing Technology,* vol. 132, pp. 9-15, 2003.

[23]   D.-C. Kang, X.-C. Gao, X.-F. Meng, and Z.-H. Wang, "Study on the deformation mode of conventional spinning of plates," *Journal of Materials Processing Technology,* vol. 91, pp. 226-230, 1999.

[24]   E. Quigley and J. Monaghan, "Metal forming: an analysis of spinning processes," *Journal of Materials Processing Technology,* vol. 103, pp. 114-119, 2000.

[25]   J. Frisch and M. Achmad, "An Experimental Study of Computer Controlled Shear Spinning," in *Proceedings of the Twentieth International Machine Tool Design and Research Conference*, 1980, pp. 25-28.

[26]   D. Pollitt, "The Practice and Potential of Flow Forming Processes," *Rotary Metalworking Processes,* pp. 19-32, 1979.

[27]   C. Wong, T. Dean, and J. Lin, "A review of spinning, shear forming and flow forming processes," *International Journal of Machine Tools and Manufacture,* vol. 43, pp. 1419-1435, 2003.

[28]   R. P. Evert and J. A. Miller, "Stretch-forming process," *U.S. Patent 4,704,886,* 1987.

[29]   N.-M. Wang and M. Wenner, "Elastic-viscoplastic analyses of simple stretch forming problems," in *Mechanics of Sheet Metal Forming*, ed: Springer, 1978, pp. 367-402.

[30]   C. WICK, "STRETCH FORMING-BETTER PARTS LOWER COSTS," *Machinery,* vol. 75, pp. 96-&, 1968.

[31]   A. H. Clausen, O. S. Hopperstad, and M. Langseth, "Stretch bending of aluminium extrusions for car bumpers," *Journal of Materials Processing Technology,* vol. 102, pp. 241-248, 2000.

[32]   F. Vollertsen, "Sheet Metal Forming," in *Micro Metal Forming*, ed: Springer, 2013, pp. 135-176.

[33]   F. Vollertsen, Z. Hu, H. S. Niehoff, and C. Theiler, "State of the art in micro forming and investigations into micro deep drawing," *Journal of Materials Processing Technology,* vol. 151, pp. 70-79, 2004.

[34]   R. Hill, *The mathematical theory of plasticity* vol. 11: Oxford university press, 1998.

[35]   H. Kim, J. H. Sung, R. Sivakumar, and T. Altan, "Evaluation of stamping lubricants using the deep drawing test," *International Journal of Machine Tools and Manufacture,* vol. 47, pp. 2120-2132, 2007.

[36]   H. Hornauer, "Beitrag zu einem Fehlerkatalog-Fehler beim Herstellen von Formteilen mittels Verfahren des Umformens und Trennens," *Blech.(6),* pp. 107-120, 1959.

[37]   L. Menezes and C. Teodosiu, "Three-dimensional numerical simulation of the deep-drawing process using solid finite elements," *Journal of Materials Processing Technology,* vol. 97, pp. 100-106, 2000.

[38]   S. Kobayashi, S. Kobayashi, S.-I. Oh, and T. Altan, *Metal forming and the finite-element method* vol. 4: Oxford University Press on Demand, 1989.

[39]   R. Blake, R. Pearson, A. Revell, and W. Simon, "Laser thermal forming of sheet metal parts using desktop laser systems," in *International Congress on Applications of Lasers & Electro-Optics*, 1997, pp. E66-E75.

[40]   P. Cheng and S. Lin, "An analytical model for the temperature field in the laser forming of sheet metal," *Journal of Materials Processing Technology,* vol. 101, pp. 260-267, 2000.

[41]   A. Göttmann, J. Diettrich, G. Bergweiler, M. Bambach, G. Hirt, P. Loosen, *et al.,* "Laser-assisted asymmetric incremental sheet forming of titanium sheet metal parts," *Production Engineering,* vol. 5, pp. 263-271, 2011.

[42]   S. P. Keeler and W. A. Backofen, "Plastic instability and fracture in sheets stretched over rigid punches," *Asm Trans Q,* vol. 56, pp. 25-48, 1963.

[43]   G. M. Goodwin, "Application of strain analysis to sheet metal forming problems in the press shop," *SAE Transactions,* pp. 380-387, 1968.

[44]   K. Nakazima, T. Kikuma, and K. Hasuka, "Study on the formability of steel sheets," *YAWATA TECH REP, SEPT. 1968,--264--, 8517-8530,* 1968.

[45]   V. Hasek, "Untersuchung und Theoretische Beschreibung wichtiger Einflussgrössen auf das Grenzformanderungsschaubild," *Institute of Metal Forming Report, University of Stuttgart, West Germany,* pp. 213-220, 1978.

[46]   T. B. Stoughton, "A general forming limit criterion for sheet metal forming," *International Journal of Mechanical Sciences,* vol. 42, pp. 1-27, 2000.

[47]   S. Kim, H. Huh, H. Bok, and M. Moon, "Forming limit diagram of auto-body steel sheets for high-speed sheet metal forming," *Journal of Materials Processing Technology,* vol. 211, pp. 851-862, 2011.

[48]   A. Assempour, R. Hashemi, K. Abrinia, M. Ganjiani, and E. Masoumi, "A methodology for prediction of forming limit stress diagrams considering the strain path effect," *Computational materials science,* vol. 45, pp. 195-204, 2009.

[49]   M. Koç, E. Billur, and Ö. N. Cora, "An experimental study on the comparative assessment of hydraulic bulge test analysis methods," *Materials & Design,* vol. 32, pp. 272-281, 2011.

[50]   S. Fukui, H. Kudo, K. Yoshida, and H. Okawa, "A Method for Testing of Deep-Drawability of Sheet Metals," *Report of the Institute of Science and Technology, University of Tokyo,* vol. 6, pp. 351-357, 1952.

[51]   J. Cognard, "The mechanics of the wedge test," *The Journal of Adhesion,* vol. 20, pp. 1-13, 1986.

[52]   S. Chung and H. Swift, "Cup-drawing from a flat blank: Part I. Experimental investigation," *Proceedings of the institution of mechanical engineers,* vol. 165, pp. 199-211, 1951.

[53]   A. Heinz, A. Haszler, C. Keidel, S. Moldenhauer, R. Benedictus, and W. Miller, "Recent development in aluminium alloys for aerospace applications," *Materials Science and Engineering: A,* vol. 280, pp. 102-107, 2000.

[54]   N.-K. Li, G. Lin, B. Nie, and J.-A. Liu, "Aluminum alloy material and its heat treatment technology," *Beijing Metallurgical Industry Press,* 2012.

[55] W. Miller, L. Zhuang, J. Bottema, A. J. Wittebrood, P. De Smet, A. Haszler, *et al.*, "Recent development in aluminium alloys for the automotive industry," *Materials Science and Engineering: A,* vol. 280, pp. 37-49, 2000.

[56] R. A. Sielski, "Research needs in aluminum structure," *Ships and Offshore Structures,* vol. 3, pp. 57-65, 2008.

[57] N. R. Mandal, *Aluminium welding*: Woodhead publishing, 2001.

[58] T. Anderson, "Troubleshooting in aluminium welding," *Svetsaren no,* vol. 2, 2000.

[59] X.-b. Fan, Z.-b. He, W.-x. Zhou, and S.-j. Yuan, "Formability and strengthening mechanism of solution treated Al–Mg–Si alloy sheet under hot stamping conditions," *Journal of Materials Processing Technology,* vol. 228, pp. 179-185, 2016.

[60] X. Fan, Z. He, S. Yuan, and P. Lin, "Investigation on strengthening of 6A02 aluminum alloy sheet in hot forming-quenching integrated process with warm forming-dies," *Materials Science and Engineering: A,* vol. 587, pp. 221-227, 2013.

[61] G. Mrówka-Nowotnik and J. Sieniawski, "Influence of heat treatment on the microstructure and mechanical properties of 6005 and 6082 aluminium alloys," *Journal of Materials Processing Technology,* vol. 162, pp. 367-372, 2005.

[62] P. A. Rometsch, Y. Zhang, and S. Knight, "Heat treatment of 7xxx series aluminium alloys—Some recent developments," *Transactions of Nonferrous Metals Society of China,* vol. 24, pp. 2003-2017, 2014.

[63] J. F. W. Leuthesser and J. A. Fox, "Apparatus for bulging hollow metal blanks to shape in a mold and control mechanism therefor," *U.S. Patent 2,713,314,* 1955.

[64] K.-H. Chang, *Product Manufacturing and Cost Estimating Using CAD/CAE: The Computer Aided Engineering Design Series*: Academic Press, 2013.

[65] S. Yuan, Z. He, and G. Liu, "New developments of hydroforming in China," *Materials transactions,* vol. 53, pp. 787-795, 2012.

[66] B.-S. Kang, B.-M. Son, and J. Kim, "A comparative study of stamping and hydroforming processes for an automobile fuel tank using FEM," *International Journal of Machine Tools and Manufacture,* vol. 44, pp. 87-94, 2004.

[67] P. K. Mallick, *Materials, design and manufacturing for lightweight vehicles*: Elsevier, 2010.

[68] M. Tolazzi, "Hydroforming applications in automotive: a review," *International journal of material forming,* vol. 3, pp. 307-310, 2010.

[69] L. Lang, J. Danckert, and K. B. Nielsen, "Investigation into the effect of pre-bulging during hydromechanical deep drawing with uniform pressure onto the blank," *International Journal of Machine Tools and Manufacture,* vol. 44, pp. 649-657, 2004.

[70] R. Kolleck and H. Cherek, "Active hydromechanical deep drawing a new process for lightweight design manufacturing," in *Proceedings of the SheMet International Conference*, 2001, pp. 177-182.

[71] A. Aginagalde, A. Orus, J. Esnaola, I. Torca, L. Galdos, and C. Garcia, "Warm hydroforming of lightweight metal sheets," in *AIP Conference Proceedings*, 2007, pp. 1175-1180.

[72] L. Lang, P. Du, B. Liu, G. Cai, and K. Liu, "Pressure rate controlled unified constitutive equations based on microstructure evolution for warm

hydroforming," *Journal of Alloys and Compounds,* vol. 574, pp. 41-48, 2013.

[73]   G. Palumbo, A. Piccininni, P. Guglielmi, and G. Di Michele, "Warm HydroForming of the heat treatable aluminium alloy AC170PX," *Journal of Manufacturing Processes,* vol. 20, pp. 24-32, 2015.

[74]   C. Hartl, "Research and advances in fundamentals and industrial applications of hydroforming," *Journal of Materials Processing Technology,* vol. 167, pp. 383-392, 2005.

[75]   N. Abedrabbo, M. A. Zampaloni, and F. Pourboghrat, "Wrinkling control in aluminum sheet hydroforming," *International Journal of Mechanical Sciences,* vol. 47, pp. 333-358, 2005.

[76]   K. Jackson and J. Allwood, "The mechanics of incremental sheet forming," *Journal of materials processing technology,* vol. 209, pp. 1158-1174, 2009.

[77]   K. Dai, Z. R. Wang, and Y. Fang, "CNC incremental sheet forming of an axially symmetric specimen and the locus of optimization," *Journal of Materials Processing Technology,* vol. 102, pp. 164-167, 5/15/ 2000.

[78]   T. J. Kim and D. Y. Yang, "Improvement of formability for the incremental sheet metal forming process," *International Journal of Mechanical Sciences,* vol. 42, pp. 1271-1286, 7// 2000.

[79]   Y. Kim and J. Park, "Effect of process parameters on formability in incremental forming of sheet metal," *Journal of materials processing technology,* vol. 130, pp. 42-46, 2002.

[80]   J.-J. Park and Y.-H. Kim, "Fundamental studies on the incremental sheet metal forming technique," *Journal of Materials Processing Technology,* vol. 140, pp. 447-453, 9/22/ 2003.

[81]   S. GmbH. and S. GmbH, *Metal forming handbook*: Springer Science & Business Media, 1998.

[82]   L. Fratini, G. Ambrogio, R. Di Lorenzo, L. Filice, and F. Micari, "Influence of mechanical properties of the sheet material on formability in single point incremental forming," *CIRP Annals - Manufacturing Technology,* vol. 53, pp. 207-210, // 2004.

[83]   M.-S. Shim and J.-J. Park, "The formability of aluminum sheet in incremental forming," *Journal of Materials Processing Technology,* vol. 113, pp. 654-658, 6/15/ 2001.

[84]   L. Filice, L. Fratini, and F. Micari, "Analysis of material formability in incremental forming," in *CIRP annals-Manufacturing technology* vol. 51, ed, 2002, pp. 199-202.

[85]   Y. Ji and J. Park, "Formability of magnesium AZ31 sheet in the incremental forming at warm temperature," *Journal of materials processing technology,* vol. 201, pp. 354-358, 2008.

[86]   J. Duflou, B. Callebaut, J. Verbert, and H. De Baerdemaeker, "Laser assisted incremental forming: formability and accuracy improvement," *CIRP annals,* vol. 56, pp. 273-276, 2007.

[87]   G. Fan, L. Gao, G. Hussain, and Z. Wu, "Electric hot incremental forming: A novel technique," *International Journal of Machine Tools and Manufacture,* vol. 48, pp. 1688-1692, 2008.

[88]   G. Ambrogio, S. Bruschi, A. Ghiotti, and L. Filice, "Formability of AZ31 magnesium alloy in warm incremental forming process," *International Journal of Material Forming,* vol. 2, p. 5, 2009.

[89]   T. Maeno, K.-i. Mori, and R. Yachi, "Hot stamping of high-strength aluminium alloy aircraft parts using quick heating," *CIRP Annals,* vol. 66, pp. 269-272, 2017.

[90]   F. Grabner, B. Gruber, C. Schlögl, and C. Chimani, "Cryogenic Sheet Metal Forming-An Overview," in *Materials Science Forum*, 2018, pp. 1397-1403.

[91]   R. Schneider, B. Heine, R. Grant, R. Kelsch, F. Gerstner, and T. Hägle, "Mechanical behaviour of automobile relevant aluminium wrought alloys at low temperatures," *International Aluminium Journal,* vol. 88, pp. 77-82, 2012.

[92]   Y.-c. Huang, X.-y. Yan, and Q. Tao, "Microstructure and mechanical properties of cryo-rolled AA6061 Al alloy," *Transactions of Nonferrous Metals Society of China,* vol. 26, pp. 12-18, 2016.

[93]   J. Jin, X. Wang, L. Deng, and J. Luo, "A single-step hot stamping-forging process for aluminum alloy shell parts with nonuniform thickness," *Journal of Materials Processing Technology,* vol. 228, pp. 170-178, 2016.

[94]   H. Karbasian and A. E. Tekkaya, "A review on hot stamping," *Journal of Materials Processing Technology,* vol. 210, pp. 2103-2118, 2010.

[95]   M. Merklein and J. Lechler, "Determination of material and process characteristics for hot stamping processes of quenchable ultra high strength steels with respect to a FE-based process design," *SAE International Journal of Materials and Manufacturing,* vol. 1, pp. 411-426, 2009.

[96]   P. F. Bariani, S. Bruschi, A. Ghiotti, and F. Michieletto, "Hot stamping of AA5083 aluminium alloy sheets," *CIRP Annals,* vol. 62, pp. 251-254, 2013.

[97]   X. Liu, K. Ji, O. El Fakir, H. Fang, M. M. Gharbi, and L. Wang, "Determination of the interfacial heat transfer coefficient for a hot aluminium stamping process," *Journal of Materials Processing Technology,* vol. 247, pp. 158-170, 2017.

[98]   H. Hoffmann, H. So, and H. Steinbeiss, "Design of hot stamping tools with cooling system," *CIRP annals,* vol. 56, pp. 269-272, 2007.

[99]   J. Lin, T. Dean, and R. Garrett, "A process in forming high strength and complex-shaped Al-alloy sheet components," *UK Patent WO2008059242,* 2008.

[100]   W. Xiao, B. Wang, and K. Zheng, "An experimental and numerical investigation on the formability of AA7075 sheet in hot stamping condition," *The International Journal of Advanced Manufacturing Technology,* vol. 92, pp. 3299-3309, 2017.

[101]   N. Li, Z. T. Shao, J. G. Lin, and T. A. Dean, "Investigation of uniaxial tensile properties of AA6082 under HFQ® conditions," in *Key Engineering Materials*, 2016, pp. 337-344.

[102]   O. El Fakir, L. Wang, D. Balint, J. P. Dear, J. Lin, and T. A. Dean, "Numerical study of the solution heat treatment, forming, and in-die quenching (HFQ) process on AA5754," *International Journal of Machine Tools and Manufacture,* vol. 87, pp. 39-48, 2014.

[103]   L. Wang, M. Strangwood, D. Balint, J. Lin, and T. Dean, "Formability and failure mechanisms of AA2024 under hot forming conditions," *Materials Science and Engineering: A,* vol. 528, pp. 2648-2656, 2011.

[104]   M. S. Mohamed, A. D. Foster, J. Lin, D. S. Balint, and T. A. Dean, "Investigation of deformation and failure features in hot stamping of

AA6082: Experimentation and modelling," *International Journal of Machine Tools and Manufacture,* vol. 53, pp. 27-38, 2012.

[105]   J. Liu, A. L. Wang, H. X. Gao, O. El Fakir, X. Luan, L. L. Wang, *et al.*, "Studies on the Hot Forming and Cold-Die Quenching of AA6082 Tailor Welded Blanks," in *Key Engineering Materials*, 2016, pp. 941-947.

[106]   Z. Jing, B.-y. Wang, J.-g. Lin, and F. Lei, "Forming defects in aluminum alloy hot stamping of side-door impact beam," *Transactions of Nonferrous Metals Society of China,* vol. 24, pp. 3611-3620, 2014.

[107]   S.-j. Yuan, X.-b. Fan, and Z.-b. He, "Hot forming-quenching integrated process with cold-hot dies for 2A12 aluminum alloy sheet," *Procedia Engineering,* vol. 81, pp. 1780-1785, 2014.

[108]   F. Tan, M. Li, and Z. Cai, "Research on the process of multi-point forming for the customized titanium alloy cranial prosthesis," *Journal of materials processing technology,* vol. 187, pp. 453-457, 2007.

[109]   J. M. Papazian, "Tools of change," *Mechanical Engineering Magazine Select Articles,* vol. 124, pp. 52-55, 2002.

[110]   D. F. Walczyk and D. E. Hardt, "Design and analysis of reconfigurable discrete dies for sheet metal forming," *Journal of Manufacturing Systems,* vol. 17, pp. 436-454, 1998.

[111]   V. Păunoiu, D. Nicoară, M. Banu, C. Maier, O. Ciocan, and A. Epureanu, "Design an experimental reconfigurable die for sheet metal forming," *The Annals of" Dunarea de Jos" University of Galati, Fascicle V, Technologies in machine building,* vol. 24, pp. 60-65, 2006.

[112]   E. Haas, R. C. Schwarz, and J. M. Papazian, "Design and test of a reconfigurable forming die," *Journal of Manufacturing processes,* vol. 4, pp. 77-85, 2002.

[113]   D. F. Walczyk and Y.-T. Im, "A hydraulically-actuated reconfigurable tool for flexible fabrication: implementation and control," *J. Manuf. Sci. Eng.,* vol. 122, pp. 562-568, 1999.

[114]   M. Li, Z. Cai, Z. Sui, and X. Li, "Principle and applications of multi-point matched-die forming for sheet metal," *Proceedings of the Institution of Mechanical Engineers, Part B: Journal of Engineering Manufacture,* vol. 222, pp. 581-589, 2008.

[115]   Q. Zhang, Z. Wang, and T. Dean, "The mechanics of multi-point sandwich forming," *International Journal of Machine Tools and Manufacture,* vol. 48, pp. 1495-1503, 2008.

[116]   A. Elghawail, K. Essa, M. Abosaf, A. Tolipov, S. Su, and D. Pham, "Low-cost metal-forming process using an elastic punch and a reconfigurable multi-pin die," *International Journal of Material Forming,* vol. 12, pp. 391-401, 2019.

[117]   S. Wang, Z. Cai, and M. Li, "Numerical investigation of the influence of punch element in multi-point stretch forming process," *The International Journal of Advanced Manufacturing Technology,* vol. 49, pp. 475-483, 2010.

[118]   F. Nishioka, "An automatic bending of plates by the universal press with multiple piston heads (Second report: practicality researcher)," *Journal of the Society of Naval Architects of Japan,* vol. 133, pp. 291-305, 1973.

[119]   R. Webb and D. E. Hardt, "A transfer function description of sheet metal forming for process control," *Journal of engineering for industry,* vol. 113, pp. 44-52, 1991.

[120] D. F. Walczyk and D. E. Hardt, "Design and analysis of reconfigurable discrete dies for sheet metal forming," *Journal of Manufacturing Systems,* vol. 17, pp. 436-453, 1998.

[121] M. Li, K. Nakamura, S. Watanabe, and Y. Akutsu, "Study of the basic principles (1st report: research on multi-point forming for sheet metal)," in *Proc. of the Japanese Spring conf. for Technology of Plasticity*, 1992, pp. 519-522.

[122] L. Mingzhe, L. Chunguo, and C. Qingmin, "Research on multi-point forming of three-dimensional sheet metal parts," *M Geiger et al. Advanced Technology of Plasticity. Germany: Springer,* pp. 189-194, 1999.

[123] Z.-Y. Cai and M.-Z. Li, "Multi-point forming of three-dimensional sheet metal and the control of the forming process," *International Journal of Pressure Vessels and Piping,* vol. 79, pp. 289-296, 2002.

[124] Z.-Y. Cai and M.-Z. Li, "Finite element simulation of multi-point sheet forming process based on implicit scheme," *Journal of Materials Processing Technology,* vol. 161, pp. 449-455, 2005.

[125] V. Paunoiu, P. Cekan, E. Gavan, and D. Nicoara, "Numerical simulations in reconfigurable multipoint forming," *International Journal of Material Forming,* vol. 1, pp. 181-184, 2008.

[126] B. Davoodi and B. Zareh-Desari, "Assessment of forming parameters influencing spring-back in multi-point forming process: a comprehensive experimental and numerical study," *Materials & Design,* vol. 59, pp. 103-114, 2014.

[127] B.-b. Jia and W.-W. Wang, "Shape accuracy analysis of multi-point forming process for sheet metal under normal full constrained conditions," *International Journal of Material Forming,* pp. 1-11, 2017.

[128] M. Yaşar, Z. Korkmaz, and M. Gavas, "Forming sheet metals by means of multi-point deep drawing method," *Materials & design,* vol. 28, pp. 2647-2653, 2007.

[129] Z.-Y. Cai, S.-H. Wang, X.-D. Xu, and M.-Z. Li, "Numerical simulation for the multi-point stretch forming process of sheet metal," *Journal of materials processing technology,* vol. 209, pp. 396-407, 2009.

[130] X.-p. Gong, M.-z. Li, Q.-p. Lu, and Z.-q. Peng, "Research on continuous multi-point forming method for rotary surface," *Journal of Materials Processing Technology,* vol. 212, pp. 227-236, 2012.

[131] Y. Luo, W. Yang, Z. Liu, Y. Wang, and R. Du, "Numerical simulation and experimental study on cyclic multi-point incremental forming process," *The International Journal of Advanced Manufacturing Technology,* vol. 85, pp. 1249-1259, 2016.

[132] Q. Liu, C. Lu, W. Fu, K. Tieu, M. Li, and X. Gong, "Optimization of cushion conditions in micro multi-point sheet forming," *Journal of Materials Processing Technology,* vol. 212, pp. 672-677, 2012.

[133] L. Li, Y.-H. Seo, S.-C. Heo, B.-S. Kang, and J. Kim, "Numerical simulations on reducing the unloading springback with multi-step multi-point forming technology," *The International Journal of Advanced Manufacturing Technology,* vol. 48, pp. 45-61, 2010.

[134] J.-J. Chen, M.-Z. Li, W. Liu, and C.-T. Wang, "Sectional multipoint forming technology for large-size sheet metal," *The International Journal of Advanced Manufacturing Technology,* vol. 25, pp. 935-939, 2005.

[135]   Z. Qian, M. Li, and F. Tan, "The analyse on the process of multi-point forming for dish head," *Journal of materials processing technology,* vol. 187, pp. 471-475, 2007.

[136]   N. Boudeau and J.-C. Gelin, "Necking in sheet metal forming. Influence of macroscopic and microscopic properties of materials," *International journal of mechanical sciences,* vol. 42, pp. 2209-2232, 2000.

[137]   J. Cao, H. Yao, A. Karafillis, and M. C. Boyce, "Prediction of localized thinning in sheet metal using a general anisotropic yield criterion," *International Journal of Plasticity,* vol. 16, pp. 1105-1129, 2000.

[138]   Z.-Y. Cai, S.-H. Wang, and M.-Z. Li, "Numerical investigation of multi-point forming process for sheet metal: wrinkling, dimpling and springback," *The International Journal of Advanced Manufacturing Technology,* vol. 37, pp. 927-936, 2008.

[139]   Z. Marciniak and K. Kuczyński, "Limit strains in the processes of stretch-forming sheet metal," *International journal of mechanical sciences,* vol. 9, pp. 609-620, 1967.

[140]   R. Sowerby and J. Duncan, "Failure in sheet metal in biaxial tension," *International Journal of Mechanical Sciences,* vol. 13, pp. 217-229, 1971.

[141]   R. Hill, "Theoretical plasticity of textured aggregates," in *Mathematical Proceedings of the Cambridge Philosophical Society*, 1979, pp. 179-191.

[142]   V. Uthaisangsuk, U. Prahl, S. Münstermann, and W. Bleck, "Experimental and numerical failure criterion for formability prediction in sheet metal forming," *Computational materials science,* vol. 43, pp. 43-50, 2008.

[143]   Ø. Fyllingen, O. Hopperstad, O.-G. Lademo, and M. Langseth, "Estimation of forming limit diagrams by the use of the finite element method and Monte Carlo simulation," *Computers & Structures,* vol. 87, pp. 128-139, 2009.

[144]   X. Duan, M. Jain, and D. S. Wilkinson, "Development of a heterogeneous microstructurally based finite element model for the prediction of forming limit diagram for sheet material," *Metallurgical and materials transactions A,* vol. 37, p. 3489, 2006.

[145]   H. N. Han and K.-H. Kim, "A ductile fracture criterion in sheet metal forming process," *Journal of Materials Processing Tech.,* vol. 142, pp. 231-238, 2003.

[146]   J. J. Yang, "Finite element simulation of metal forming processes in ABAQUS," 1992.

[147]   J. Cao and M. Boyce, "A predictive tool for delaying wrinkling and tearing failures in sheet metal forming," *Journal of Engineering Materials and Technology,* vol. 119, pp. 354-365, 1997.

[148]   C.-g. LIU, Z.-y. CAI, and M.-z. LI, "Dimple formation and its elimination in multi-point forming for sheet metal [J]," *Journal of Jilin University of Technology (Natural Science Edition),* vol. 1, 2004.

[149]   A. Tolipov, A. Elghawail, S. Shushing, D. Pham, and K. Essa, "Experimental research and numerical optimisation of multi-point sheet metal forming implementation using a solid elastic cushion system," in *Journal of Physics: Conference Series*, 2017, p. 012120.

[150]   H. Al-Qureshi, "Analysis of simultaneous sheet metal forming operations using elastomer technique," *Journal of materials processing technology,* vol. 125, pp. 751-755, 2002.

[151] X. Wang and J. Cao, "On the prediction of side-wall wrinkling in sheet metal forming processes," *International Journal of Mechanical Sciences,* vol. 42, pp. 2369-2394, 2000.

[152] L. Peng, X. Lai, and M. Li, "Transition surface design for blank holder in multi-point forming," *International Journal of Machine Tools and Manufacture,* vol. 46, pp. 1336-1342, 2006.

[153] K. Chung and O. Richmond, "The mechanics of ideal forming," *Journal of applied mechanics,* vol. 61, pp. 176-181, 1994.

[154] C. Zhongyi and L. Mingzhe, "Optimum path forming technique for sheet metal and its realization in multi-point forming," *Journal of Materials Processing Technology,* vol. 110, pp. 136-141, 2001.

[155] M. Li, J. Yao, Z. Cai, and S. Li, "The research on multi-point alternate forming of sheet metal to minimize springback," *Suxing Gongcheng Xuebao(Journal of Plasticity Engineering)(China)(China),* vol. 7, pp. 22-25, 2000.

[156] Q.-F. Zhang, Z.-Y. Cai, Y. Zhang, and M.-Z. Li, "Springback compensation method for doubly curved plate in multi-point forming," *Materials & Design,* vol. 47, pp. 377-385, 2013.

[157] C. Liu, M. Li, and W. Fu, "Principles and apparatus of multi-point forming for sheet metal," *The International Journal of Advanced Manufacturing Technology,* vol. 35, pp. 1227-1233, 2008.

[158] T. Altan, S. Oh, and H. Gegel, "Metal forming: fundamentals and applications (ASM Series in Metal Processing)," *ASM, Metals Park,* 1983.

[159] C. R. Boër, N. M. Rebelo, H. A. Rydstad, and G. Schröder, *Process modelling of metal forming and thermomechanical treatment*: Springer Science & Business Media, 2012.

[160] P. Dewhurst and I. Collins, "A matrix technique for constructing slip-line field solutions to a class of plane strain plasticity problems," *International Journal for Numerical Methods in Engineering,* vol. 7, pp. 357-378, 1973.

[161] E. G. Thomsen, J. Bierbower, and C. T. Yang, *An experimental investigation of the mechanics of plastic deformation of metals*: University of California Press, 1954.

[162] B. Aritzur, "Handbook of metal-forming processes," 1983.

[163] R. Hill, "A general method of analysis for metal-working processes," *Journal of the Mechanics and Physics of Solids,* vol. 11, pp. 305-326, 1963.

[164] D. Woo, "On the complete solution of the deep-drawing problem," *International Journal of Mechanical Sciences,* vol. 10, pp. 83-94, 1968.

[165] R. Courant, "Variational methods for the solution of problems of equilibrium and vibrations-Bull. Amer. Math. Soc., V. 49," 1943.

[166] R. W. Clough, "The finite element method in plane stress analysis," in *Proceedings of 2nd ASCE Conference on Electronic Computation, Pittsburgh Pa., Sept. 8 and 9, 1960*, 1960.

[167] A. S. Wifi, "An incremental complete solution of the stretch-forming and deep-drawing of a circular blank using a hemispherical punch," *International Journal of Mechanical Sciences,* vol. 18, pp. 23-31, 1976.

[168] M. Gotoh and F. Ishise, "A finite element analysis of rigid-plastic deformation of the flange in a deep-drawing process based on a fourth-degree yield function," *International Journal of Mechanical Sciences,* vol. 20, pp. 423-435, 1978.

[169]   N.-M. Wang and B. Budiansky, "Analysis of sheet metal stamping by a finite-element method," *Journal of Applied Mechanics,* vol. 45, pp. 73-82, 1978.

[170]   S. Tang, E. Chu, and S. K. Samanta, "Finite element prediction of the deformed shape of an automotive body panel during preformed stage," *Numerical Methods in Industrial Forming Processes,* pp. 629-640, 1982.

[171]   O. C. Zienkiewicz, R. L. Taylor, O. C. Zienkiewicz, and R. L. Taylor, *The finite element method* vol. 36: McGraw-hill London, 1977.

[172]   A. E. Tekkaya, "State-of-the-art of simulation of sheet metal forming," *Journal of Materials Processing Technology,* vol. 103, pp. 14-22, 2000.

[173]   W. Chung, B. Kim, S. Lee, H. Ryu, and M. Joun, "Finite element simulation of plate or sheet metal forming processes using tetrahedral MINI-elements," *Journal of Mechanical Science and Technology,* vol. 28, pp. 237-243, 2014.

[174]   D.-Y. Yang, D. Jung, I. Song, D. Yoo, and J. Lee, "Comparative investigation into implicit, explicit, and iterative implicit/explicit schemes for the simulation of sheet-metal forming processes," *Journal of Materials Processing Technology,* vol. 50, pp. 39-53, 1995.

[175]   M. A. Ablat and A. Qattawi, "Numerical simulation of sheet metal forming: a review," *The International Journal of Advanced Manufacturing Technology,* vol. 89, pp. 1235-1250, 2017.

[176]   P.-A. Raviart and J.-M. Thomas, "A mixed finite element method for 2-nd order elliptic problems," in *Mathematical aspects of finite element methods*, ed: Springer, 1977, pp. 292-315.

[177]   O. C. Zienkiewicz and R. L. Taylor, *The finite element method for solid and structural mechanics*: Elsevier, 2005.

[178]   J.-M. Jin, *The finite element method in electromagnetics*: John Wiley & Sons, 2015.

[179]   T. J. Hughes, *The finite element method: linear static and dynamic finite element analysis*: Courier Corporation, 2012.

[180]   A. Makinouchi, C. Teodosiu, and T. Nakagawa, "Advance in FEM simulation and its related technologies in sheet metal forming," *CIRP Annals,* vol. 47, pp. 641-649, 1998.

[181]   M. Tisza, "Numerical modelling and simulation in sheet metal forming," *Journal of Materials Processing Technology,* vol. 151, pp. 58-62, 2004.

[182]   J.-P. Geng, K. B. Tan, and G.-R. Liu, "Application of finite element analysis in implant dentistry: a review of the literature," *The Journal of prosthetic dentistry,* vol. 85, pp. 585-598, 2001.

[183]   R. Huiskes and E. Chao, "A survey of finite element analysis in orthopedic biomechanics: the first decade," *Journal of biomechanics,* vol. 16, pp. 385-409, 1983.

[184]   S. Gu, "Application of finite element method in mechanical design of automotive parts," in *IOP Conference Series: Materials Science and Engineering*, 2017, p. 012180.

[185]   M. Lee, C. Kim, E. Pavlina, and F. Barlat, "Advances in sheet forming—materials modeling, numerical simulation, and press technologies," *Journal of Manufacturing Science and Engineering,* vol. 133, p. 061001, 2011.

[186]   A. U. Manual, "Version 6.13-2," *Dassault Systémes Simulia Corp., Providence, Rhode Island, USA,* 2013.

176

[187] Z. Zhuang, X. You, J. Liao, S. Cen, X. Shen, and M. Liang, "Finite element analysis and application based on ABAQUS," *Beijing, TsinghuaUniversityPress,* 2009.

[188] L. Taylor, J. Cao, A. Karafillis, and M. Boyce, "Numerical simulations of sheet-metal forming," *Journal of Materials Processing Technology,* vol. 50, pp. 168-179, 1995.

[189] O. Pantalé, J.-L. Bacaria, O. Dalverny, R. Rakotomalala, and S. Caperaa, "2D and 3D numerical models of metal cutting with damage effects," *Computer methods in applied mechanics and engineering,* vol. 193, pp. 4383-4399, 2004.

[190] S. Romeed, S. Fok, and N. Wilson, "A comparison of 2D and 3D finite element analysis of a restored tooth," *Journal of oral rehabilitation,* vol. 33, pp. 209-215, 2006.

[191] F. Gao, D. Wu, H. Cheng, and X. Fan, "Fast simplification and interactive rendering for large FEM mesh model," *Machinery Design & Manufacture,* vol. 4, pp. 15-17, 2011.

[192] H. Mounir, A. Nizar, and B. Abdelmajid, "CAD model simplification using a removing details and merging faces technique for a FEM simulation," *Journal of Mechanical Science and Technology,* vol. 26, pp. 3539-3548, 2012.

[193] S. Bruschi, T. Altan, D. Banabic, P. Bariani, A. Brosius, J. Cao*, et al.*, "Testing and modelling of material behaviour and formability in sheet metal forming," *CIRP Annals,* vol. 63, pp. 727-749, 2014.

[194] R. Zhang, Z. Shao, and J. Lin, "A review on modelling techniques for formability prediction of sheet metal forming," *International Journal of Lightweight Materials and Manufacture,* vol. 1, pp. 115-125, 2018.

[195] R. Hill, "On discontinuous plastic states, with special reference to localized necking in thin sheets," *Journal of the Mechanics and Physics of Solids,* vol. 1, pp. 19-30, 1952.

[196] H. W. Swift, "Plastic instability under plane stress," *Journal of the Mechanics and Physics of Solids,* vol. 1, pp. 1-18, 1952.

[197] H. Li, M. Fu, J. Lu, and H. Yang, "Ductile fracture: experiments and computations," *International journal of plasticity,* vol. 27, pp. 147-180, 2011.

[198] A. Freudenthal, "The Inelastic Behaviour of Engineering Materials and Structures, 1950," ed: Wiley, New York.

[199] J. Chen, X. Zhou, and J. Chen, "Sheet metal forming limit prediction based on plastic deformation energy," *Journal of Materials Processing Technology,* vol. 210, pp. 315-322, 2010.

[200] B. Farahmand, G. Bockrath, and J. Glassco, *Fatigue and fracture mechanics of high risk parts: application of LEFM & FMDM theory*: Springer Science & Business Media, 2012.

[201] X.-P. Xu and A. Needleman, "Numerical simulations of fast crack growth in brittle solids," *Journal of the Mechanics and Physics of Solids,* vol. 42, pp. 1397-1434, 1994.

[202] N. Moës, J. Dolbow, and T. Belytschko, "A finite element method for crack growth without remeshing," *International journal for numerical methods in engineering,* vol. 46, pp. 131-150, 1999.

[203] D. J. Benson, Y. Bazilevs, E. De Luycker, M. C. Hsu, M. Scott, T. Hughes*, et al.*, "A generalized finite element formulation for arbitrary basis

functions: from isogeometric analysis to XFEM," *International Journal for Numerical Methods in Engineering,* vol. 83, pp. 765-785, 2010.

[204] P. M. Areias and T. Belytschko, "Non-linear analysis of shells with arbitrary evolving cracks using XFEM," *International Journal for Numerical Methods in Engineering,* vol. 62, pp. 384-415, 2005.

[205] M. Shahzad, A. Kamran, M. Z. Siddiqui, and M. Farhan, "Mechanical characterization and FE modelling of a hyperelastic material," *Materials Research,* vol. 18, pp. 918-924, 2015.

[206] Z. Shao, N. Li, J. Lin, and T. Dean, "Formability evaluation for sheet metals under hot stamping conditions by a novel biaxial testing system and a new materials model," *International Journal of Mechanical Sciences,* vol. 120, pp. 149-158, 2017.

[207] G. Adam, D. Balint, T. Dean, J. Dear, O. El Fakir, A. Foster*, et al.*, "Method of forming parts from sheet metal alloy," *U.S. Patent 10,465,271.,* 2019.

Appendix A. Equipment refinement

A.1 Reconfiguring the fast cooling station

Originally six gas springs were mounted on the lower die of the contact cooling station to provide counter acting force when the hydraulic press moved down. But in the initial design the counter forces between the contact cooling station and multi-point forming tool were different, which resulted in an imbalance of the hydraulic press. To improve the imbalance four new gas springs with reduced capacity were ordered to replace the old ones. The new springs were placed on each corner of the lower die. After this modification the total initial force was reduced to 1000 daN from the original 18000 daN. Since the new gas springs were smaller, some other parts needed to be manufactured, these were adjusted base mounts, new contact plate extensions, new mechanical stops and cylinder flanges. The specification of the old and new gas springs and CAD drawings are shown in Appendix B.

Details of the reconfiguration procedures are shown as follows

1. Before the adjustment made on the tooling two G clamps were used to clamp the lower cooling die to the upper one tightly on both sides with air input and output design and then they were lifted up, as shown in Figure A-1.
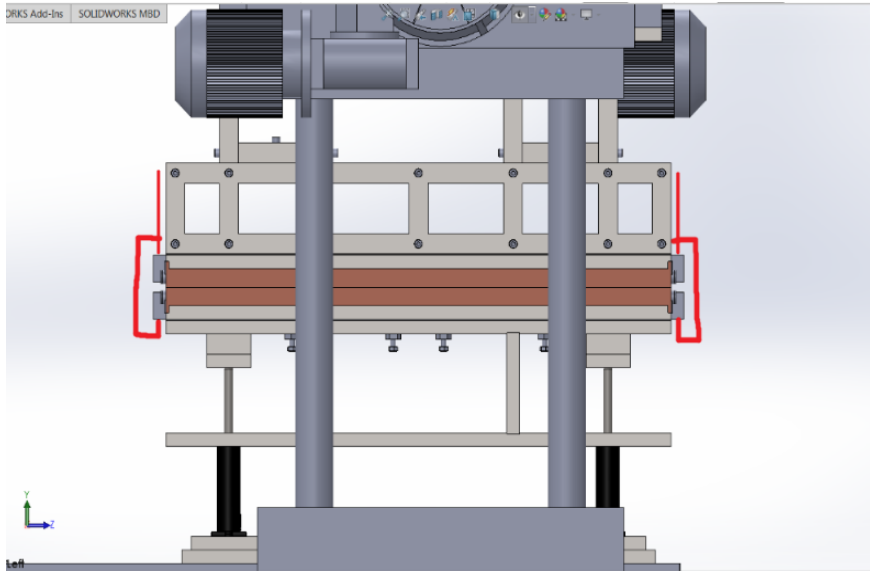
Figure A-1 Cooling dies clamped by G clamp

2. After the old gas springs were taken off, the base mounts were used for the new ones to fit, with holes to be made into slots. Firstly half of the new gas spring holders were screwed on the old mounting plate. Then the gas spring was placed in the holder, and screwed onto the other half. These screws should be tightened to fix the gas springs when being pressed down.
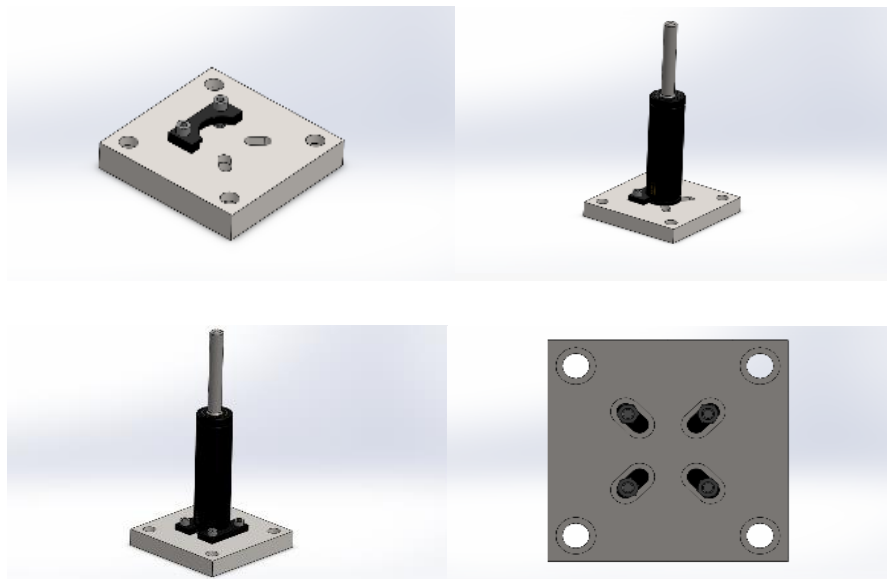

Figure A-2 Fastening of the new gas spring

3. Since the new gas springs are shorter, new contact plate extensions were employed to extend the height of the contact plate by 30mm in order to keep the tool height equal. The new extended contact plate was combined with the old contact plate and they were screwed into the lower die.
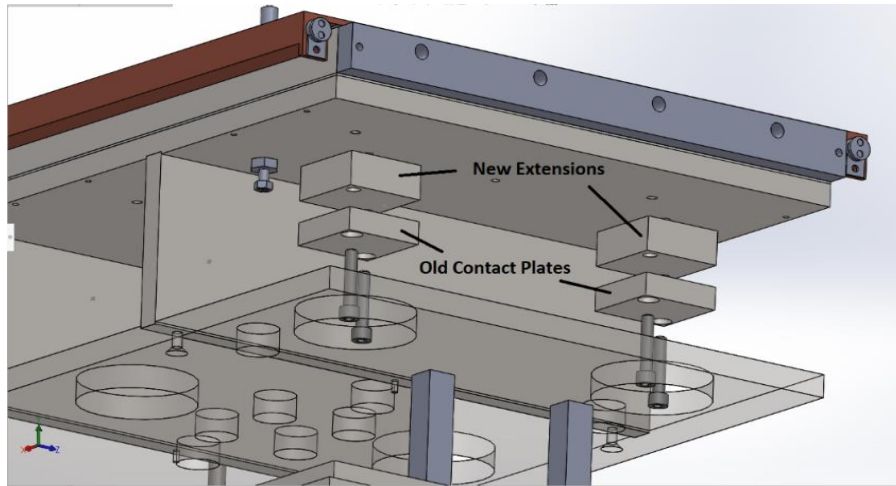
Figure A-3 Extension of the contact plate

4. The gas spring was placed through the hole, and the gas spring base plates were screwed onto the mounting plate. In the meantime, new mechanical stops were fixed to their previous positions to prevent the cooling station from over compressing. Finally, cylinder flanges with a small diameter were located to prevent the new gas springs from turning over when the force on the springs was not vertical.
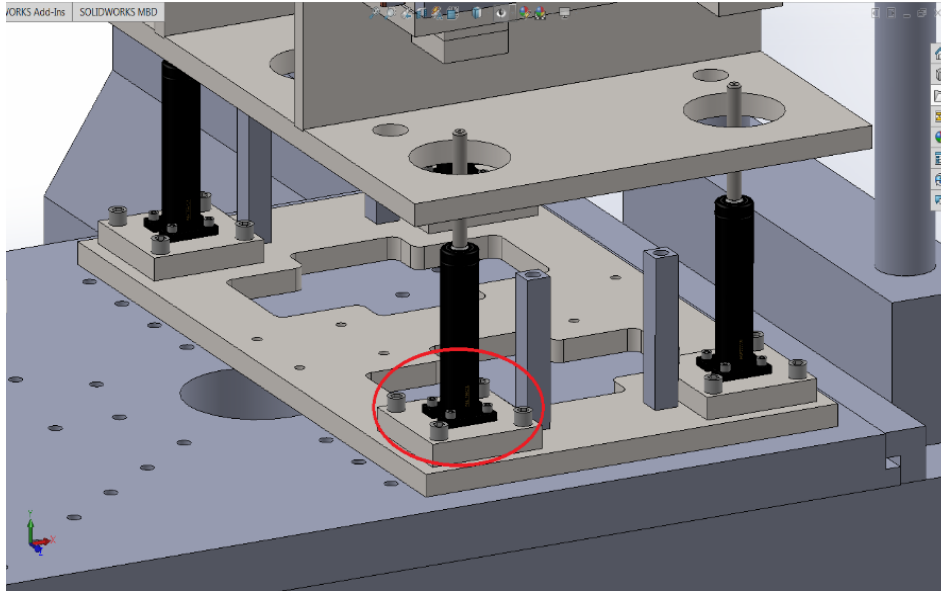
Figure A-4 Re-location of the gas springs, mechanical stops and flanges

A.2 Blank holder assembly

Originally during the forming process, the heated and fast cooled blank was transferred to the multi-point forming tool, after which a blank holder was applied on the blank to control the sliding of the blank material along the surface of the die-plate and reduce wrinkling. But there are two major problems for this procedure especially for hot forming: one is that the adjustment of the blank holder position may cause a handling burning issue although thermal insulated gloves are worn; the other is that the placement and adjustment procedure may cause great heat loss, thus the forming temperature is not within the desired range. To solve these problems and simplify the handling procedures, the blank holder was fixed to the blocks of the upper forming tool with countersinks and an illustration is shown in Figure A-5. After this modification no more adjustments are required to be made during the whole process.
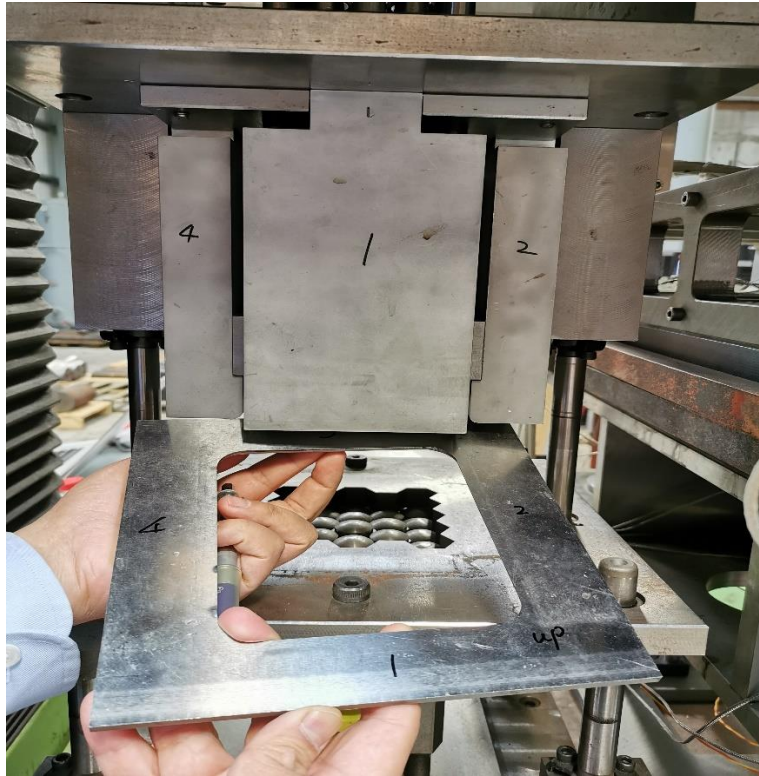
Figure A-5 Illustration of fixing blank holder to the upper blocks of forming tool

To fix the blank holder, firstly four holes need to be drilled using countersink drill bits at each edge of the blank holder and the bottom of each block, labelling as 1, 2, 3 and 4 separately to make sure there is no obvious gap on the lower surface. The positions of the holes in the blank holder and the blocks must fit each other so that they can be screwed together. The fitting direction should be carefully considered because the lower surface of the blank holder has a round fillet of 3mm, which makes the material flow of the formed blank smoother when pressed down. The engineering drawing of the blank holder is shown in Appendix B. The depth of the holes in the blocks depends on the specification of the screws.

A.3 Metal blank locating

The location of the blank holder is fixed without any adjustment. However, before the forming stage it is still necessary to adjust the position of the heated blank. The hot blank is usually transferred by using a plier to avoid handling burning issues, so it is very difficult and time consuming to locate a precise position. To make this easy, we planned to drill two holes on the stripper plate of the lower die and use dowels as stoppers. Although compared with more holes, there may be small movements and displacements from the exact position, it is a balance of performance and modification cost. After this modification, the blank is located once it touches the two stoppers on the side.

The engineering drawing location of the two drill holes is presented in Appendix C. The stopper used here is a 12mm plain steel parallel dowel pin with 3mm diameter following the DIN 6325 specification standard. To ensure clearance installation is available, the holes should be H7 as least. The depth of the hole is selected as 11.5mm to allow 0.5mm clearance above the die surface. The dowel holes are designed to be outside the pressing area to avoid damage of the tool.

A.4 Machine thermal insulation

It can be seen in Figure 6-3 that the hydraulic ram is protected by a rubber sleeve, the heat induced by the fast cooling station may destroy the rubber and thus cause potential risks. In this situation an insulation plate was planned to be cut and hung to prevent heat transfer as shown in Figure A-6. The insulation plate can move with the press and withstand temperature up to 1000 $^\circ$C.
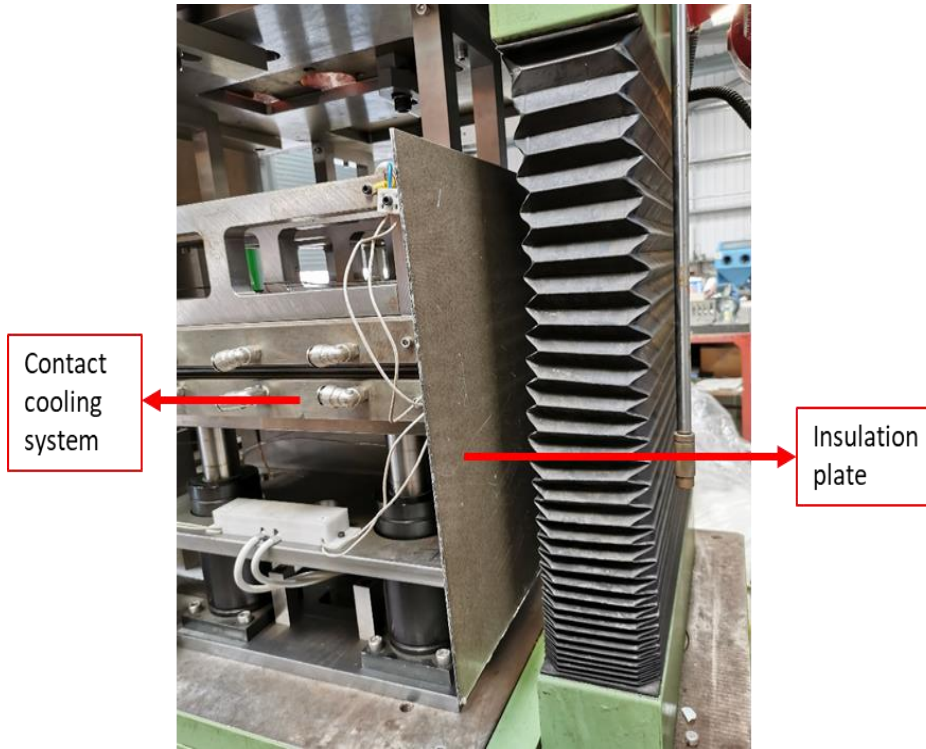
Figure A-6 Insulation plate

Appendix B. Gas spring specification and reconfiguration of the fast contact cooling station

To balance the counter forces of the hydraulic press between the fast contact-cooling station and multi-point forming tool, six gas springs from the fast contact-cooling station were changed to four new gas springs with reduced capacity. Figure B-1 shows the specification of old and new gas spring in terms of dimension and pressure capacity. In addition, some more parts were manufactured to match the spring gas dimension change in order to maintain the initial design of the fast contact-cooling station, as shown in Figure B-2.


PRODUCT CODE
ISNG3000-080

Description:
The ISNG range is the optimum design for gas spring durability and conforms to the ISO11901 gas spring standard.

BODY DIAMETER:	95 mm
PISTON DIAMETER:	50 mm
INITIAL FORCE:	3000 daN
MAXIMUM FORCE:	4408 daN
STROKE:	80 mm
L MIN:	200 mm
LENGTH:	280 mm
SAFETY MARGIN:	3 mm
PCD:	60 mm
TAPPED HOLE DIAMETER:	M8
TAPPED HOLE DEPTH:	13 mm
WEIGHT:	7.50 Kg
MAX PRESSURE:	150 Bar
MIN PRESSURE:	20 Bar
MAX PISTON VELOCITY:	1.6M/Sec

(a)

PRODUCT CODE
ISNG0250-100

Description:
The ISNG range is the optimum design for gas spring durability and conforms to the ISO11901 gas spring standard.

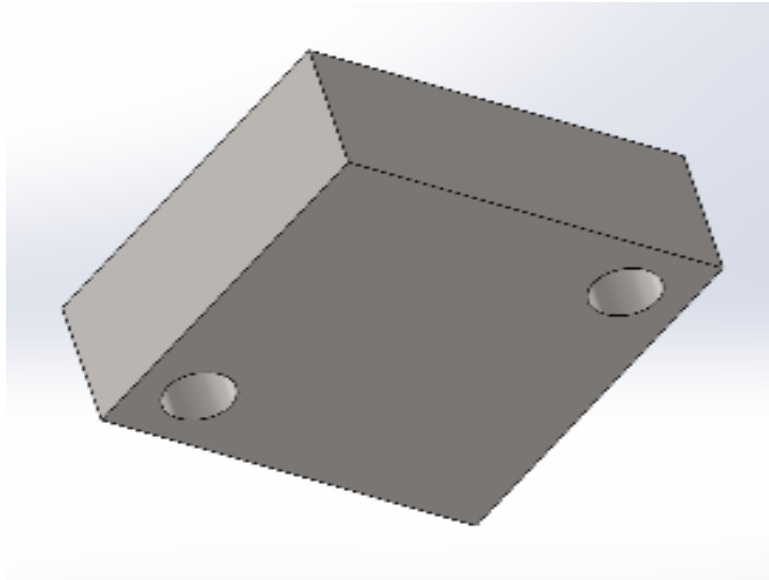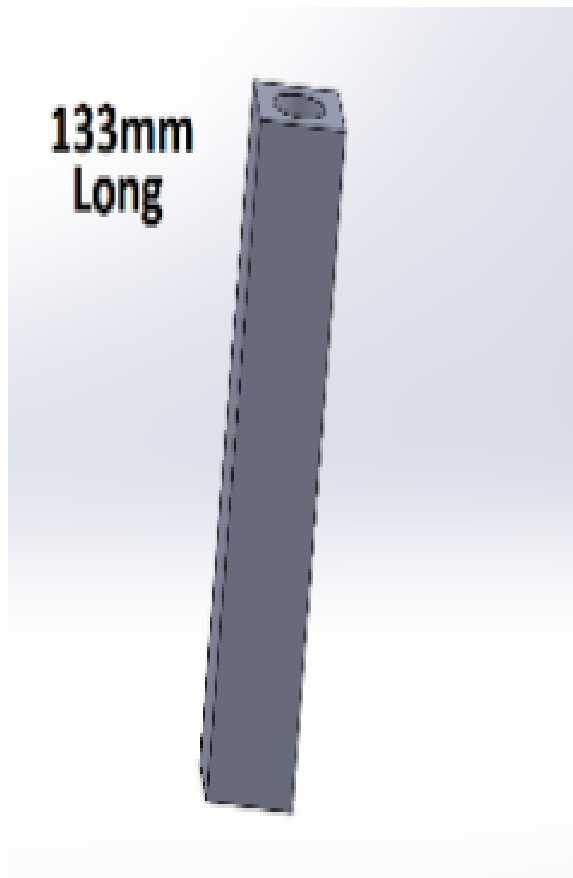|	
BODY DIAMETER:	38 mm
PISTON DIAMETER:	14 mm
INITIAL FORCE:	250 daN
MAXIMUM FORCE:	301 daN
STROKE:	100 mm
L MIN:	150 mm
LENGTH:	250 mm
SAFETY MARGIN:	2 mm
PCD:	18/25 mm
TAPPED HOLE DIAMETER:	M6
TAPPED HOLE DEPTH:	8 mm
WEIGHT:	0.87 Kg
MAX PRESSURE:	150 Bar
MIN PRESSURE:	20 Bar
MAX PISTON VELOCITY:	1.6M/Sec
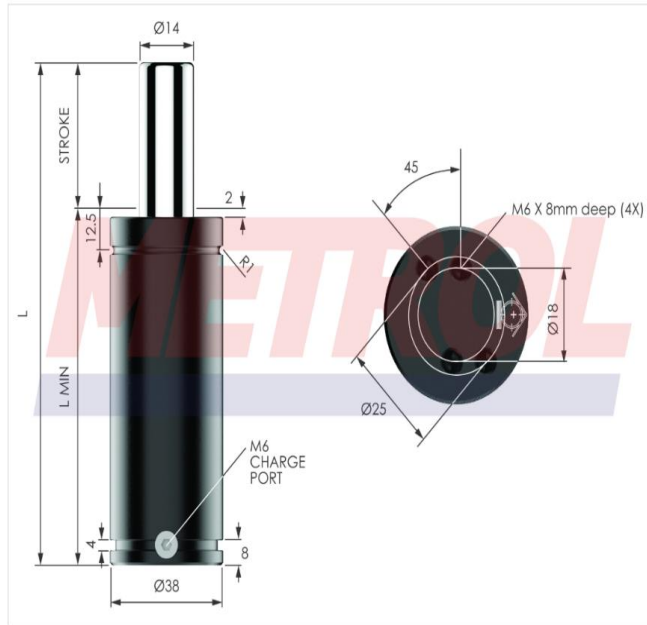
(b)

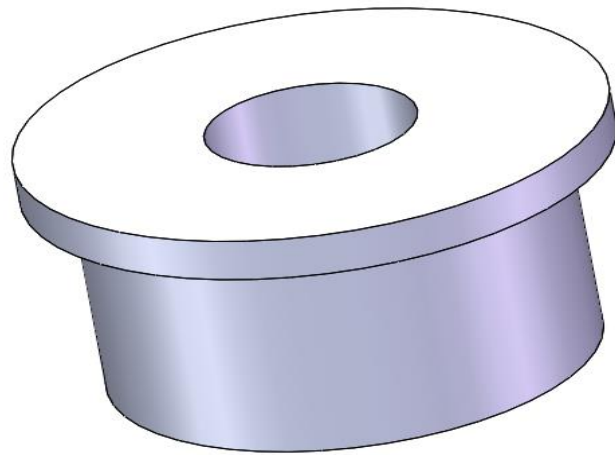Figure B-1 Specification of gas springs: (a) original and (b) new

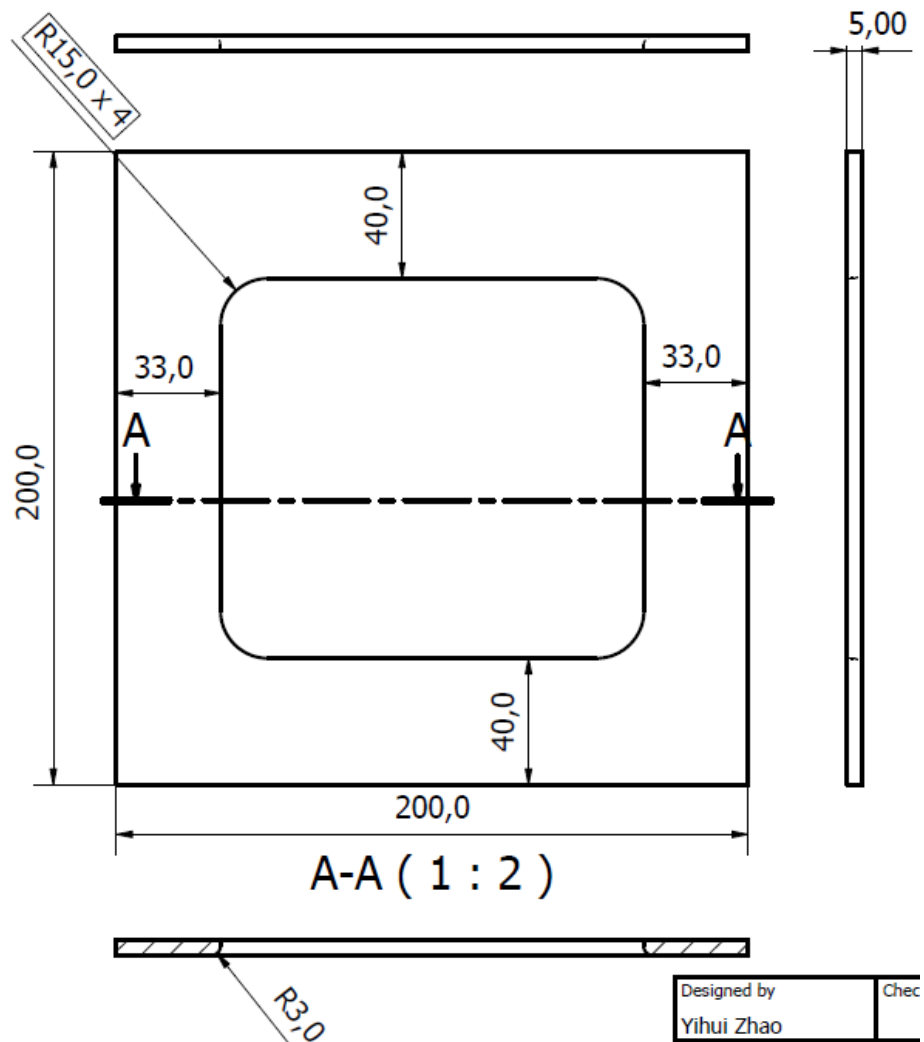
(a)

(b)

133mm
Long
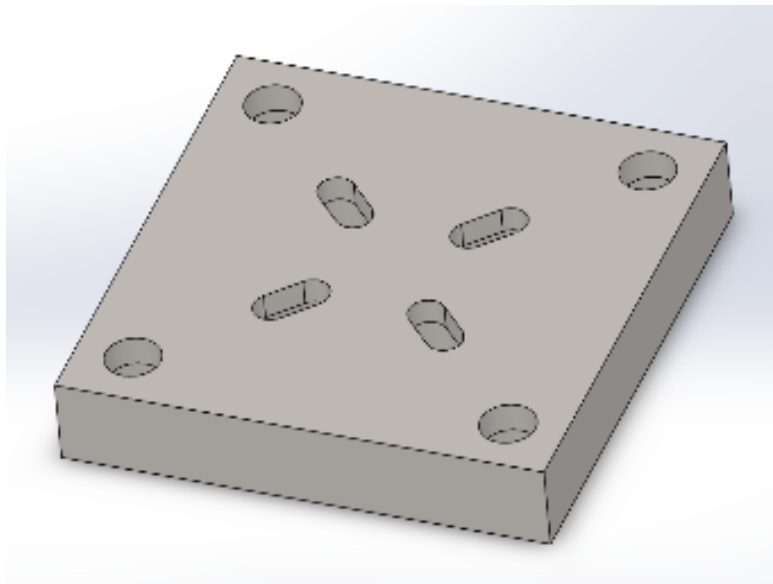
(c)

(d)

Figure B-2 Adjusted parts: (a) adjusted base mounts, (b) new contact

plate extensions (c) new stops and (d) cylinder flange

Appendix C. Engineering drawing of blank holder and its locating

Blank holder:

Location of dowel holes: